

5-2010

Vehicle Steering Systems - Hardware-in-the-Loop Simulator, Driving Preferences, and Vehicle Intervention

Jesse Black

Clemson University, jdblack@clemson.edu

Follow this and additional works at: https://tigerprints.clemson.edu/all_dissertations



Part of the [Engineering Mechanics Commons](#)

Recommended Citation

Black, Jesse, "Vehicle Steering Systems - Hardware-in-the-Loop Simulator, Driving Preferences, and Vehicle Intervention" (2010). *All Dissertations*. 515.

https://tigerprints.clemson.edu/all_dissertations/515

This Dissertation is brought to you for free and open access by the Dissertations at TigerPrints. It has been accepted for inclusion in All Dissertations by an authorized administrator of TigerPrints. For more information, please contact kokeefe@clemson.edu.

VEHICLE STEERING SYSTEMS - HARDWARE-IN-THE-LOOP SIMULATOR,
DRIVING PREFERENCES, AND VEHICLE INTERVENTION

A Dissertation
Presented to
the Graduate School of
Clemson University

In Partial Fulfillment
of the Requirements for the Degree
Doctor of Philosophy
Mechanical Engineering

by
Jesse David Black
May 2010

Accepted by:
Dr. John Wagner, Committee Chair
Dr. Darren Dawson
Dr. Ardalan Vahidi
Dr. Fred Switzer

ABSTRACT

The steering system is a critical component of all ground vehicles regardless of their propulsion source. Chassis directional control is provided by the steering system, which in turn relays valuable feedback about the road and vehicle behavior. As the primary feedback channel to the driver, the steering system also delivers the initial perception of a vehicle's handling and responsiveness to the consumer. Consequently, the steering system is an important aspect of the vehicle's evaluation and purchasing process, even if drivers are unaware of its direct influence in their decision making. With automobile purchases potentially hinging on the steering system, a need exists for a better understanding of steering preference through a focused research project. In this investigation, driver steering preferences have been studied using an advanced hardware-in-the-loop automobile steering simulator. Additionally, vehicle run-off-road situations have been studied, which occur when some of the vehicle wheels drift off the road surface and the driver recovers through steering commands.

The Clemson University steering simulator underwent three significant generations of refinements to realize a state-of-the-art automotive engineering tool suitable for human subject testing. The first and third generation refinements focused on creating an immersive environment, while the second generation introduced the accurate reproduction of steering feel found in hydraulic systems and real-time adjustable steering feel. This laboratory simulator was the first known validated

driving simulator developed for the sole purpose of supporting driver steering preference studies. The steering simulator successfully passed all validation tests (two pilot studies) leading to an extensive demographics-based driver preference study with 43 subjects. This study reflected the following preliminary trends: Drivers who used their vehicles for utility purposes preferred quicker steering ratios and heavier efforts in residential, country, and highway environments. In contrast, car enthusiasts preferred quick steering ratios in residential and country environments and light steering effort on the highway. Finally, rural drivers preferred quicker steering ratios on country roads. These relationships may be used to set steering targets for future vehicle developments to accurately match vehicles to their intended market segments.

The second research aspect was the development of an objective steering metric to evaluate a driver's steering preference. In past simulator studies, driver feedback has been gathered extensively using written questionnaires. However, this delays the testing procedure and introduces an outside influence that may skew results. Through the data collected in this project, a robust objective steering preference metric has been proposed to gather steering preferences without directly communicating with the driver. The weighted steering preference metric demonstrated an excellent correlation with survey responses of $r = -0.39$ regardless of steering setting. This global steering preference metric used a combination of yaw rate, $\dot{\psi}$, longitudinal acceleration, a_x , and lateral acceleration, a_y . The objective data was further dissected and it was discovered that changes made to the steering

ratio resulted in a correlation of $r = -0.55$ between the objective data and subjective response from the test subjects. This substantial correlation relied on the longitudinal acceleration, a_x , left front tire angle, δ_{lf} , and throttle position, TPS.

Beyond steering preferences, vehicle safety remains a major concern for automotive manufacturers. One important type of crash results from the vehicle leaving the road surface and then returning abruptly due to large steering wheel inputs: road runoff and return. A subset of run-off-road crashes that involves a steep hard shoulder has been labeled “shoulder induced accidents”. An active steering controller was developed to mitigate these “shoulder induced accidents”. A cornering stiffness estimation technique, using a Kalman filter, was coupled with a full state feedback controller and “driver intention” module to create a safe solution without excessive intervention. The concept was designed to not only work for shoulder induced accidents, but also for similar road surface fluctuations like patched ice. The vehicle crossed the centerline after 1.0s in the baseline case; the controller was able to improve this to 1.3s for a 30% improvement regardless of driver expertise level. For the case of an attentive driver, the final heading angle of the vehicle was reduced by 47% from 0.48 rad to 0.255 rad.

These laboratory investigations have clearly demonstrated that advancements in driver preference and vehicle safety may be realized using simulator technology. The opportunity to apply these tools should result in better vehicles and greater safety of driver and occupants. With the development of the objective steering preference metric, future research opportunities exist. For prior steering preference research, the

feedback loop has typically required interaction with the subject to rate a setting before continuing. However, the objective steering preference metric allows this step to be automated, opening the door for the development of an automatic tuning steering system.

ACKNOWLEDGMENTS

I would like to thank and acknowledge Honda R&D Americas, Inc. for providing extensive support. Specifically I would like to thank David Thompson, Dr. Bill Post, and Mike Kinstle for constantly pushing the research forward.

I would also like to thank Erhun Iyasere for his hard work in the trenches with me.

TABLE OF CONTENTS

	Page
TITLE PAGE	i
ABSTRACT	ii
ACKNOWLEDGMENTS	vi
LIST OF TABLES	ix
LIST OF FIGURES	xi
NOMENCLATURE	xviii
CHAPTER	
I. INTRODUCTION	1
Clemson University Steering Simulator	1
Subjective Steering Preferences.....	3
Objective Steering Preferences	5
Steering Intervention for Vehicle Road Runoff.....	6
Organization of Dissertation	9
II. STEERING SIMULATOR DEVELOPMENT	10
First Generation Steering Simulator	10
Second Generation Steering Simulator	15
Third Generation (Current) Steering Simulator	28
III. DRIVER PREFERENCE STUDIES	36
Pilot Studies 1 and 2	36
Demographics Study	54

Table of Contents (Continued)

	Page
IV. CREATION OF A STEERING PREFERENCE OBJECTIVE METRIC FOR INNOVATIVE STEERING FEATURES	71
Hypothesis.....	75
Analysis Method	75
Presentation and Discussion of Test Results	81
Summary	89
V. ACTIVE STEERING FOR VEHICLE ROAD RUNOFF.....	91
Description of Vehicle Behavior During a Shoulder Induced Accident.....	93
Shoulder Induced Accident Vehicle Dynamics	97
Training and Active Control for SIA Mitigation	102
Active Steering Control	105
VI. CONCLUSION AND FUTURE RESEARCH.....	144
Summary	144
Future Research Challenges.....	146
APPENDICES	149
A: Pilot Study 1 and 2 Scenario Questionnaire	150
B: Pilot Study 1 Raw Data.....	152
C: Pilot Study 2 Raw Data.....	154
D: Final Demographics Questionnaire.....	156
E: Demographics Questionnaire Data	161
F: Final Scenario Questionnaire.....	167
G: Demographics Study Raw Data	169
H: Simulator Operation.....	191
I: Active Steering Controller Simulink Block Diagram	198
J: Normalized Objective Metrics.....	199
REFERENCES	206

LIST OF TABLES

Table	Page
2.1 Tuned parameters in steering model to create accurate replication of steering torque for a 2006 Honda CR-V.....	25
3.1 Pilot study vehicle steering configurations with variations in steering ratio and steering torque.....	39
3.2 Pilot study 1 percent deviations of the mean for all scenarios within each question grouping; shading denotes the two most popular steering configurations, C1 and C5.....	46
3.3 Pilot study 2 percent deviations of the mean for all scenarios within each question grouping; shading denotes the most popular steering configuration, C4.....	53
3.4 Summary of the five steering configurations used in demographics study; configuration C6 was delisted due to poor results in the pilot studies	56
3.5 Three designed roadway environments utilized in the demographics study	56
3.6 The fifteen scenarios with corresponding steering configuration and roadways for the demographics study.....	57
3.7 Latin square run order showing driving scenario (steering configuration and roadway) versus driving order for groups of fifteen drivers.....	58
3.8 Average response, \bar{q}_{ij} , of each subject ($i=1,2,\dots,43$) for each question ($j=1,2,\dots,9$) used to normalize the response data for fifteen configurations to eliminate question bias.....	65
3.9 Qualitative interpretation the of correlation, r , and p-value used to evaluate the strength of results for the demographic study	67

List of Tables (Continued)

Table	Page
3.10 Correlations, r , between the demographic groups and steering systems preferences with related p-measures based on questionnaire data	68
4.1 Data channels, H_c , investigated to determine correlation between objective data and subjective human responses	76
4.2 Qualitative interpretation of correlation, r , with four categories: poor, moderate, excellent, and unrealistic correlations.....	81
4.3 Global normalized questionnaire data, Q_{ik} , used for all correlations with objective metrics	83
4.4 Correlation coefficients between objective metrics and questionnaire results with best correlation of $r = -0.32$ for yaw rate, $\dot{\psi}$, metric.....	84
4.5 Weighting factors, w_c , for weighted metric, J_w , giving maximum correlations of $r = -0.39$, $r = -0.55$, and $r = -0.15$ for Global ($k = 1-5$), Ratio ($k = 2,3$), and Effort ($k = 4,5$) respectively where k denotes the steering configuration	87
5.1 Table of parameter values for a small sedan simulated in CarSim 6	125
5.2 Summary of driver and controller time variables showing symbol, unit, and case values.....	128
5.3 Summary of test cases for shoulder induced accident control system with driver reaction times, τ_d , controller reaction times, τ_e , final vehicle heading angle, ψ_f , time to lane crossing, Δt_c , peak yaw rate, $\dot{\psi}_{\max}$, peak lateral velocity, $v_{y_{\max}}$, peak slip angle, β_{\max} , driver behavior, intervention time period, and performance rank in terms of vehicle safety	142

LIST OF FIGURES

Figure	Page
1.1 Clemson University steering simulator with immersive driving environment.....	3
1.2 Steering design problem which illustrates how safety and enjoyment interact with the environment and demographic groups using limited system parameters	4
2.1 Honda Initiation Grant (HIG) stand alone steering simulator bench with hydraulic rack and pinion assembly	11
2.2 First generation driving simulator cab with fixed base and privacy curtain to isolate human subject.....	12
2.3 First generation steering servo-motor with steering stub shaft mounted below dashboard gauges	13
2.4 First generation driving environment with authentic vehicle cabin and single projected view	15
2.5 Second generation steering simulator with single projected view; operating station relocated behind the vehicle cabin.....	16
2.6 Working dashboard gauges and lights improve the realism of the environment for test subjects within the vehicle cabin.....	18
2.7 Full assembly of new steering motor mounted in dashboard with support points attached to banana brackets.....	19
2.8 Comparison of the simulation and experimental results from the holding effort test.....	26
2.9 Comparison of the simulation and experimental data from fixed frequency sinusoidal input (0.25, 0.50, 1.0 Hz) test at 60 kph. The solid line is the test data while the dotted line is the result of the simulation.....	27

List of Figures (Continued)

Figure	Page
2.10 Comparison of the simulation and experimental data from fixed frequency sinusoidal input (0.25, 0.50, 1.0 Hz) test at 120 kph. The solid line is the test data while the dotted line is the result of the simulation.....	28
2.11 Longitudinal motion base installed beneath simulator cab with tensioning spring to keep cab balanced	31
2.12 Motion control box with (a) emergency stop and (b) amplifier to control the position of the motion base.....	31
2.13 Three screen projection with 120 degree field of view for the driver in vehicle cabin.....	32
2.14 Schematic of the steering simulator showing the interaction of inputs and outputs with the dSPACE 1103 processor board and support computers	35
3.1 Winding country road and residential driving environment (R2 and R1) used for the first pilot study	38
3.2 Pilot study 1 “global” steering configuration preference calculated as mean response from questionnaire	40
3.3 Pilot study 1 “fun” steering configuration preference calculated as mean response from questionnaire	42
3.4 Pilot study 1 “control” steering configuration preference calculated as mean response from questionnaire	43
3.5 Pilot study 1 “ease” steering configuration preference calculated as mean response from questionnaire	44
3.6 Pilot study 1 “safety” steering configuration preference calculated as mean response from questionnaire	45
3.7 Highway driving environment (R3) used for pilot study 2 with pylons to force drivers to change lanes.....	47

List of Figures (Continued)

Figure	Page
3.8 Pilot study 2 “global” steering configuration preference calculated as mean response from questionnaire	48
3.9 Pilot study 2 “fun” steering configuration preference calculated as mean response from questionnaire	49
3.10 Pilot study 2 “control” steering configuration preference calculated as mean response from questionnaire	50
3.11 Pilot study 2 “ease” steering configuration preference calculated as mean response from questionnaire	51
3.12 Pilot study 2 “safety” steering configuration preference calculated as mean response from questionnaire	52
3.13 Breakdown of demographics categorization for all 43 human subjects participating in the simulator study with (a) Fun, (b) Utility, and (c) Enthusiast.....	61
4.1 Steering angle for test subject 20 driving steering configurations C8 and C7 on road surface R2; the solid line (C8) was identified through questionnaire feedback as the preferred setting while the dotted line (C7) was not preferred.....	74
4.2 Analysis methodology flowchart for creating a weighted objective metric that may predict driver steering preference.....	80
4.3 Plot of normalized yaw rate metric, J_{norm_6} , vs. normalized questionnaire data, Q , to visualize the moderate correlation of $r = -0.32$	84
4.4 Plot of weighted metric, J_w , vs. normalized questionnaire data, Q , to visualize the moderate correlation of $r = -0.39$	86
4.5 Plot of weighted steering ratio metric, J_w , vs. normalized questionnaire data, Q , for changes in steering ratio ($k = 2, 3$) to visualize the correlation of $r = -0.55$	88

List of Figures (Continued)

Figure		Page
4.6	Plot of weighted steering effort metric, J_w , vs. normalized questionnaire data, Q , for changes in steering effort ($k = 4, 5$) to visualize the correlation of $r = -0.15$	89
5.1	Configuration diagrams for an (a) electric power steering, and (b) steer-by-wire system in a ground vehicle	93
5.2	Passenger vehicle with two tires off road surface	94
5.3	Front tire caught against the road shoulder prior to the vehicle's return to the road surface	94
5.4	Vehicle immediately after re-entry onto the road surface with a large commanded front wheel steer angle	95
5.5	Vehicle less than one second after re-entry with large yaw angle and approaching roadway double solid line	96
5.6	Low order vehicle model with front and rear tire slip angles, yaw angle, and sideslip angle with commanded speed and steer angle	100
5.7	Vehicle trajectory during an emulated shoulder induced accident (simulated J-turn); roadway double solid line at 3 meters crossed by vehicle traveling at 72 kph	101
5.8	Lateral vehicle position versus time for shoulder induced accident; roadway double solid line crossed within one second for vehicle traveling at 72 kph	101
5.9	Yaw versus time for shoulder induced accident; roadway centerline crossed at $t = 1$ second for vehicle traveling at 72 kph	102

List of Figures (Continued)

Figure		Page
5.10	Schematic diagram of active steering controller with driver steering input angle δ_{sw} being supplemented by the steering controller to create the front wheel angle δ	106
5.11	The input steering wheel angle to validate the estimation strategy for tire cornering stiffness with frequency and amplitude of $f = 0.25Hz$ and $\delta_{sw} = 90^\circ$	118
5.12	Estimated front cornering stiffness, $\hat{C}_{\alpha f}$, on a road surface changing from $\mu = 0.85$ to $\mu = 0.3$ and back with $v_x = 60kph$	120
5.13	Estimated front cornering stiffness, $\hat{C}_{\alpha r}$, on a road surface changing from $\mu = 0.85$ to $\mu = 0.3$ and back with $v_x = 60kph$	120
5.14	Yaw rate for the CarSim vs. estimated chassis model on a road surface changing from $\mu = 0.85$ to $\mu = 0.3$ and back with $v_x = 60kph$	121
5.15	Error in yaw rate between CarSim and bicycle model on a road surface changing from $\mu = 0.85$ to $\mu = 0.3$ and back with $v_x = 60kph$	121
5.16	Lateral acceleration for the CarSim vehicle model on a road surface changing from $\mu = 0.85$ to $\mu = 0.3$ and back with $v_x = 60kph$	122
5.17	Visual representation of driver intention module showing intended intervention intervals of steering controller; controller designed to assist during the $\Delta t = \tau_e$ time period following a tire/road equivalent friction transition.....	124

List of Figures (Continued)

Figure	Page
5.18 Friction coefficient during simulated shoulder induced maneuver stepping from $\mu = 0.85$ to $\mu = 0$ (wheels off road surface) at $t = 25s$ and back to $\mu = 0.85$ (wheels on road surface) at $t = 28s$	129
5.19 Road wheel angle, δ , during SIA event with driver reaction time of $\tau_d = 2s$ and controller settings of $\tau_e = 0s$ (Case #1 - uncontrolled baseline), $\tau_e = 2s$ (Case #2), and $\tau_e = 1s$ (Case #3)	131
5.20 Yaw rate, $\dot{\psi}$, during SIA event with driver reaction time of $\tau_d = 2s$ and controller settings of $\tau_e = 0s$ (Case #1 - uncontrolled baseline), $\tau_e = 2s$ (Case #2), and $\tau_e = 1s$ (Case #3)	133
5.21 Vehicle slip angle, β , during SIA event with driver reaction time of $\tau_d = 2s$ and controller settings of $\tau_e = 0s$ (Case #1 - uncontrolled baseline), $\tau_e = 2s$ (Case #2), and $\tau_e = 1s$ (Case #3)	133
5.22 Lateral velocity, v_y , during SIA event with driver reaction time of $\tau_d = 2s$ and controller settings of $\tau_e = 0s$ (Case #1 - uncontrolled baseline), $\tau_e = 2s$ (Case #2), and $\tau_e = 1s$ (Case #3)	134
5.23 Lateral position, Y , during SIA event with driver reaction time of $\tau_d = 2s$ and controller settings of $\tau_e = 0s$ (Case #1 - uncontrolled baseline), $\tau_e = 2s$ (Case #2), and $\tau_e = 1s$ (Case #3)	134
5.24 Vehicle trajectory during SIA event with driver reaction time of $\tau_d = 2s$ and controller settings of $\tau_e = 0s$ (Case #1 - uncontrolled baseline), $\tau_e = 2s$ (Case #2), and $\tau_e = 1s$ (Case #3)	135

List of Figures (Continued)

Figure	Page
5.25 Steering angle, δ , during SIA event with driver reaction time of $\tau_d = 1$ s and controller settings of $\tau_e = 0$ s (Case #4 - uncontrolled baseline), $\tau_e = 2$ s (Case #5), and $\tau_e = 1$ s (Case #6)	137
5.26 Yaw rate, $\dot{\psi}$, during SIA event with driver reaction time of $\tau_d = 1$ s and controller settings of $\tau_e = 0$ s (Case #4 - uncontrolled baseline), $\tau_e = 2$ s (Case #5), and $\tau_e = 1$ s (Case #6)	138
5.27 Vehicle slip angle, β , during SIA event with driver reaction time of $\tau_d = 1$ s and controller settings of $\tau_e = 0$ s (Case #4 - uncontrolled baseline), $\tau_e = 2$ s (Case #5), and $\tau_e = 1$ s (Case #6)	138
5.28 Lateral velocity, v_y , during SIA event with driver reaction time of $\tau_d = 1$ s and controller settings of $\tau_e = 0$ s (Case #4 - uncontrolled baseline), $\tau_e = 2$ s (Case #5), and $\tau_e = 1$ s (Case #6)	139
5.29 Lateral position, Y , during SIA event with driver reaction time of $\tau_d = 1$ s and controller settings of $\tau_e = 0$ s (Case #4 - uncontrolled baseline), $\tau_e = 2$ s (Case #5), and $\tau_e = 1$ s (Case #6)	139
5.30 Vehicle trajectory during SIA event with driver reaction time of $\tau_d = 1$ s and controller settings of $\tau_e = 0$ s (Case #4 - uncontrolled baseline), $\tau_e = 2$ s (Case #5), and $\tau_e = 1$ s (Case #6)	140

NOMENCLATURE

Symbol	Units	Description
a	m	distance from front axle to center of gravity
a_x	m / s^2	vehicle longitudinal acceleration
a_y	m / s^2	vehicle lateral acceleration
A	deg	slalom maneuver amplitude
b	m	distance from rear axle to center of gravity
B_{rack}	$\frac{kg \cdot m}{s}$	steering rack damping
B_{sc}	$\frac{kg \cdot m^2}{s}$	steering column damping
B_w	$\frac{kg \cdot m^2}{s}$	wheel and linkage assembly damping
C_{af}	N / rad	front tire cornering stiffness
\hat{C}_{af}	N / rad	estimated front tire cornering stiffness
\tilde{C}_{af}	N / rad	driver perceived front tire cornering stiffness
C_{ar}	N / rad	rear tire cornering stiffness
\hat{C}_{ar}	N / rad	estimated rear cornering stiffness
\tilde{C}_{ar}	N / rad	driver perceived rear tire cornering stiffness
d_s	m	lateral offset of the steering axis

Nomenclature (Continued)

Symbol	Units	Description
D	-	demographic group
e_k	variable	discrete Kalman estimation error
f	Hz	slalom maneuver frequency
F_{boost}	N	power assist force
$F_{fr,rack}$	N	steering rack friction
F_y	N	tire lateral force
F_z	N	tire vertical force
H	variable	vehicle data channel
i	-	participant number
I	$kg \cdot m^2$	vehicle moment of inertia
I_{sw}	$kg \cdot m^2$	steering wheel moment of inertia
I_w	$kg \cdot m^2$	wheel and linkage assembly moment
j	-	question number
J	variable	steering preference metric
J_{norm}	-	normalized steering preference metric
J_w	-	weighted steering preference metric
k	-	steering configuration number
K	variable	continuous Kalman error weighting factor

Nomenclature (Continued)

Symbol	Units	Description
\bar{K}	-	steering ratio
K_k	variable	discrete Kalman error weighting factor
K_L	$N \cdot m$	steering linkage stiffness
K_{sc}	$N \cdot m$	steering column stiffness
K_{sw}	rad	steering angle control gain
K_T	$N \cdot m$	torsion bar stiffness
K_β	rad	slip angle control gain
$K_{\dot{\psi}}$	rad	yaw rate control gain
L	-	demographic group number
m	kg	vehicle mass
M_{AT}	$N \cdot m$	steering moment due to aligning moments
M_{sw}	$N \cdot m$	steering wheel torque
M_L	$N \cdot m$	steering moment due to lateral forces
M_{rack}	kg	steering rack mass
M_V	$N \cdot m$	steering moment due to vertical forces
M_z	$N \cdot m$	tire aligning moment
n	-	number of participants in a study

Nomenclature (Continued)

Symbol	Units	Description
N_L	m	steering linkage ratio
p	-	roadway number
P	variable	continuous Kalman error covariance
P_k	variable	discrete Kalman error covariance
q	-	questionnaire response
q_{norm}	-	normalized questionnaire response
Q	variable	process noise covariance
r	-	correlation coefficient
r_f	m	front tire radius
r_w	-	weighted correlation coefficient
R	variable	measurement noise covariance
R_p	m	pinion gear radius
S_{effort}	-	subject's effort based steering preference
S_{ratio}	-	subject's ratio based steering preference
u	variable	continuous Kalman white state noise
v	variable	continuous Kalman white measurement noise
v_k	variable	discrete Kalman white measurement noise
v_y	m / s	vehicle lateral velocity

Nomenclature (Continued)

Symbol	Units	Description
v_x	m / s	vehicle longitudinal velocity
w_c	-	weighting factor
w_k	variable	discrete Kalman white process noise
x	variable	continuous Kalman state vector
\hat{x}	variable	continuous Kalman estimated state vector
x_k	variable	discrete Kalman state vector
X	m	vehicle global x coordinate
y_{rack}	m	steering rack displacement
Y	m	vehicle global y coordinate
z	variable	continuous Kalman measurement vector
z_k	variable	discrete Kalman measurement vector
α_f	rad	front tire slip angle
α_r	rad	rear tire slip angle
β	rad	vehicle slip angle
δ	rad	front tire steering angle
δ_{sw}	rad	driver commanded steering angle
η	-	desired change in cornering stiffness
θ_{sp}	rad	spool valve angle

Nomenclature (Continued)

Symbol	Units	Description
θ_{sw}	rad	steering wheel angle
θ_{rw}	rad	front road wheel angle
θ_{tbar}	rad	torsion bar angle
λ	rad	kingpin inclination angle
μ	-	tire/road friction coefficient
$\mu_{control}$	-	mean questionnaire response for control category
μ_{ease}	-	mean questionnaire response for ease category
μ_{fun}	-	mean questionnaire response for fun category
μ_{global}	-	mean questionnaire response for global category
μ_{safety}	-	mean questionnaire response for safety category
ν	rad	caster angle
τ_d	s	driver reaction time
τ_e	s	controller assistance time
τ_{fb}	$N \cdot m$	kingpin moment
$\tau_{fr,kp}$	$N \cdot m$	kingpin friction
$\tau_{fr,sc}$	$N \cdot m$	steering column friction
τ_{sw}	$N \cdot m$	driver torque commanded at steering wheel

Nomenclature (Continued)

Symbol	Units	Description
ψ	<i>rad</i>	vehicle yaw angle

CHAPTER ONE

INTRODUCTION

The steering system is an important aspect of the automobile from operational safety and driver enjoyment perspectives. It is one of the primary control and feedback mechanisms in the driver-vehicle-road interface, both introducing and curing some of the most extreme instabilities a vehicle may face. Although drivers often receive initial vehicle training through driver education programs, intuitive use of the steering system typically comes through personal experience. For instance, wide ranging driving environments, vehicles, and behind-the-wheel driving experiences help shape a driver's steering preferences throughout the years. The diversity of these preferences and how they relate to a driver's demographics and driving behavior will be examined in this dissertation. The research has been divided into four distinct phases: simulator development, subjective steering preferences, objective steering preferences, and vehicle intervention.

1.1 Clemson University Steering Simulator

The first stage of studying the driver/vehicle steering interface was the development of a steering simulator. Many types of driving simulators exist, although most exist to study non-steering driving behavior. Steering simulator research typically focused on vehicle behavior rather than the driver's preferences. Zhang *et al.* (2000) designed a hardware-in-the-loop (HIL) steering simulator to

consider the effect of physical components, steering system dynamics and other factors like soil stiffness on off-road vehicles. Heydinger *et al.* (2002) developed a vehicle dynamics simulation model for use in the National Highway Traffic Safety Administration's (NHTSA's) National Advanced Driving Simulator. Andonian *et al.* (2003) used a fixed-based 14 DOF driving simulator to compare the lane tracking performance of test subjects using a joystick steering controller against a conventional hand wheel. Setlur *et al.* (2003) evaluated a hybrid vehicle steer-by-wire system using a hardware-in-the-loop and virtual reality test environment. The common theme is that simulators designed for human subject testing lack steering feedback realism, and those designed with accurate steering feedback were not designed for human subject testing.

The Clemson University steering simulator (refer to Figure 1.1) was developed for the sole purpose of accurately replicating an automobile's steering feel to investigate driver steering preferences. Beyond realistic steering feel, the steering had to be highly adjustable and provide environments that simulate typical driving situations. The simulator was developed in three generations, and the details of these generations are covered in Chapter 2.



Figure 1.1: Clemson University steering simulator with immersive driving environment

1.2 Subjective Steering Preferences

The concept of steering preference encompasses both safety and enjoyment. Vehicle safety regarding steering addresses the ability of the driver to command a safe and predictable trajectory for the chassis through rotation of the steering wheel. Enjoyment may be any aspect of the steering that makes the driver happy, such as an enhanced sense of speed and cornering performance or simply exceptional control over the vehicle. One may consider safety to overlap enjoyment since exceptional vehicle control may result in both driver enjoyment and safety. While a marketing perspective may encourage the development of a “fun” (i.e., enjoyable to the driver) steering setting, the global focus should always be on increasing safety. The problem

facing automotive engineers is summarized in Figure 1.2 which exhibits the complexity of designing a steering system that encompasses the specified design objectives on all environments for multiple demographic groups. Figure 1.2 hints at the possibility of a global steering design compromise, however no single setting could satisfy all design criteria simultaneously.

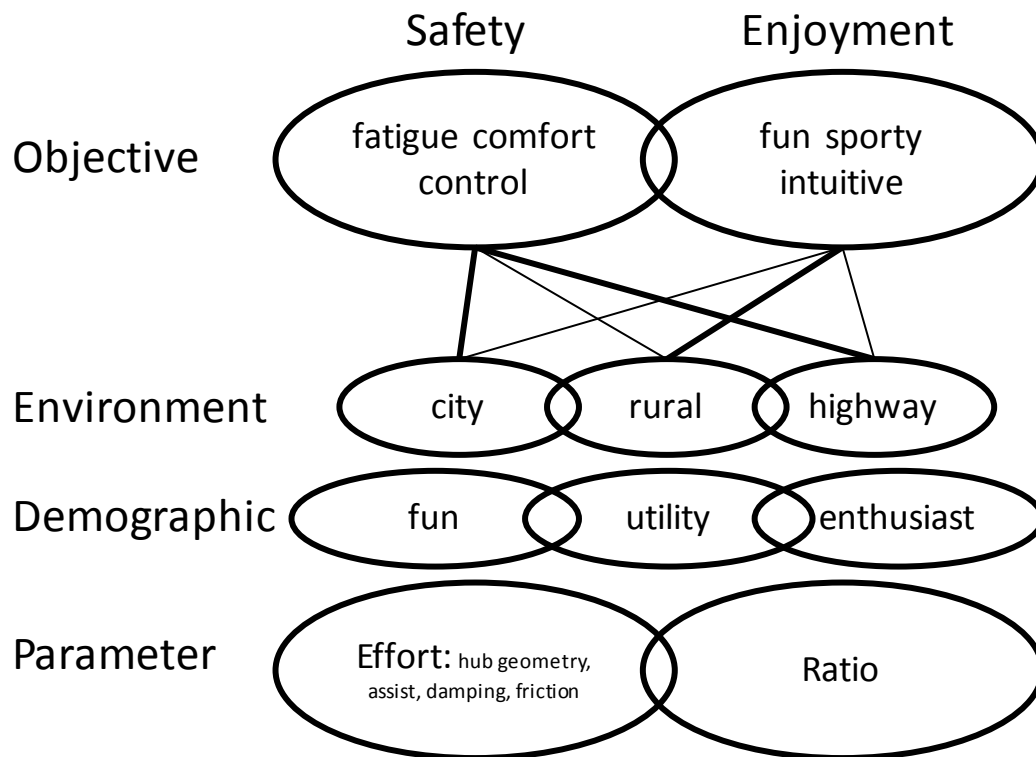


Figure 1.2: Steering design problem which illustrates how safety and enjoyment interact with the environment and demographic groups using limited system parameters

In preparation for studying driver steering preferences, the steering simulator was extensively validated to give credibility to future studies. For full validation, the simulator and testing procedure had to be capable of showing preferential differences

in both steering settings and driving environments. Furthermore, the simulator had to be validated in its sensitivity to individual driver preferences and demonstrate an ability to link drivers with similar preferences in the same demographics group. The details of this validation procedure have been covered in Chapter 3.

1.3 Objective Steering Preferences

Direct human subject feedback is an accurate and reliable method to measure a driver's steering preference; however, this method requires direct interaction with the subject and active thought to formulate a response, both of which slow down the data collection speed and distract the driver. When accuracy is more important than efficiency and safety (i.e., during an engineer's evaluation), the direct feedback method is preferred. However, circumstances may exist when driver preferences are sought in a timely, real-time manner without requiring a driver's direct attention. An objective steering preference metric may be used in such a situation to reveal a driver's steering preference simply by observing driving patterns.

Engineers have access to many relevant vehicle dynamics data channels such as yaw rate, lateral and longitudinal acceleration, steering angle, and vehicle speed. In a simulator environment, even more channels exist including tire slip angles and road position data. All of these channels can be used to describe the behavior of the vehicle. If a driver operates a vehicle differently depending on their fondness for a steering characteristic, the result of this change should be measurable in the vehicle

dynamics channels. Discovering the measurable change in vehicle response resulting from a driver's steering preference is the focus of Chapter 4.

1.4 Steering Intervention for Vehicle Road Runoff

No matter how much control a driver is given, there will always be dangerous situations that may be unavoidable. Random elements such as road obstructions (loose debris, pedestrians, animals) or changing road conditions (ice, hydroplaning) will always threaten a driver's safety and compromise an otherwise stellar level of control. To combat this, a vehicle needs to be able to intervene during these volatile situations.

Driving is a complex task that cannot yet be completely handed over to an autonomous controller. However, a driver's reaction time may not be fast enough to adjust to quickly changing road conditions. It's during these rare situations that vehicle intervention may prevent a crash. Active steering was explored as a solution to the specific problem of "shoulder induced accidents." These are crashes that occur as a result of the vehicle leaving the road shoulder, then returning abruptly, typically resulting in striking oncoming traffic or losing control of the vehicle and striking stationary obstacles on either side of the road. The key to intervention in a situation like this is the concept of "driver intention." If a driver intends to swerve abruptly to avoid an obstacle, it is imperative that an intervention system does not override this command. However, the swerve as a result of returning to the road should be overridden until the driver has time to react.

A number of recent research studies have emphasized preventing vehicle road departure through a vehicle dynamics approach. Pape *et al.* (1999) discussed the effectiveness of in-vehicle crash avoidance active safety systems as a countermeasure for run-off-road (ROR) crashes through on-road, test track, and simulator experiments designed to improve driver lane-keeping models. The authors reported that numerical studies demonstrated improved driver models for passenger vehicles and tractor trailers; however, heavy trucks present a greater challenge for improved lane-keeping technology due to instability in recovery maneuvers. Second, Deram (2004) studied lane departure crashes, specifically focusing on two research questions. First, can vehicle based parameters detect driver inattention? Second, how can such detection be integrated into a lane departure warning system (LDWS)? The findings suggested that an adaptive lane departure warning system was a viable tool for detection. The accompanying simulation studies were able to suppress up to 70% of redundant warnings. Finally, Pohl *et al.* (2007) studied a lane-keeping support system which was designed to provide assistance to a distracted driver. The authors utilized a video-based monitoring system to estimate the level of a visual distraction for distracted drivers. On-road tests indicated initial success in terms of a lane-keeping device which only intervened when a lane departure event was detected.

Recently, various research studies have shown an interest in a human factors approach to ROR crashes. First, Campbell *et al.* (2003) provided an extensive analysis of primary contributing human factors for crashes. In analyzing single vehicle ROR crashes, the authors found that the “2 leading crash contributing factors

involved speeding in 43% of crashes and resulting in a control loss in 41% of crashes”. Furthermore, the study demonstrated other primary contributing human factors for single vehicle ROR crashes including inattention (35%), driving under the influence (21%), drowsy/sleepy drivers (8%), vision obstruction for driver (3%), and driver sickness or blacking out (2%). Second, Janssen *et al.* (2006) found that that there were not many studies conducted to investigate driver behavior in ROR crashes. Furthermore, the authors found that the available studies are largely field observation studies and do not delineate best practices for reducing risk-taking behaviors. Third, LeBlanc *et al.* investigated a road departure crash warning (RDCW) system focusing on drivers that either drift off the road or take a turn too quickly. Researchers developed, validated, and field-tested the driver warning system in real time utilizing video and audio data. Findings suggested that the RDCW system improved driver lane keeping and therefore reducing the number of ROR incidents. Additionally, data on driver perception was collected through post-drive questionnaires, debriefing sessions, and focus groups. Interestingly, the authors found that “drivers who rated themselves as not prone to inattention or slips in memory found the RDCW system easier to use than drivers with higher lapse scores” (Leblanc, 2006). Finally, Sayer *et al.* (2007) conducted a field operational test to determine driver acceptance and perceived utility of a ROR crash warning system. The study found that drivers were generally positive regarding the use of the in-vehicle warning systems, and they determined lane departure warning (LDW) to be more helpful than curve speed warning (CSW). Furthermore, the subjects tended to rate the warning systems higher

for utility rather than satisfaction. Findings suggested that drivers perceived the overall warning system to increase safety regarding ROR crashes.

1.5 Organization of Dissertation

The dissertation has been organized as follows. The development of the Clemson University steering simulator will be presented in Chapter 2. Chapter 3 will capture the subjective steering preference research performed using the steering simulator. An objective steering preference metric has been developed in Chapter 4 using the data collected during the subjective testing of Chapter 3. Chapter 5 follows with the development of an active steering controller to mitigate shoulder induced accidents following run-off-road events. A summary of the presented work will be given in Chapter 6. The Appendices contain supplementary data and documentation.

CHAPTER TWO

STEERING SIMULATOR DEVELOPMENT

The Clemson University Steering Simulator was designed to replicate the steering response of a passenger automobile while offering a virtual reality driving experience for the operator. The primary focus of the simulator was to discover optimal steering characteristics to aid in the vehicle development process. The 2002 Honda Initiation Grant (HIG) established the foundation for the Clemson Steering Simulator. That research project investigated autonomous directional vehicle control and human-machine interface design and control issues. The simulator hardware and software, as well as the laboratory have been through three generations of refinement. This chapter reviews the hardware and software evolution of the steering simulator over these three generations which occurred between a 2001 and 2009 time period.

2.1 First Generation Steering Simulator

The first generation of the Clemson University Steering Simulator featured all steering and driving components packaged together into a vehicle cockpit to offer a first step of realism for the driver. Prior to the first generation, independent systems were developed as a result of the HIG with stand alone steering wheel and a rack and pinion hydraulic assembly mounted on a test stand with projected image (refer to Figure 2.1). Although functional, the components did not create a realistic environment nor did they support any type of human subject testing. A need existed

to migrate to a cab-type driving simulator with standard driver inputs and visual display.

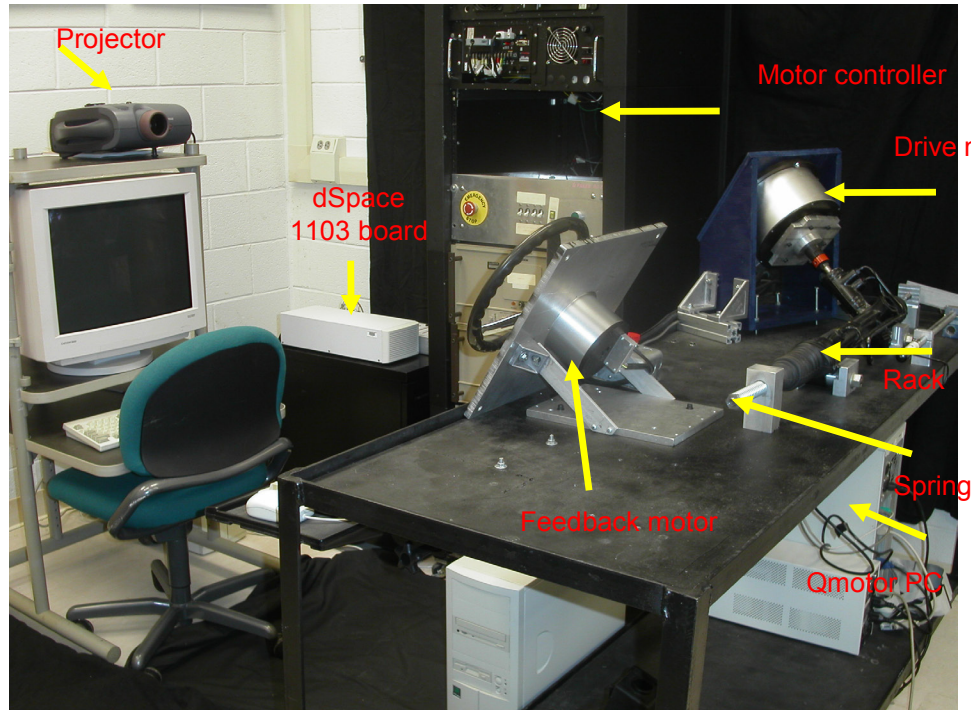


Figure 2.1: Honda Initiation Grant (HIG) stand alone steering simulator bench with hydraulic rack and pinion assembly

Cab/Driver Interface

The front half of a 2002 Honda CRV vehicle body (measuring 2,000mm length \times 1,782mm width \times 1,682mm height) formed the primary structure of the simulator (refer to Figure 2.2). The steering shaft was removed and replaced with a motor-torque sensor system at the steering wheel connection. This cab was one of the few pieces that survived through all three generations. The vehicle was delivered by Honda R&D America, Inc. (Raymond, Ohio) as a full working automobile and carefully stripped down to satisfy the simulator requirements. The engine and

transmission were removed and the back half of the vehicle was cut off to save space and allow positioning in the laboratory. In the first generation, the pedals were non-functional and the simulator ran at a fixed longitudinal velocity, v_x . The only input from the driver was through the steering wheel. The vehicle cab was placed in front of a single projector screen with a projector mounted directly above for environment visualization. The entire package was surrounded by black curtains to avoid peripheral distractions.



Figure 2.2: First generation driving simulator cab with fixed base and privacy curtain to isolate human subject

Hardware

The two primary hardware components of the first generation simulator were the servo-motor attached to the steering wheel (refer to Figure 2.3) and the

accompanying computer controller board. The motor was a direct drive NSK Megatorque Motor System with a built in resolver. It had a maximum torque output of 9.8 Nm and continuous torque output of 6.8 Nm. The motor drive was used in torque control mode. The controller board was a dSPACE 1103 rapid control prototyping board. The board allows the vehicle model to run in real-time while interfacing with the motor and resolver. The dSPACE 1103 board has the following specifications: (i) PowerPC 750 GX 1GHz processor; (ii) 32MB local RAM and 96MB Global RAM; (iii) 20 analog inputs; (iv) 8 analog outputs; (v) 32 digital I/Os; and (vi) 6 digital incremental encoder inputs.

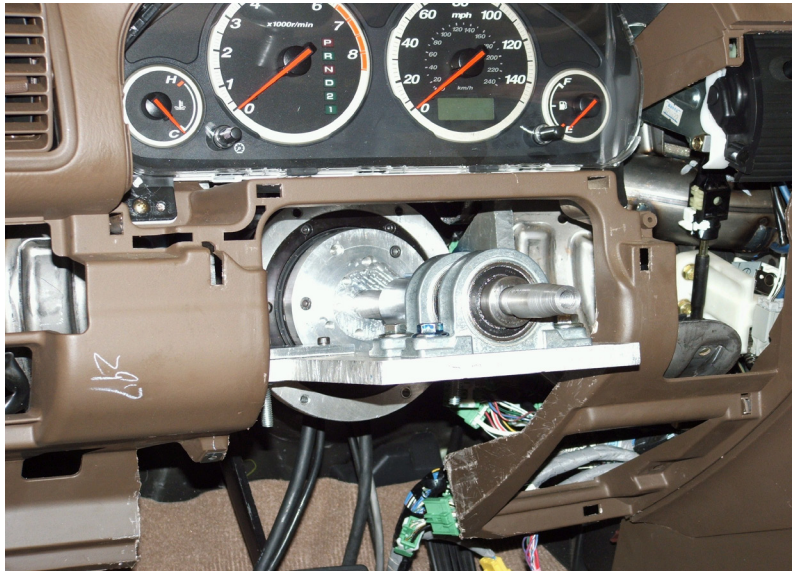


Figure 2.3: First generation steering servo-motor with steering stub shaft mounted below dashboard gauges

Vehicle Model

Initially, a Matlab/Simulink based eight degree-of-freedom vehicle model was used to simulate the vehicle dynamics (Xia, 1990). The vehicle model was strictly for handling (lateral dynamics) without a powertrain (engine, transmission) or brakes. The model was coded in Matlab and uploaded to the dSPACE controller board for interfacing with the automotive hardware. From there, the simulation was controlled from within ControlDesk, the dSPACE interfacing software.

The initial steering model featured three virtual components (spring, damper, and lateral force scaling) that could be independently turned on or off. The spring and damper were directly dependent on the angular position, θ_{sw} , and velocity, $\dot{\theta}_{sw}$, of the steering wheel. In contrast, the lateral force was proportional to the lateral force of the left and right front tires calculated by the vehicle model, F_{yl} and F_{yr} respectively. The combination of the three components created a simple estimation of the torque observed at the steering wheel, τ_{sw} , given by

$$\tau_{sw} = C_1 \theta_{sw} + C_2 \dot{\theta}_{sw} + C_3 (F_{yl} + F_{yr}) \quad (2.1)$$

where C_1 , C_2 , and C_3 were the spring, damping, and lateral force coefficients that were used to tune the steering feedback.

Virtual Environments

The driving environment was animated using MotionDesk. MotionDesk is the scene animation software that works directly with ControlDesk and the dSPACE controller board. The road profile was built piece-by-piece in a fashion similar to a train set with individual track pieces. Due to software limitations, the road had no elevation changes. Without speed control, complicated terrain was unnecessary. The driving environment from the first generation has been displayed in Figure 2.4.



Figure 2.4: First generation driving environment with authentic vehicle cabin and single projected view

2.2 Second Generation Steering Simulator

The key upgrade of the second generation steering simulator (refer to Figure 2.5) was the enhanced vehicle and steering dynamics. The previous mathematical

chassis and steering models were simple and lacked the accuracy necessary for a realistic driving experience. Consequently, steps were taken to improve and validate new automotive models while allowing for real-time modification of the driver steering feedback parameters.



Figure 2.5: Second generation steering simulator with single projected view; operating station relocated behind the vehicle cabin

CarSim Software Package

The handling dynamics of the simulator were initially controlled by an eight degree-of-freedom vehicle model. This model created a generic driving experience;

however, the vehicle response lacked the realism needed to reproduce the desired changes in steering feel. To improve the accuracy of the simulator and subsequent experimental results, this eight degree-of-freedom model was replaced by the commercial software package CarSim. CarSim is a vehicle dynamics simulation package available from Mechanical Simulation Corporation (Ann Arbor, MI). It provides accurate vehicle response simulations faster than real-time. Vehicle parameters are defined within CarSim on a system level. This means that nonlinear kinematics and compliance data can be entered for easy, accurate vehicle descriptions. CarSim meshes seamlessly with Matlab/Simulink to allow for user-defined models and control strategies to supplement or replace the CarSim mathematical models. The CarSim vehicle database used in the steering simulator was validated and supplied by Honda R&D Americas, Inc (Raymond, OH).

Cab Upgrades

The cockpit from the first generation simulator was retained for the second generation simulator. However, many upgrades were added to improve the immersive qualities of the simulator. Possibly the most important upgrade was the addition of driver accelerator and brake pedal potentiometers. With the improved CarSim vehicle model, the driver could now supply brake and throttle inputs similar to actual vehicle operation. This was a tremendous improvement to the overall driving experience for human subjects (both novice and test engineers) and compared favorably with commercial simulations. It was important to give as many sensory

cues as possible to the driver. With this in mind, the door panel speakers were wired to provide vehicle sounds. Furthermore, the dashboard gauges were connected to the dSPACE board and programmed to display engine and vehicle speed to the driver in real-time (refer to Figure 2.6). These two upgrades assisted the driver in finding and maintaining a desired speed on the various driving environments.



Figure 2.6: Working dashboard gauges and lights improve the realism of the environment for test subjects within the vehicle cabin

The final major cab upgrade was the replacement of the steering wheel feedback motor. The first generation resolver had relatively low resolution, which resulted in a grainy steering feeling. It also created limitations when trying to reproduce a friction feel in the steering wheel. The new motor, shown in Figure 2.7, created an instant improvement in steering feel with crisp, realistic friction and damping characteristics. A Danaher Motion AKM53K – ANCNR 00 was selected

which was powered by 240 VAC and provided 11.6 Nm of continuous stall torque. It was controlled by a Servostar S300 in torque control mode.

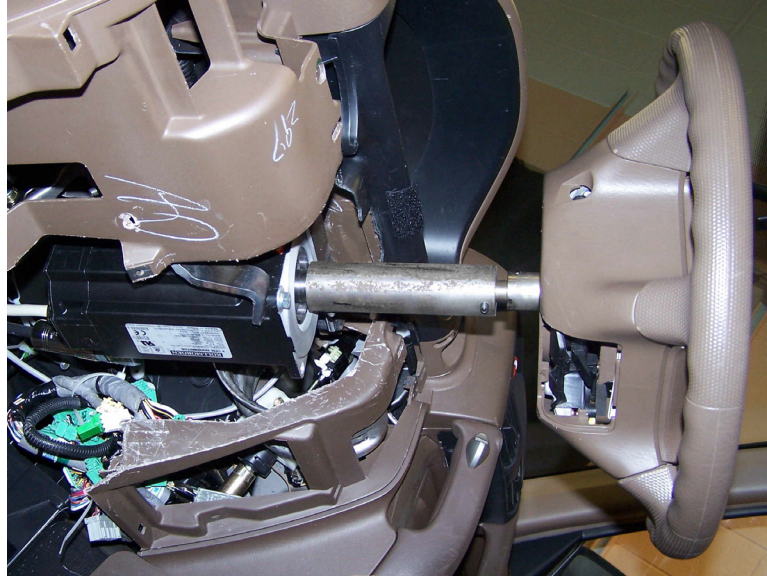


Figure 2.7: Full assembly of new steering motor mounted in dashboard with support points attached to banana brackets

Virtual Environment

With the introduction of the CarSim software package, the simulator now featured a quality scene rendering tool. Through CarSim and its accompanying animation program, “Surfanim”, custom driving environments could be generated. This was a big step in creating a realistic driving experience. CarSim allows the user to enter the (x,y,z) coordinates of the center line of the proposed road as well as add terrain, trees, pylons, and houses using a graphical user interface (GUI). Simply put, Surfanim interfaces with CarSim to render the scene in real-time based on the vehicle's coordinates.

Four driving environments were created and/or applied in the simulator for steering evaluations. These were generically classified as: city, country, highway, and proving ground. The city environment was a simple flat grid populated with houses and stop signs. It was designed to evaluate the key factors in an intersection mode (e.g., primarily high steering angles and low speed). The country environment was a hilly winding road designed to capture the fun-to-drive aspects of the steering along with directional control. The highway environment had smooth turns and occasional pylons to force drivers to change lanes, which helped evaluate the ease of control at high speeds. The proving ground had a high speed oval, a large flat paved area, and a connected race track.

Steering Feel Validation

The steering wheel torque dynamics were based on a reduced order four degree-of-freedom mass, spring, damper, and friction model. This model represented an improvement over the simple feedback model of Section 2.1. The distributed physical mass (inertia) within the model included the steering wheel, steering shaft, steering rack, and wheel/tire assembly. Tire vertical forces, F_z , lateral forces, F_y , and aligning moments, M_z , were calculated in real-time by CarSim and supplied to the steering model. These force and moment magnitudes were mapped into steering moments using the kingpin inclination angle, λ , caster angle, ν , and lateral offset

of the steering axis, d_s , using Gillespie's (1992) steering equations. The expression for the steering moment as a result of the vertical forces on the tires is given by

$$M_V = -(F_{zl} + F_{zr})d_s \sin \lambda \sin \delta + (F_{zl} - F_{zr})d_s \sin \nu \cos \delta \quad (2.2)$$

where δ denotes the steering angle at the front tires, and F_{zl} and F_{zr} are the vertical forces acting on the left and right front tires, respectively.

The expression for the steering moment as a result of the lateral forces on the tires is

$$M_L = (F_{yl} + F_{yr})r_w \tan \nu \quad (2.3)$$

where F_{yl} and F_{yr} are the lateral forces acting on the left and right front tires, respectively. The variable r_w denotes the radius of the front tires. The third component of the steering moment is a direct result of the left and right aligning moments on the front tires, M_{zl} and M_{zr} , which may be formulated as

$$M_{AT} = (M_{zl} + M_{zr}) \cos \sqrt{\lambda^2 + \nu^2} \quad (2.4)$$

The three moments were combined into one steering torque as

$$\tau_{fb} = M_V + M_L + M_{AT} \quad (2.5)$$

The steering moment, τ_{fb} , was then fed into the four degree-of-freedom model given by Mandhata *et al.* (2004) in equation (2.10) to generate the steering wheel torque, $M_{sw} = I_{sw} \ddot{\theta}_{sw}$. Steering torque assistance was modeled as a tunable power function

with respect to the torsion bar twist angle, θ_{tbar} (refer to equation (2.9)). This allowed the assist boost curve to be set to replicate most power steering systems.

The steering system model structure was comprised of four differential equations. The input to the steering system was the driver input torque command, τ_{sw} , resulting in the angular displacement of the steering wheel θ_{sw} , given by

$$\ddot{\theta}_{sw} = \frac{1}{I_{sw}} \left[\tau_{sw} - B_{sc} (\dot{\theta}_{sw} - \dot{\theta}_{sp}) - K_{sc} (\theta_{sw} - \theta_{sp}) - \tau_{fr,sc} \right] \quad (2.6)$$

where θ_{sw} , $\dot{\theta}_{sw}$, $\ddot{\theta}_{sw} \in \mathbb{R}^1$ denote the angular position, velocity, and acceleration, respectively, of the steering wheel, and θ_{sp} , $\dot{\theta}_{sp}$ represent the spool valve angular displacement and velocity. The parameters I_{sw} , B_{sc} , K_{sc} , and $\tau_{fr,sc}$ denote the lumped steering wheel and column inertia, damping, stiffness, and the dry friction, respectively. The steering column and torsion bar stiffness act as two linear springs in series because the spool valve was modeled as an element with negligible inertia.

The angular displacement of the spool valve, θ_{sp} , was a result of the torsion bar windup and may be formulated as

$$\dot{\theta}_{sp} = \dot{\theta}_{sw} + \frac{1}{B_{sc}} \left[K_{sc} (\theta_{sw} - \theta_{sp}) - K_T (\theta_{tbar}) \right] \quad (2.7)$$

where K_T denotes the torsion bar's stiffness and θ_{tbar} its angular displacement. The torsion bar twist also resulted in the transmission of driver input torque to the pinion gear of the rack and pinion system. This pinion torque was transformed into the rack

force that is resisted by the feedback forces from the tire-road interface consisting of the aligning torque and tire-spin inertia.

The governing equation for the rack displacement may be written as

$$\ddot{y}_{rack} = \frac{1}{M_{rack}} \left[\frac{K_T}{R_p} (\theta_{tbar}) - B_{rack} \dot{y}_{rack} - F_{fr,rack} - \frac{2K_L}{N_L} \left(\frac{y_{rack}}{N_L} - \theta_{rw} \right) + F_{boost} \right] \quad (2.8)$$

where y_{rack} is the rack displacement, θ_{rw} is the angular displacement of the front road wheels, and F_{boost} is the power assist force modeled to be dependent on the torsion bar displacement. The parameters K_L and N_L are constants which represent the steering linkage stiffness and ratio of the steering wheel angle to road wheel angle, respectively. The terms M_{rack} , B_{rack} and $F_{fr,rack}$ denote the rack's mass, damping and inherent friction.

The torsion bar twist, which measured the relative displacement between the spool valve and the pinion gear, was given as

$$\theta_{tbar} = \theta_{sp} - \frac{y_{rack}}{R_p} \quad (2.9)$$

where R_p denotes the radius of the pinion gear. Finally, the governing equation of motion for the wheel and linkage assembly was expressed as

$$\ddot{\theta}_{rw} = \frac{1}{I_w} \left[K_L \left(\frac{y_{rack}}{N_L} - \theta_{rw} \right) - B_w \dot{\theta}_{rw} - \tau_{fr,kp} - \tau_{fb} \right] \quad (2.10)$$

where $\tau_{fr,kp}$ and τ_{fb} denote the kingpin friction and aligning torques at the tire-road interface per equation (2.5), respectively. The parameters I_w and B_w represent the lumped inertia and damping of the wheel and linkage assembly.

The primary focus of the simulator was not simply to accurately replicate steering feel, but to be able to adjust this feel in real-time to determine driver preference. This adjustability was aided greatly by the dSPACE ControlDesk software package that allows all variables within the model to be monitored and adjusted during the simulation.

The steering model was validated by tuning the steering feel to match a 2006 Honda CR-V with experimental proving ground (Transportation Research Center, Liberty, Ohio) data provided by Honda R&D Americas, Inc. The goal was to match test results over the operating range to provide the most realistic feel. The system parameters were not strictly held to their real world value as steering feel realism outweighed individual parameter accuracy. To this end, the steering simulator was validated against static holding effort and fixed frequency sinusoidal input. The final tuned parameters are given in Table 2.1.

The holding effort test was performed on a 50m radius circle. This test consisted of steering the vehicle so that it tracked a painted circle while gradually increasing the speed. The steering torque was measured at different speeds while the driver kept the vehicle on the circle. Figure 2.8 shows the simulation and experimental results for steering torque versus lateral acceleration. Note that the

analytical and test points corresponded to within 7% which is acceptable for the steering design studies. As expected, the steering torque increased until the tires reached their saturation point due to the design of the steering system.

Symbol	Value	Units	Symbol	Value	Units
B_{rack}	0.136	$\frac{kg \cdot m}{s}$	K_T	67.8	$N \cdot m$
B_{sc}	1.423	$\frac{kg \cdot m^2}{s}$	M_{rack}	29.4	kg
B_w	900	$\frac{kg \cdot m^2}{s}$	N_L	0.118	m
d_s	0.063	m	r_w	0.341	m
$F_{fr,rack}$	44.5	N	R_p	7.37E-3	m
I_{sw}	6.78E-5	$kg \cdot m^2$	λ	0.232	rad
I_w	1.356	$kg \cdot m^2$	ν	0.037	rad
K_L	48.8E-3	$N \cdot m$	$\tau_{fr,sc}$	0.6	$N \cdot m$
K_{sc}	33.9	$N \cdot m$	$\tau_{fr,kp}$	80	$N \cdot m$

Table 2.1: Tuned parameters in steering model to create accurate replication of steering torque for a 2006 Honda CR-V

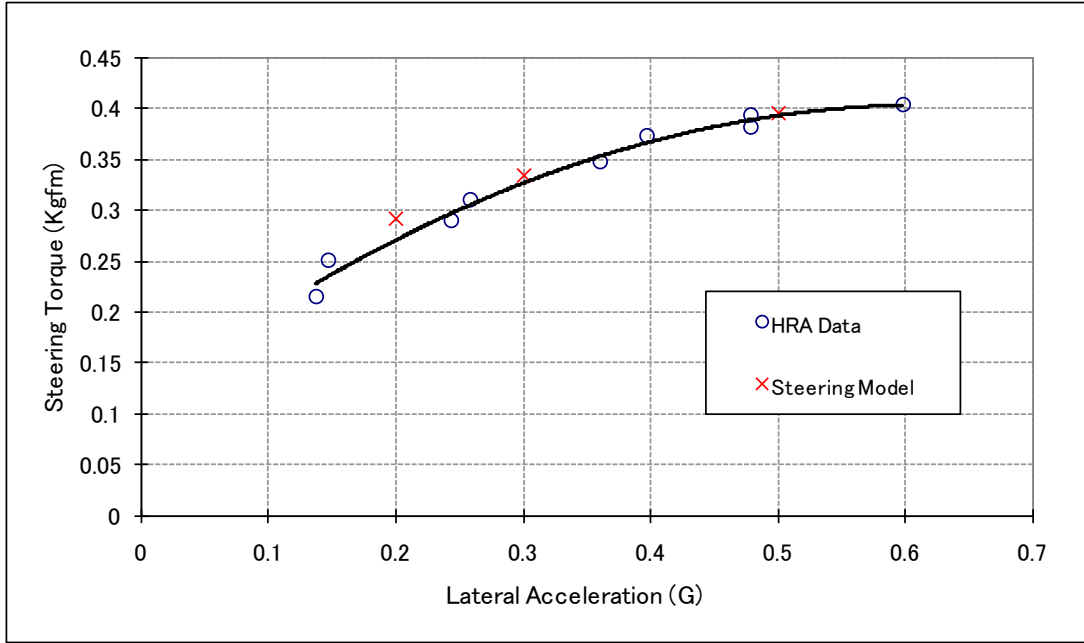


Figure 2.8: Comparison of the simulation and experimental results from the holding effort test

The slalom test employed a fixed frequency sinusoidal input at a constant speed, $\delta_{sw} = A \sin \omega t$ with $\omega = 2\pi f$. Figures 2.9 and 2.10 display the simulation and experimental results from the fixed frequency sinusoidal input test, where the y-axis measures the steering wheel torque. Steering wheel excitations of $f = 0.25\text{Hz}$, 0.50Hz , and 1.00Hz were used with amplitudes of $A = 20^\circ$ or 25° depending on test. The tests were performed at $v_x = 60\text{kph}$ and 120kph . This test highlights the gain and hysteresis of the steering torque in the typical operating range. The simulation model showed excellent correlation to the experimental results over the conventional operating range. The small nuances of the angle-effort dynamics (i.e., steering wheel rotational angle versus measured torque at the steering wheel) were successfully captured. The hysteresis bulged through center at the 60kph while tightening to a

more “S-like” shape at 120kph. At the highest speed and steering frequency, the model lost accuracy, most likely due to the tire model within CarSim. However, this combination of speed and frequency is only encountered during evasive maneuvers, so the discrepancy was deemed acceptable.

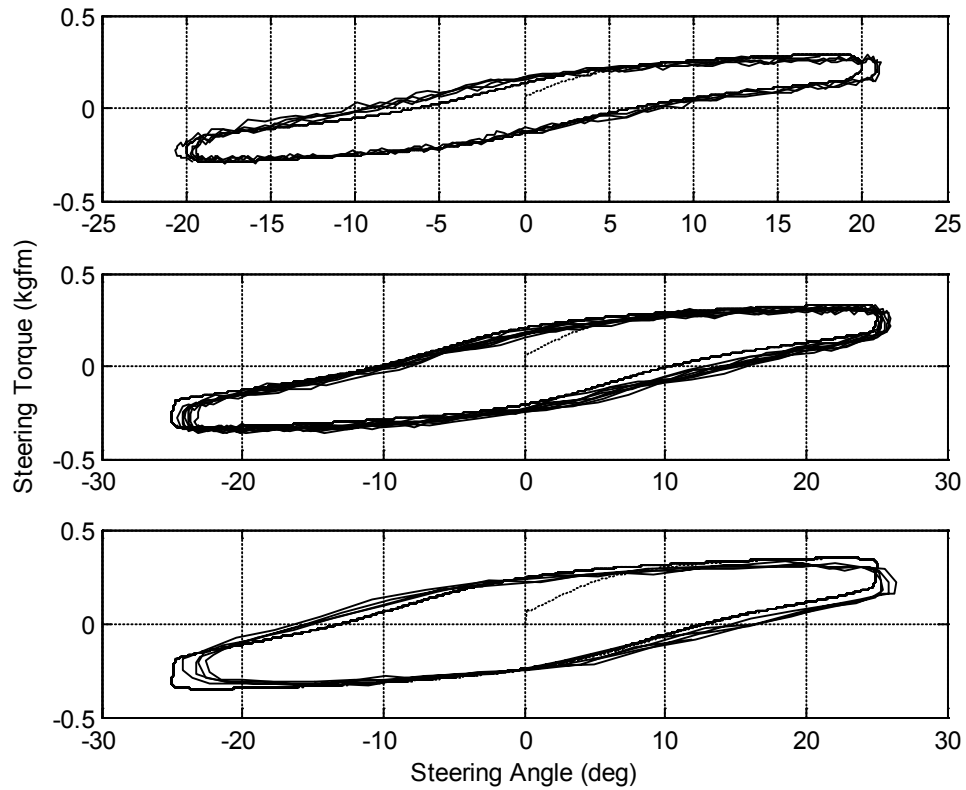


Figure 2.9: Comparison of the simulation and experimental data from fixed frequency sinusoidal input (0.25, 0.50, 1.0 Hz) test at 60 kph. The solid line is the test data while the dotted line is the result of the simulation

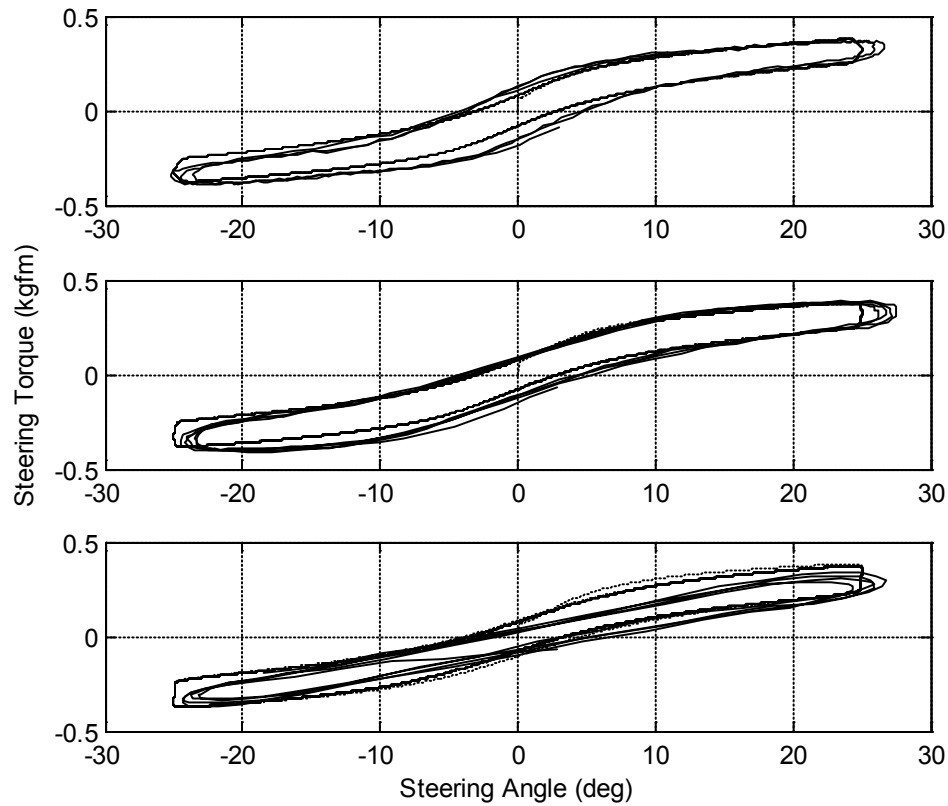


Figure 2.10: Comparison of the simulation and experimental data from fixed frequency sinusoidal input (0.25, 0.50, 1.0 Hz) test at 120 kph. The solid line is the test data while the dotted line is the result of the simulation.

2.3 Third Generation (Current) Steering Simulator

The third generation of the Clemson University Steering Simulator offered greater realism in driver immersion for a better driving experience. A series of non-steering upgrades were introduced. The upgrades were focused on improving the driving experience as a whole to eliminate distractions that might contaminate the steering evaluation. Regardless of how accurate the steering feedback, human subjects must believe that they are truly driving an automobile to give an accurate

judgment about their steering preference. Cues that remind subjects that they are driving a simulator have the potential to ruin the perception of the steering feedback.

Motion Base

Prior to the third generation, the Clemson University Steering Simulator had a fixed (no motion) base. This means that the driver did not experience any motion (longitudinal, lateral, vertical, yaw, roll, pitch) of the vehicle cab while driving. A primary concern with the simulator was braking realism. Stopping distances were difficult to judge with only visual feedback; full stopping force was often used when it was not necessary. Braking realism does not seem important in a steering simulator at first, but this one area would remind drivers that they were in a simulator and taint the steering evaluation. With the addition of pitch feedback, drivers could better judge their decelerations and their perceived realism improved.

The IDEAS (Interactive Driver Evaluation & Assessment Systems) Company (Oceanside, CA) creates custom driving simulators for training and classroom use. They fabricated and installed a custom motion base for the Honda CR-V half-cab (refer to Figure 2.11). The motion base contained a curved track that the simulator rode on while an electric motor moves the cab forward or backwards. The curved track turned the longitudinal motion into a pitching sensation similar to the pitch a driver experiences while accelerating and decelerating in an automobile. With the motion base activated, drivers could sense the acceleration of the vehicle through the

pitching motion, allowing for more accurate braking when approaching an intersection.

The motion base was designed to give 6° of travel along the curved track. It accomplished this using a DC motor and a set of powerful springs that balanced the vehicle in the center of the track. By balancing the vehicle, the power required by the motor was greatly reduced since it did not need to overcome the weight of the vehicle cabin. However, the cabin weight was still a limitation. Despite the suspension and subframe being removed from the vehicle, the cabin weighed enough to add a noticeable delay (300-500ms) in the motion base response. This delay necessitated that the motion base be tuned to only provide small motions that would be triggered during the largest accelerations. By doing this, the motion base added a realistic feedback channel to the driver without becoming a distraction. Figure 2.12 displays two images of the motion base control box outer panel and enclosed electronic components. The outside of the box contains an emergency stop button since the motion base was the most dangerous component to both the participants and itself. The amplifier located at the interior top of the box controlled the power to the motor using position feedback from a potentiometer.

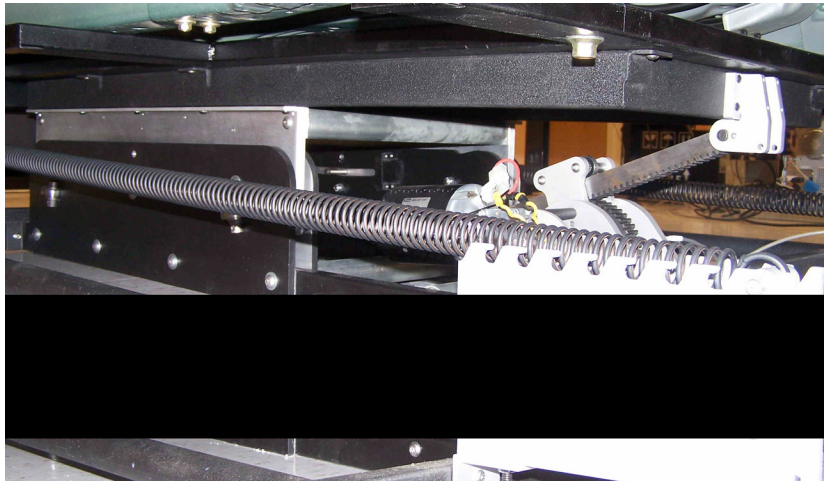


Figure 2.11: Longitudinal motion base installed beneath simulator cab with tensioning springs to keep cab balanced



Figure 2.12: Motion control box with (a) emergency stop and (b) amplifier to control the position of the motion base

Three Screen Projection System

A single projected view was used through the first two generations of the steering simulator which provided a horizontal field of view of approximately 40 degrees. While adequate for a simple driving experience, the lack of peripheral views gave a lower sense of speed and made it difficult to navigate tight turns common at intersections. The visual display was upgraded to three projected screens (refer to

Figure 2.13), increasing the field of view to 120 degrees. This required a custom animator upgrade to ensure all the screens were synchronized on a dedicated graphics computer with a dual output video card.



Figure 2.13: Three screen projection with 120 degree field of view for the driver in vehicle cabin

Three ultra short throw projectors (NEC WT610E) allowed a ground mounting solution and avoided the complex ceiling location with mounting difficulties. These projectors improved the portability of the simulator. However, the primary drawback of ultra short throw projectors is that screen irregularities are magnified due to the sharp projection angle. The sense of vehicle speed and navigational ability were immediately improved upon installation of the three screens. Beyond these intended effects, the sensation of the vehicle dynamics also improved greatly. A wider field of view allowed the driver to have a greater feel for the

direction of the velocity vector with respect to the vehicle's orientation. This was especially evident in a lateral vehicle slide when the driver could look into the direction of travel even though the view was not oriented to match. This unintended effect improves the value of the simulator as a "limit" (i.e., high lateral acceleration) evaluation tool.

Brake Feel

The final upgrade in the third generation of the simulator was the improvement of brake pedal feel. Prior to this generation, a hybrid spring and partially bled brake system created resistance while pressing the brake pedal. The system provided a usable pedal feel, but it lacked consistency and did not offer the smooth damped feeling of a power assist brake system. An improvement was sought with small dampers, but a suitable feeling could not be created. Instead, a solution was devised to use the Honda factory brake booster system in conjunction with the fully operational base brake system.

The brake lines were connected to the two front calipers with rotors still present. The rear brake lines were plugged, and the brake system was bled to make the front brakes fully operational. An external 110 VAC vacuum pump was connected to the brake booster to supply the vacuum typically created by the engine. This solution offered the driver the proper force buildup when depressing the brake pedal. However, the only drawback was the vacuum pump sound level which could

be potentially distracting to the driver. A quieter pump is recommended to ensure that the brake system does not interfere with the overall driving experience.

System Integration

The integration of the system hardware, software, and external peripherals has been shown in Figure 2.14. The primary interaction was between the command center PC and the dSPACE 1103 processor board. While operating, the dSPACE board handled all vehicle dynamics calculations, which freed the command center PC to handle one of the animation screens. The other two animation screens were handled by the image generating PC with data sent from the command center PC using TCP/IP. The steering model was implemented in Matlab/Simulink in such a way to allow all steering parameters to be changed in real time through the dSPACE software, ControlDesk. ControlDesk was used to interface between the command center PC and the dSPACE board, and this software handled run control, data monitoring, and variable changes. Finally, the dSPACE board controlled all hardware inputs and outputs with physical wiring to the interface panel, allowing the driver to interact with the vehicle and steering models.

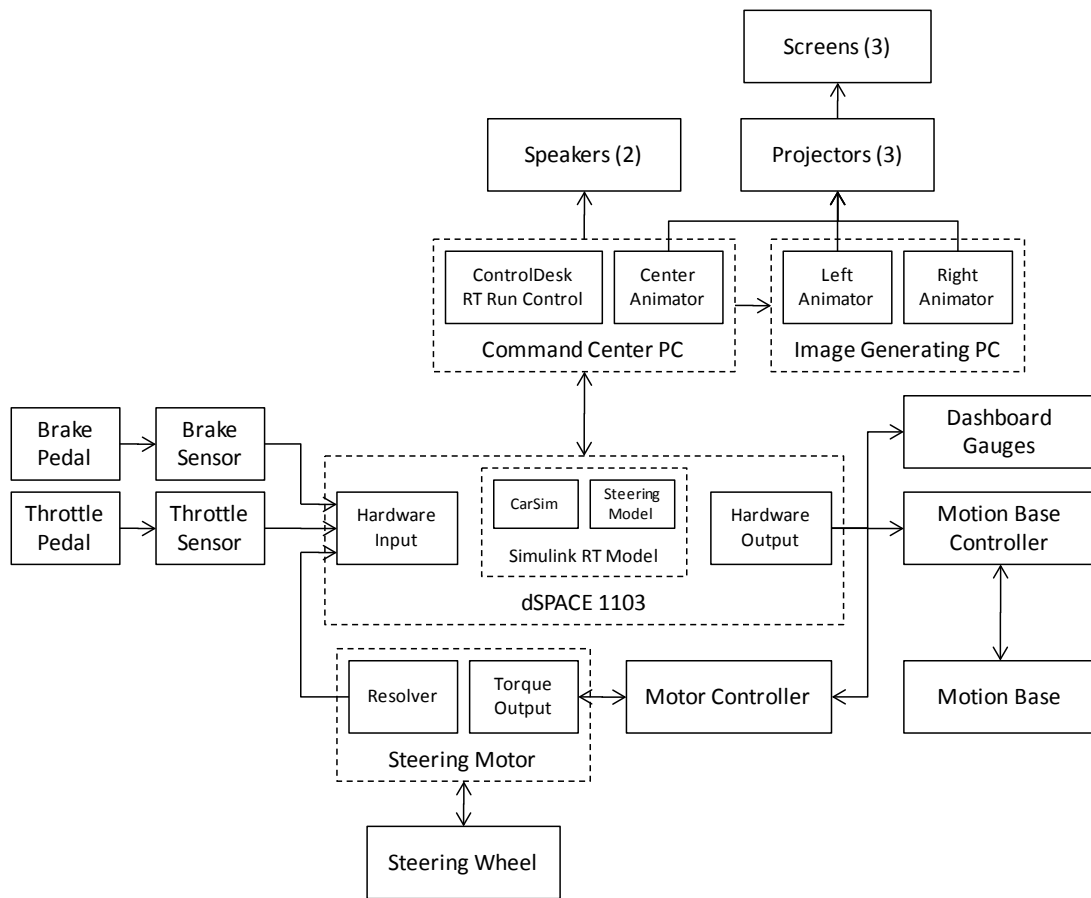


Figure 2.14: Schematic of the steering simulator showing the interaction of inputs and outputs with the dSPACE 1103 processor board and support computers

CHAPTER THREE

DRIVER PREFERENCE STUDIES

The Clemson steering simulator was designed and fabricated to replicate the “feel” of automotive steering subsystems. Alone, the automotive hardware-in-the-loop tool was a good engineering exercise and a fun endeavor, but it needed to add value to the overall vehicle development process. A series of human subject based psychology tests were performed to validate and initially apply the simulator as an engineering tool for investigating driver steering preferences. There were three questions to be answered during the study: (1) Can drivers sense different steering settings and show a preference? (2) Do preferences change depending on the driving scenario? (3) Does the driver demographic influence steering preference? The three questions were evaluated through three rounds of human subject tests conducted at Clemson University which have been denoted as Pilot Study 1, Pilot Study 2, and Demographics Study. In this chapter, the methodology and results from the three studies will be presented and discussed to answer the posed questions. In addition, a forecast on ground vehicle steering system technology evolution will be stated based on these findings.

3.1 Pilot Studies 1 and 2

Two pilot studies were performed with the steering simulator as it entered its second generation of integrated hardware and software (refer to Section 2.2). As

stated previously, there were three questions to be answered during the validation studies. The pilot studies approached the first two questions: (1) Can drivers sense different steering settings and show a preference, and (2) Do preferences change depending on the driving scenario? Two separate human subject studies were performed to answer these questions; a comprehensive plan was submitted and approved by the Clemson University Institutional Review Board (IRB). The only change made between studies was the virtual driving environment; the first study used combined country and residential roads, while the second study utilized a highway. This approach allowed the second question to be answered by comparing the results from the two pilot studies.

Pilot Study 1 Procedure

The first pilot study was a low ($0 < v_x < 40kph$) to medium ($40 \leq v_x < 70kph$) speed steering preference study. Eleven ($n=11$) participants each drove six steering configurations, C1-C6, that varied both the steering ratio and torque scaling. After each run, the driver filled out a questionnaire to determine his/her preference for the given steering configuration (refer to Appendix A). The driving environment was a hybrid roadway with access to a winding country road and residential area as shown in Figure 3.1. The country road, R2, contained modest elevation changes and blind corners to force the drivers to react instinctively. This road exposed both the on-center, $|\theta_{sw}| < 20^\circ$, and off-center, $|\theta_{sw}| > 20^\circ$, characteristics of the steering system at

medium speeds ($40 \leq v_x < 70 \text{ kph}$). The residential zone, R1, was a simple grid layout with 4-way stops at all intersections and houses scattered throughout. The low speed ($0 < v_x < 40 \text{ kph}$) off-center steering characteristics and returnability should be revealed during this section of the road.

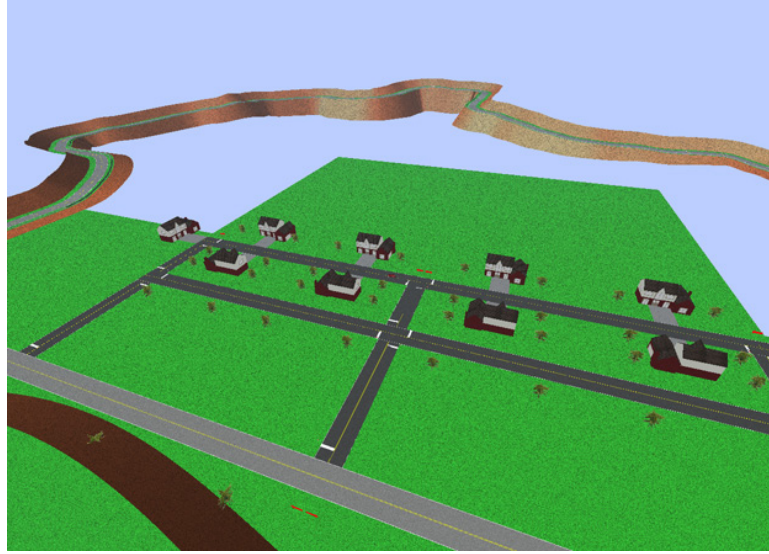


Figure 3.1: Winding country road and residential driving environment (R2 and R1) used for the first pilot study

The six steering configurations, C1-C6, used in the first pilot study have been listed in Table 3.1. The baseline configuration, C1, was the replicated real world steering feel of the 2006 Honda CR-V production vehicle validated in Section 2.2. The baseline configuration was scaled up and down by approximately 20% in both the steering ratio and torque output to create four more configurations, C2-C5. The steering ratio corresponds to the relationship between steering wheel rotation, δ_{sw} , and road wheel angle, δ . The steering torque is the direct scaling of the target torque of the steering wheel servomotor. The final configuration, C6, was a variable gain

steering (VGS) ratio configuration in which a VGS algorithm adjusted the steering ratio in real-time to keep the yaw gain constant at all vehicle speeds. The yaw gain is the ratio of the yaw rate to the steering wheel input, $\dot{\psi} : \delta_{sw}$. If the steering ratio is adjusted to keep the yaw gain constant, then the response of the vehicle could potentially become more predictable to the driver.

Configuration	Description
C1	Honda CRV Baseline (18:1 Steering Ratio)
C2	15:1 Steering Ratio
C3	22.5:1 Steering Ratio
C4	20% Heavier Steering Torque
C5	20% Lighter Steering Torque
C6	Variable Gain Steering (VGS) Ratio

Table 3.1: Pilot study vehicle steering configurations with variations in steering ratio and steering torque

The study participants were asked to drive both sections (winding country road, residential) of the road course until they were comfortable answering the questionnaire. This ensured that the drivers had sufficient time to familiarize themselves with both the simulator and the virtual environment. Although this helped the reliability of the results, the participants were prone to drive for extended periods of time if not given a fixed run interval. Due to the small sample size of the dual pilot studies and the minimal number of steering configurations, extended drive times did not pose a problem.

Pilot Study 1 Test Results

The collected survey data (refer to Appendix B) was analyzed by considering the mean response of all drivers ($n=11$ test subjects) for a given steering configuration setting. The questions were divided into categories (Global $\{1,2,...,16\}$, Fun $XX = \{8\}$, Control $YY = \{1,3,5,7,11,16\}$, Ease $ZZ = \{2,6,10,14,15\}$, Safety $VV = \{4,9,12,13\}$) and analyzed together. In Figures 3.2 through 3.6, the graphs depict the mean values of the evaluated categories against the respective configurations. The survey questions were answered on a scale of 1 to 7, with 7 being the best (strongly agree) and 1 assigned as the worst (strongly disagree). In other words, the plots show the mean response for each steering configuration.

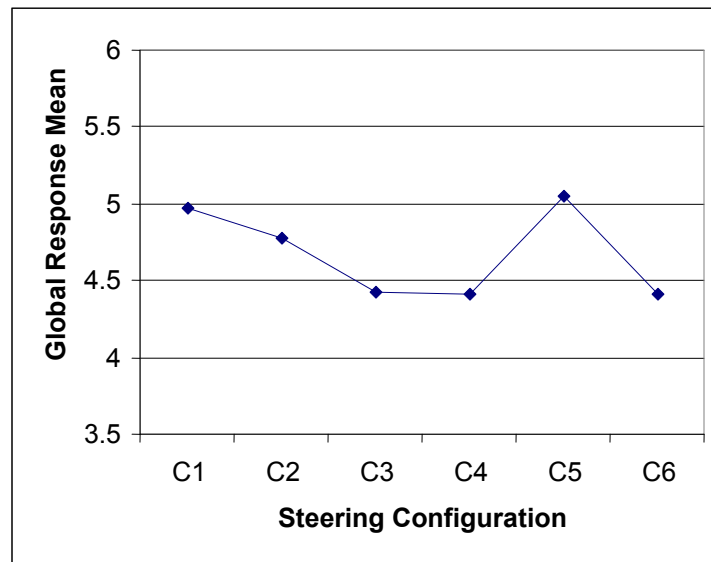


Figure 3.2: Pilot study 1 “global” steering configuration preference calculated as mean response from questionnaire

The global means, μ_{global} , were calculated using all (m=16) questions from the survey given by

$$\mu_{global_k} = \frac{1}{nm} \sum_{j=1}^{m=16} \sum_{i=1}^{n=11} q_j(i) \text{ for } (C_k = 1, 2, \dots, 6) \quad (3.1)$$

where n is the number of participants, m is the number of questions represented in the respective question category, q is the question answer using the 1-7 scale, and C_j is the steering configuration. Configuration C1 and C5 appear to be the overall favored scenarios as shown in Figure 3.2. This was acceptable because C1 was the baseline factory steering setting, and C5 required less steering torque (only 80% driver effort required compared to baseline) allowing the tighter turns of the country and residential roads to be easily navigated. However, a global view of the data may be insufficient to properly evaluate the steering configurations and make any firm conclusions. To ensure a thorough analysis, the data was analyzed with respect to each question sub-category (Fun, Control, Ease, and Safety).

While configuration C5 was slightly favored in the global view, it is clear from Figure 3.3 that configuration C1 was considered to be the most fun to drive. The fun sub-category, μ_{fun} , was formulated as

$$\mu_{fun_k} = \frac{1}{nm} \sum_{j=1}^{m=1} \sum_{i=1}^{n=11} q_{XX_j}(i) \text{ for } (C_k = 1, 2, \dots, 6) \quad (3.2)$$

where XX is the subset of questions related to the fun aspects of the steering configuration defined previously. This is more telling about the lighter steering effort

of configuration C5 in that it is less fun to drive, even if drivers may favor it overall. The factory configuration was most favored which offers a compromise in the steering ratio and torque. This begs the question: what aspects of configuration C5 did drivers prefer from a global perspective?

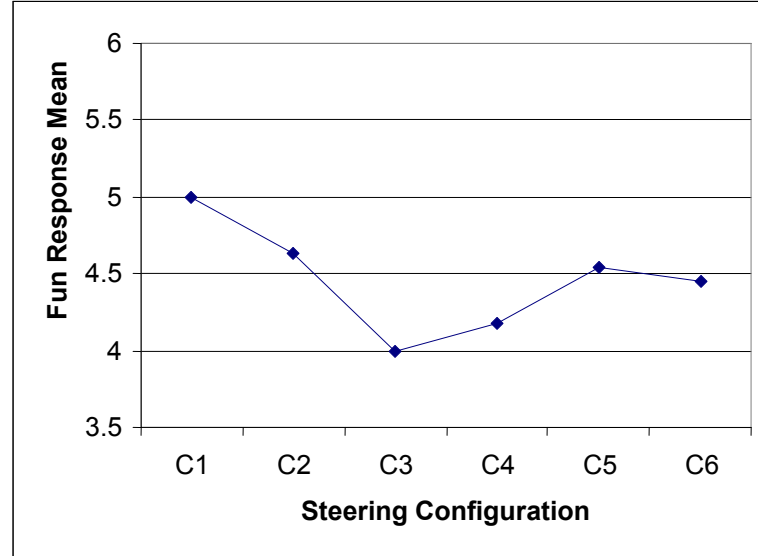


Figure 3.3: Pilot study 1 “fun” steering configuration preference calculated as mean response from questionnaire

As shown in Figure 3.4, configuration C5 ranked the highest in control, $\mu_{control}$, amongst the tested configurations by a significant margin. The control sub-category was calculated as

$$\mu_{control_k} = \frac{1}{nm} \sum_{j=1}^{m=6} \sum_{i=1}^{n=11} q_{YY_j}(i) \text{ for } (C_k = 1, 2, \dots, 6) \quad (3.3)$$

where YY is the subset of questions related to the control aspects of the steering configuration defined previously. This offers some insight into the basis for configuration C5 (lighter steering effort) demonstrating perceived strength in the

global result. The result was acceptable because the lighter steering effort may allow for crisp steering inputs while navigating the tight turns of the country and residential environments.

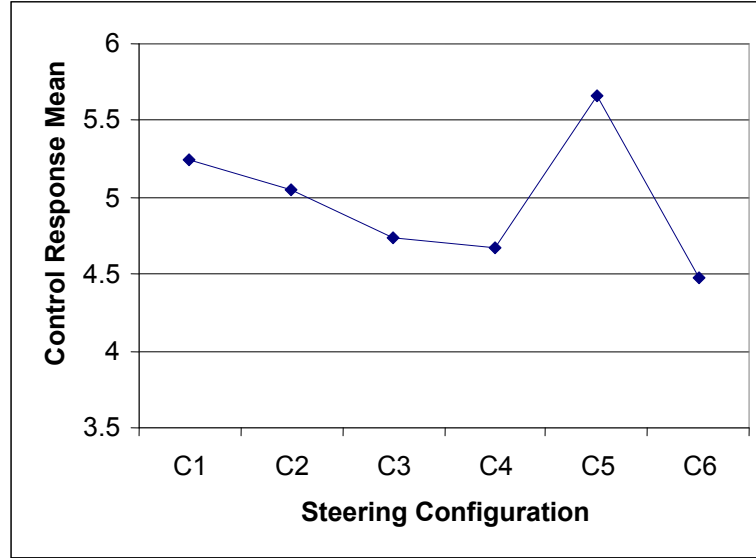


Figure 3.4: Pilot study 1 “control” steering configuration preference calculated as mean response from questionnaire

The ease of operation, μ_{ease} , was another criterion for the driving simulator analysis given by

$$\mu_{ease_k} = \frac{1}{nm} \sum_{j=1}^{m=5} \sum_{i=1}^{n=11} q_{ZZ_j}(i) \text{ for } (C_k = 1, 2, \dots, 6) \quad (3.4)$$

where ZZ is the subset of questions related to the ease aspects of the steering configuration defined previously. The analysis shown in Figure 3.5 splits the six configurations in half with configurations C1, C2, and C5 placing higher than configurations C3, C4, and C6. While configurations C1 and C5 may be expected at this point, the strength of C2 (quicker steering ratio) is worthy of discussion. A

quicker steering ratio (15:1, meaning less steering wheel angle required for a given road wheel angle) allows for a smaller steering wheel angular input while achieving the same vehicle response. It is understandable why this configuration may be easier to drive in a residential area. This setting was consistently rated ahead of the remaining three configurations, but always behind the baseline. This suggests that the steering ratio should be biased in this direction (i.e., quicker ratio) since the potential loss in driver preference is reduced.

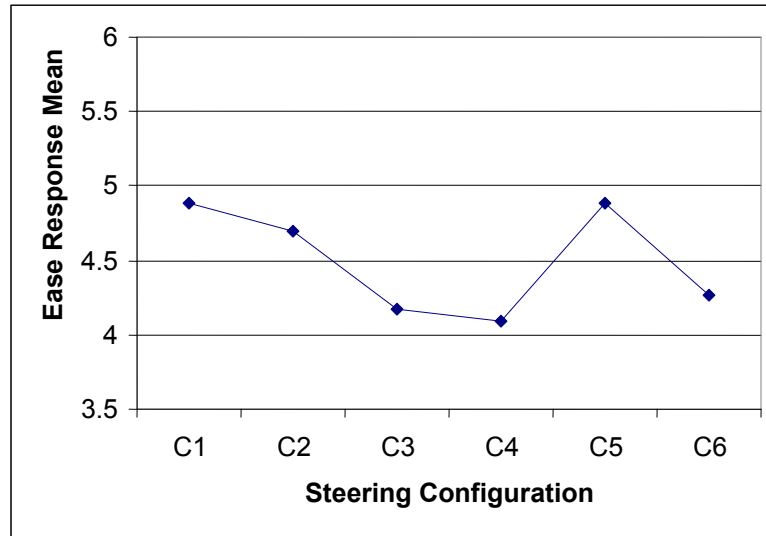


Figure 3.5: Pilot study 1 “ease” steering configuration preference calculated as mean response from questionnaire

Finally, the safety, μ_{safety} , was also used as a set of evaluation questions and may be calculated by

$$\mu_{safety_k} = \frac{1}{nm} \sum_{j=1}^{m=4} \sum_{i=1}^{n=11} q_{VV_j}(i) \text{ for } C_k = 1, 2, \dots, 6 \quad (3.5)$$

where VV is the subset of questions related to the safety aspects of the steering configuration defined previously. Interestingly enough, no significant results could be determined. All of the configurations differed only slightly as shown in Figure 3.6. This implies that the sensation of safety may not be directly connected to the steering system for the country and residential roads.

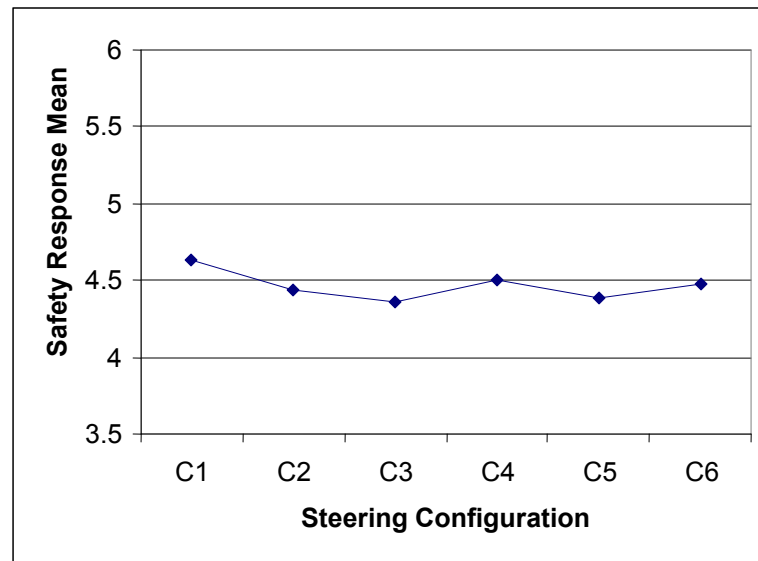


Figure 3.6: Pilot study 1 “safety” steering configuration preference calculated as mean response from questionnaire

A comprehensive summary of the question sub-category results has been illustrated in Table 3.2, which depicts the percent deviation from the mean for each configuration within the five question groupings. To construct the table, the average of all results (C1-C6) in a given question sub-category (Global, Fun, Control, Ease, Safety) was calculated. The percent difference from this average was then calculated for each individual steering configuration. For instance, the average of the Global category was 4.68 (refer to Figure 3.2). The percent difference of configuration C1

was $\frac{4.97 - 4.68}{4.68} = 6.4\%$. A large positive percentage implies that the configuration was favored for the given question grouping. This allows individual steering settings to be analyzed across all question sub-categories at once. Notice how configurations C3, C4, and C6 are below 1% for all question groups. This shows just how disliked these settings were by the human test subjects. The VGS steering setting, C6, was the least liked setting for the “control” question group. The VGS setting was designed specifically to improve the controllability of the vehicle, and this result led to the abandonment of the algorithm. Alternatively, configurations C1 and C5 (shaded) both showed significant positive percentages across most question categories.

	Global	Fun	Control	Ease	Safety
C1	6.4%	11.9%	5.4%	8.5%	3.8%
C2	2.1%	3.7%	1.5%	4.4%	-0.8%
C3	-5.4%	-10.5%	-4.7%	-7.4%	-2.3%
C4	-5.6%	-6.4%	-6.0%	-9.0%	0.8%
C5	8.1%	1.7%	13.8%	8.5%	-1.8%
C6	-5.7%	-0.3%	-10.0%	-5.0%	0.3%

Table 3.2: Pilot study 1 percent deviations of the mean for all scenarios within each question grouping; shading denotes the two most popular steering configurations, C1 and C5

Pilot Study 2 Procedure

The driving environment was changed to a highway layout, R3, for the second pilot study. The highway environment was a long, looped six lane roadway with a concrete median as shown in Figure 3.7. Traffic was not available, but pylons were introduced to force drivers to change lanes. The drivers were allowed to drive as long

as they wished at highway speeds until they were satisfied with their appraisal of the steering system. Nine ($n=9$) participants each drove six steering configurations, filling out a questionnaire after each run.

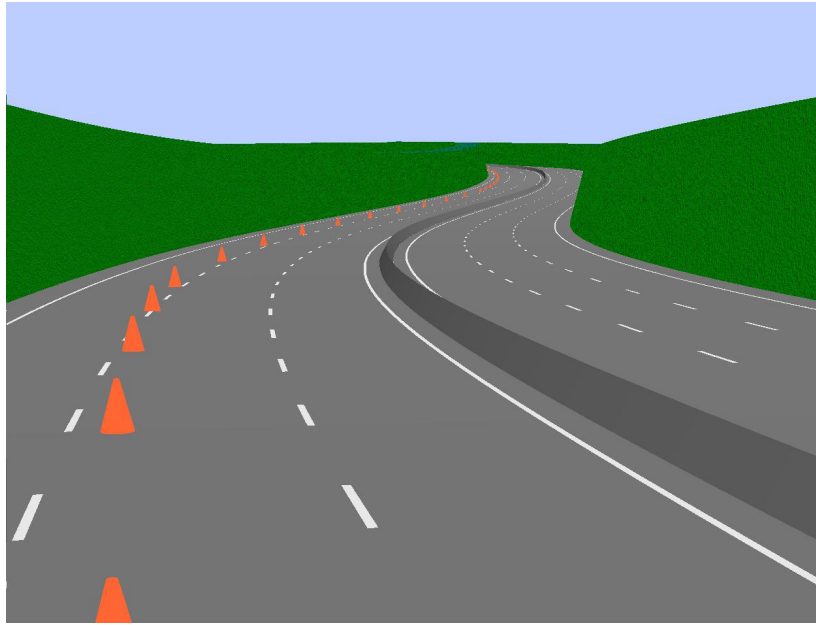


Figure 3.7: Highway driving environment (R3) used for pilot study 2 with pylons to force drivers to change lanes

Pilot Study 2 Test Results

The results of the second pilot study were analyzed in the same way as the first pilot study (refer to Appendix C). The survey questions were again divided into five groups (Global, Fun, Control, Ease, Safety) and the results of each steering configuration were averaged for all drivers per equations (3.1) through (3.5) with $n=9$. Figure 3.8 shows the global results for the second pilot study. A result that stands out from the global design analysis was configuration C4, a heavier steering feel due to larger steering torque requirements. This configuration was one of the

three least favored during the first pilot study per Figure 3.2. Although surprising, this result is understandable since a heavier steering feel may provide stability to aid in lane keeping on a highway. However, the four other question groupings should be analyzed before this result can be confirmed.

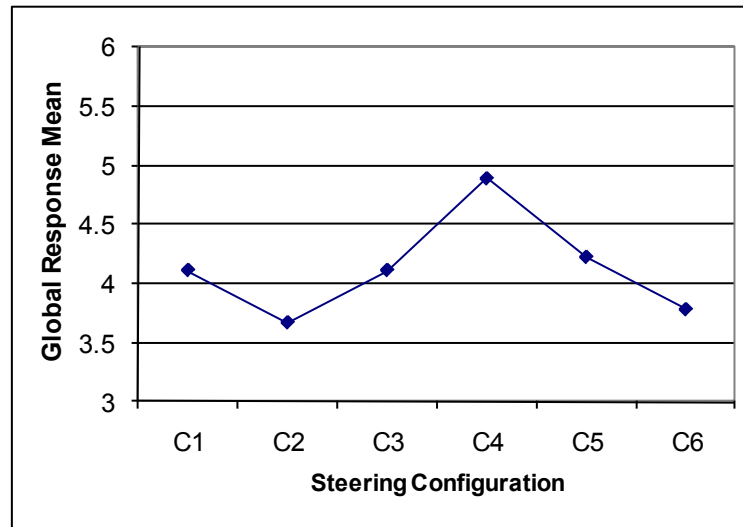


Figure 3.8: Pilot study 2 “global” steering configuration preference calculated as mean response from questionnaire

The Fun question results, shown in Figure 3.9 reveal three features that merit some consideration. A slower steering ratio, C3, and heavier effort, C4, were both preferred with mean values of 4.55 and 4.90, respectively. These were the two least favorites in the first pilot study as shown in Figure 3.3. This continues the trend that drivers may prefer different steering settings on the highway. None-the-less, a common trend may be observed with the VGS results, C6. Across both pilot studies, it was never rated highly with response mean values of 4.48 and 3.45. This may

support the idea that drivers prefer a fixed steering setting that they are familiar with rather than a continually adjusting setting based on the vehicle speed.

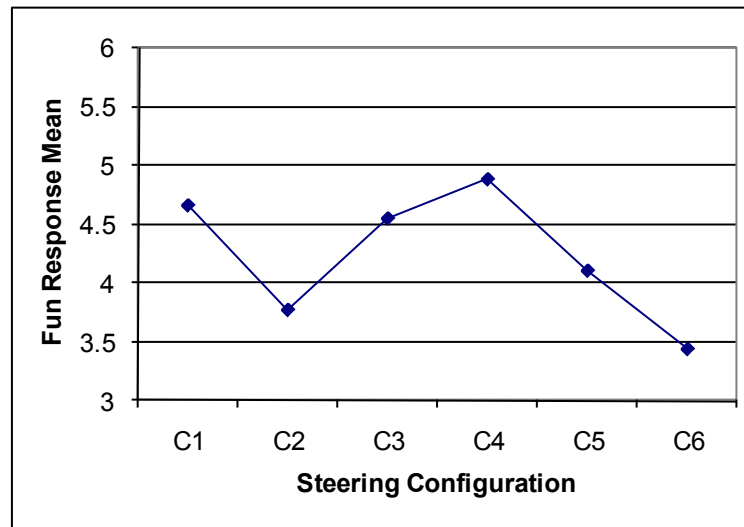


Figure 3.9: Pilot study 2 “fun” steering configuration preference calculated as mean response from questionnaire

Figure 3.10 shows the results for the control questions which pertain to the perceived response of the vehicle to driver commanded steering maneuvers. A heavier steering feeling, C4, offers drivers a better sense of control, while the baseline, C1, once again comes through as a favorite. This confirms the suspicion that a heavier steering torque provides increased stability for lane keeping on highways. This is contrary to pilot study 1 where lighter steering torque, C5, was overwhelmingly preferred in Figure 3.4. Surprisingly, drivers did not distinguish between steering ratio changes based on the similarity in results between

configurations C2 and C3. Again, the variable gain steering, C6, was not highly rated by the test subjects.

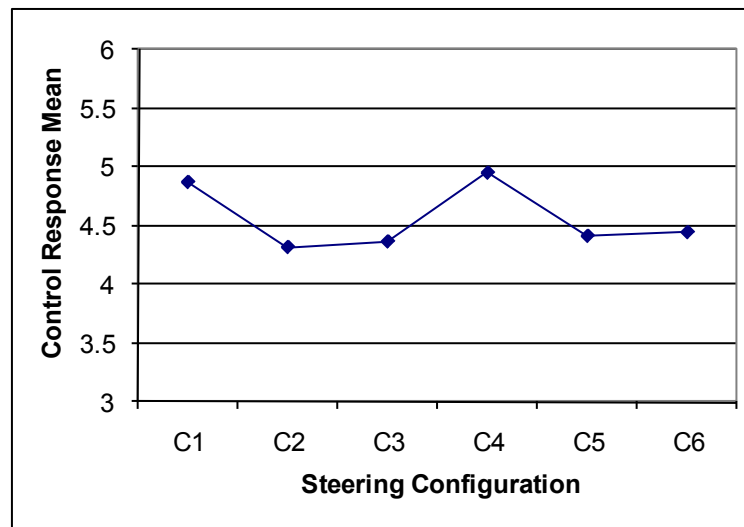


Figure 3.10: Pilot study 2 “control” steering configuration preference calculated as mean response from questionnaire

The ease question results shown in Figure 3.11 were not as decisive as the four other metrics. A stiffer steering feel was preferred, C4, but the second favorite was a lighter steering feel, C5. This likely shows that the drivers were not making clear and consistent judgments about the “ease” of the steering on the highway environment. Specifically, the highway environment was a relatively easy course to begin with, so a combination of traffic and driver distractions should be introduced for an improved “ease” test result.

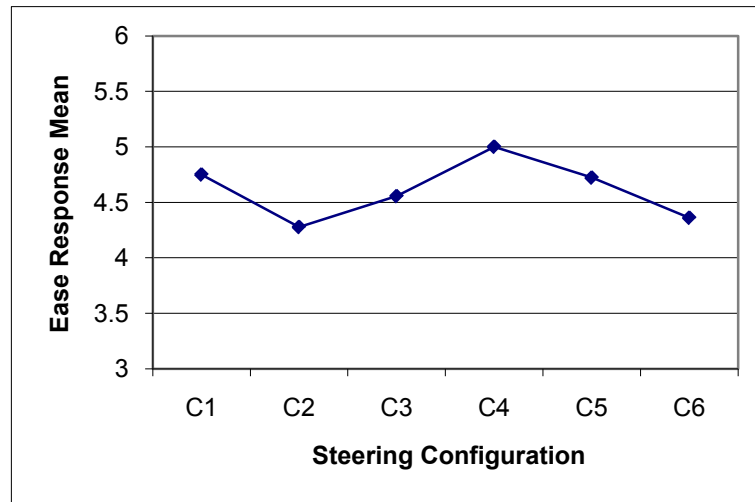


Figure 3.11: Pilot study 2 “ease” steering configuration preference calculated as mean response from questionnaire

Figure 3.12 shows the safety question results for the highway road. Once again, the stiffer (heavier) steering feel, C4, was favored among the test participants and C2 (quicker steering ratio) the least. The safety results were more pronounced than those in pilot study 1 per Figure 3.6, which may support the idea that the higher vehicle operating speeds tap into the fear and survival instincts of the given participant.

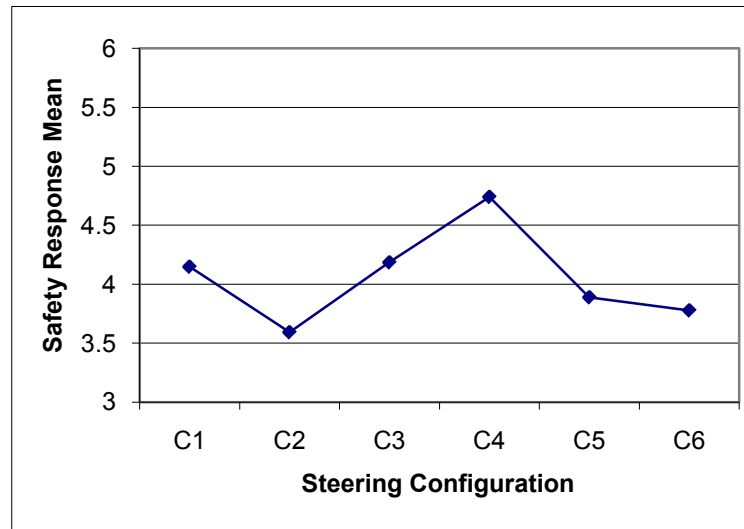


Figure 3.12: Pilot study 2 “safety” steering configuration preference calculated as mean response from questionnaire

Overall, the second pilot study reveals that the configuration C4, heavier steering torque, was the favorite on the highway environment based on Figures 3.8-3.12. The results for the second pilot study have been summarized in Table 3.3, which shows the dramatic bias towards configuration C4 by the test subjects. For instance, this configuration was positively rated for all evaluation categories with overwhelming preference in global, fun, and safety. However, this configuration was one of the least favorites for the country and residential road environment per the first pilot study (refer to Figures 3.2-3.6). This observation confirms that steering preferences change depending on the driving scenario.

	Global	Fun	Control	Ease	Safety
C1	-0.4%	10.0%	6.8%	3.0%	2.3%
C2	-11.2%	-10.9%	-5.3%	-7.2%	-11.4%
C3	-0.4%	7.4%	-4.3%	-1.2%	3.2%
C4	18.4%	15.3%	8.6%	8.4%	16.9%
C5	2.2%	-3.1%	-3.2%	2.4%	-4.1%
C6	-8.5%	-18.8%	-2.6%	-5.4%	-6.8%

Table 3.3: Pilot study 2 percent deviations of the mean for all scenarios within each question grouping; shading denotes the most popular steering configuration, C4

Pilot Study Conclusions

The two questions poised for the pilot studies have been fully answered in this chapter. First, drivers showed a consistent, logical preference for specific steering configurations, and these preferences were collected using a questionnaire. Second, the steering preferences were shown to be different depending on the driving environment. For slower country and residential driving (pilot study 1), drivers preferred the baseline, C1, or a lighter steering effort, C5. For highway driving (pilot study 2), a heavier steering effort, C4, was preferred. The findings match the expected *a priori* preferences considering the driving environments and the demands on the driver. For instance, a winding road requires quick steering changes while highway driving requires precision. These two pilot studies proved that the simulator can extract generic steering preference data from drivers. However, the selected steering settings were discrete so only general design directions can be concluded from the presented results. In other words, the method used in the pilot studies cannot find an exact optimal steering setting.

3.2 Demographics Study

Upon completion of the two pilot studies, the simulator was applied in a demographics study which used a larger pool of human test subjects at Clemson University. The study goal was to determine the simulator's effectiveness as a tool for investigating automotive steering preferences between demographic groups. In evaluating this issue, the required tools and methodologies should be developed to streamline future large scale simulator-based studies. The study ultimately contributed to future simulator applications through the development of steering system design targets and overall consumer preference trends for envisioned production vehicles. Previous collaborative Honda R&D Americas, Inc. (HRA) - Clemson University research activities focused on determining driver preferences in different roadway environments. Those investigations demonstrated an ability to collect driver preference information through the use of paper questionnaires. The next evolutionary step in the engineering/human factors process was to categorize these drivers and then link their steering preferences into a classification metric for a better understanding of the steering system design paradigms. Simply put, the success of this demographic study should allow future investigations to accurately target specific population groups and reliably determine the favored steering characteristics.

Modification Based on Pilot Studies

During the two pilot studies, the test subjects were allowed to drive the virtual reality roadway scenarios for as long as they desired. Although this helped the drivers to provide accurate feedback, it made the laboratory driving experience potentially time consuming. The pilot studies only required the drivers to experience six different steering system configurations (C1-C6) in a single driving environment. With an increase to 15 different scenarios (e.g., steering, roadway) in the demographics study, strict time limits were placed on the runs to ensure the timely completion and to avoid test subject burnout (fatigue). For example, the residential environment was restricted to 90 seconds of driving time. Similarly, the country and highway environments ended at a specific location on the roads which resulted in approximately 60 seconds of driving time.

Test Procedure

The human test subjects were largely recruited from Clemson University's undergraduate Department of Psychology classes. These subjects were given extra course credit for participating in the study, thereby eliminating the need to provide monetary compensation. This was a reliable resource for fresh test subjects that can be utilized in future studies. For the demographics study, data was gathered with $n=43$ human subjects over the course of two academic semesters (Summer 1 2007 and Summer 2 2007).

Each human subject completed a matrix of five steering configurations (C1-C5) on three driving environments (R1-R3) for a total of 15 scenarios as listed in Tables 3.4 through 3.6.

Steering Configuration	Description
C1	Baseline Honda CR-V (18:1 Ratio)
C2	15:1 Steering Ratio
C3	22.5:1 Steering Ratio
C4	20% Heavier Steering Torque
C5	20% Lighter Steering Torque

Table 3.4: Summary of the five steering configurations used in demographics study; configuration C6 was delisted due to poor results in the pilot studies

The steering configurations in Table 3.4 provided a good generic spread for the demographics study. It was important to capture changes in both the steering angle and the steering effort domains; the 20% modifiers allowed settings that were noticeable but not overwhelming. The three roadway environments available in the study have been summarized in Table 3.5 and correspond to the pilot study environments.

Road	Description
R1 - Residential	Low Speed, Stop Signs
R2 - Country	Medium Speed, Fun Winding Road
R3 - Highway	High Speed, Gradual Curves, Lane Changes

Table 3.5: Three designed roadway environments utilized in the demographics study

The fifteen scenarios (refer to Table 3.6) were placed into a randomized Latin Square format that was designed to eliminate run order effects. Table 3.7 lists the run order for the configurations that were applied to the first fifteen test subjects and then repeated for each subsequent block of fifteen subjects until testing was completed.

Scenario	Steering Configuration	Road Category
1	C1	R1
2	C2	
3	C3	
4	C4	
5	C5	
6	C1	R2
7	C2	
8	C3	
9	C4	
10	C5	
11	C1	R3
12	C2	
13	C3	
14	C4	
15	C5	

Table 3.6: The fifteen scenarios with corresponding steering configuration and roadways for the demographics study

A standardized approach was utilized in the 257 Fluor Daniel Engineering Innovation Building Driving Simulator Laboratory while hosting the tests. On arrival, the human subjects were asked to read a brief statement concerning risks, anonymity, and voluntary participation. They then filled out a three page questionnaire (refer to Appendix D) which was designed to classify their driving and purchasing styles. After a brief overview of the simulator controls and testing procedure, the subjects began driving with Run #1, corresponding to column two in the Latin Square chart displayed in Table 3.7. All of the driving environments were designed with either a time limit or endpoint to ensure the timely completion of each scenario. After the successful conclusion of a given scenario, the driver was asked to fill out a nine question survey (refer to Appendix F) about their satisfaction with the

particular steering configuration. Both the demographics questionnaires and the scenario surveys were subsequently used to analyze the driver preferences.

Subject	Run														
	1	2	3	4	5	6	7	8	9	10	11	12	13	14	15
1	1	12	9	14	6	3	5	8	10	13	2	15	11	7	4
2	12	9	14	6	3	5	8	10	13	2	15	11	7	4	1
3	9	14	6	3	5	8	10	13	2	15	11	7	4	1	12
4	14	6	3	5	8	10	13	2	15	11	7	4	1	12	9
5	6	3	5	8	10	13	2	15	11	7	4	1	12	9	14
6	3	5	8	10	13	2	15	11	7	4	1	12	9	14	6
7	5	8	10	13	2	15	11	7	4	1	12	9	14	6	3
8	8	10	13	2	15	11	7	4	1	12	9	14	6	3	5
9	10	13	2	15	11	7	4	1	12	9	14	6	3	5	8
10	13	2	15	11	7	4	1	12	9	14	6	3	5	8	10
11	2	15	11	7	4	1	12	9	14	6	3	5	8	10	13
12	15	11	7	4	1	12	9	14	6	3	5	8	10	13	2
13	11	7	4	1	12	9	14	6	3	5	8	10	13	2	15
14	7	4	1	12	9	14	6	3	5	8	10	13	2	15	11
15	4	1	12	9	14	6	3	5	8	10	13	2	15	11	7

Table 3.7: Latin square run order showing driving scenario (steering configuration and roadway) versus driving order for groups of fifteen drivers

Questionnaire Development

The success of the demographics study depended heavily on the development of two questionnaires: demographics and scenario. The demographics questionnaire needed to accurately categorize each driver within a specific demographic group selected for the study. The demographics were not limited to traditional (i.e., age, gender) classifiers, but also tried to categorize participants as a type of driver (i.e.,

enthusiast, utility) and automotive selection criteria (i.e., vehicle type). Conversely, the scenario questionnaire needed to quickly tap into the driver's opinion of a given steering system setting.

The one time thirty-eight (38) question demographics survey did not have a time constraint. However, it was important to obtain the broadest range of information possible about a participant in an efficient manner. The participants were asked about traditional demographics (i.e., age, gender), their most recent car purchase (i.e., model, cost, and reason for buying), and generic relevant questions (e.g., video game experience, how important steering is, etc.). The aim was to primarily categorize drivers by the three demographics: fun, utility, and car enthusiast. A fun driver (D_1) was looking for a "fun driving experience" and focused on the performance characteristics of the vehicle. A utility driver (D_2) used their vehicle as a tool and preferred efficiency, or convenience, over performance. Finally, an enthusiast driver (D_3) saw their vehicle as a source of pride and may focus on the visual appeal or brand rather than performance or utility.

The subjects were not categorized as a specific demographic type, but rather graded on how much each category represented them. In other words, drivers were not forced to have sole membership in one category but could belong to each to varying amounts. Subsequently, each demographic category turned into a continuous variable that identified each subject on "how much" or "how little" the given category pertained to them (all drivers were represented within each demographic to some degree). An arbitrary cutoff could be set to declare a subset of the group as the listed

demographic, but it would be biased. The final demographics questionnaire may be found in Appendix D. The questions corresponding to the demographic categories were: Fun $D_1 = \{17,19,21,23,30\}$, Utility $D_2 = \{12,13,14,31,32\}$, and Car Enthusiast $D_3 = \{15,16,18,22,28,29,34,35,36,37,38\}$. Furthermore, question 8-11 which pertained to the typical driving location of the subject were considered independently for analysis. The remaining questions were either traditional demographics (i.e., age, gender) or uncategorized open response questions (i.e., make and model of current vehicle). The demographic breakdown from the study is shown in Figure 3.13. The response scale was between 1 and 7, with 1 not being represented by the respective demographic group and 7 heavily belonging to the respective group. Notice how subject #1 ranked in the top 5 for the fun and enthusiast demographics while being the lowest ranked in the utility demographic. This subject drove a BMW M Roadster, which would match his demographic profile. As proof that the demographic groups are independent, subject #20 was in the bottom 5 for the enthusiast demographic, yet top 10 in the fun demographic. She was also in the top 5 for utility, and such a profile matched well with the Honda Accord she drove.

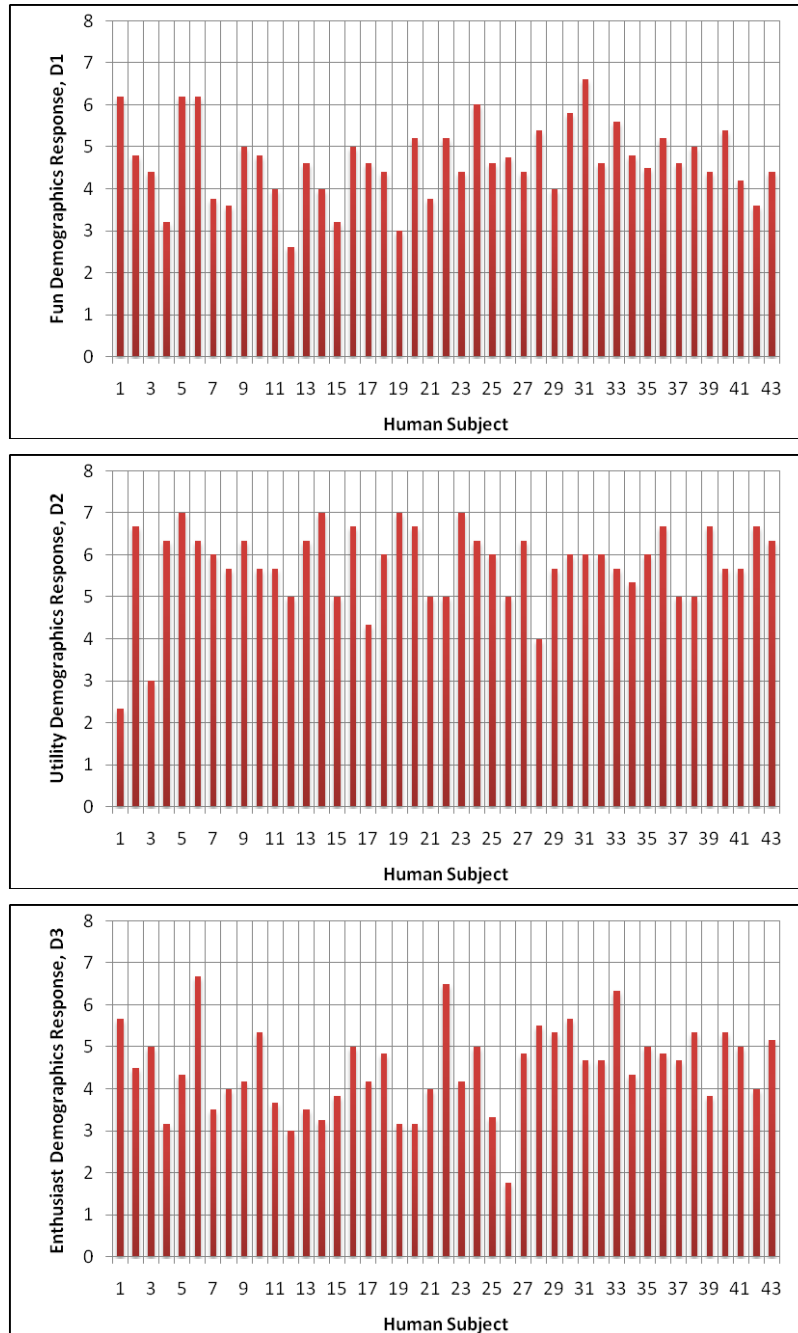


Figure 3.13: Breakdown of demographic categorization for all 43 human subjects participating in the simulator study with (a) Fun, (b) Utility, and (c) Enthusiast

The scenario questionnaire began as the bank of sixteen questions from the pilot studies (refer to Appendix A). The questionnaire's completion speed was a strong concern since fifteen unique scenario questionnaires would need to be completed by each participant during the testing session. Consequently, the questionnaire was refined through an on-line participation survey performed with Clemson University undergraduate psychology students. Three underlying factors (fun, control, and ease) were determined, and the questionnaire was meticulously trimmed from sixteen to nine questions while aiming to keep these three factors intact. Note that the safety category from the two pilot studies was dropped from consideration because it was deemed that the simulator environment was unable to effectively tap into a subject's perception of personal and/or vehicle safety. The final version of the trimmed questionnaire has been presented in Appendix F.

Demographics Results

To evaluate the demographic results, a set of special preference metrics were created to simplify the human subject data collection process. The original data has been listed in Appendix G. First, the nine question questionnaire data gathered after each of the fifteen scenarios completed by each subject was normalized into a $q_{norm_{ijk}}$ value. For a given driver and question, an average response was calculated from all

the questionnaires. The response values were scaled based on the average magnitude, \bar{q}_{ij} , per question given as

$$\bar{q}_{ij} = \frac{1}{15} \sum_{k=1}^{15} q_{ijk} \text{ for } (i = 1, 2, \dots, 43), (j = 1, 2, \dots, 9) \quad (3.6a)$$

$$q_{norm_{ijk}} = \frac{q_{ijk}}{\bar{q}_{ij}} \text{ for } (i = 1, 2, \dots, 43), (j = 1, 2, \dots, 9), (k = 1, 2, \dots, 15) \quad (3.6b)$$

where q_{ijk} is a given question response. The subscripts i, j, and k denote the human subject number, question number on questionnaire, and scenario number, respectively. The average response values used to normalize the data are given in Table 3.8. For instance, subject 1 had an average response of 1.7 for question 9. This individual never believed the steering was too sensitive. By normalizing the responses, the subject's global simulator/question bias was removed so that these responses would not skew the results unnecessarily. Please remember that the questionnaire scale ranged from 1 (disagree) to 7 (agree) in integer increments. The data were normalized where an average response would be represented by 1.

After normalizing the questionnaire data, each driver was assigned two values, S_{ratio} and S_{effort} , per roadway (R1-R3) for the steering ratio (C2-C3) and steering effort responses (C4-C5) to collapse the subject's responses into preference metrics. The differences between the two opposing configurations, S_{ratio} and S_{effort} , becomes

$$S_{ratio_{ip}} = \sum_{j=1}^9 \left(q_{norm_{ij}(k=2,7,12)} - q_{norm_{ij}(k=3,8,13)} \right) \text{ for } (i = 1, 2, \dots, 43), (p = 1, 2, 3) \quad (3.7)$$

$$S_{effort_{ip}} = \sum_{j=1}^9 \left(q_{norm_{ij}(k=4,9,14)} - q_{norm_{ij}(k=5,10,15)} \right) \text{ for } (i = 1, 2, \dots, 43), (p = 1, 2, 3) \quad (3.8)$$

with p corresponding to the three roadways (R1-R3) per Table 3.6. These parameters effectively eliminated simulator bias, leaving behind a value for how sensitive the subject was to steering ratio and/or steering effort changes. No preference was represented by a zero. A larger positive S_{ratio} or S_{effort} value represented a preference for a quicker steering ratio, C2, or heavier steering effort, C4, respectively. Inversely, a larger negative S_{ratio} or S_{effort} value represented a preference for a slower steering ratio, C3, or lighter steering effort, C5, respectively. A value of zero implied that the subject was not sensitive to changes in the respective setting. Overall, these preference metrics provided continuous variables to correlate with the demographic metrics.

The baseline steering configuration, C1, was not used in this analysis because the human subjects' direction and preference for steering system extremes was more important for this study (i.e., what is the influence of steering ratio and effort).

Subject	Question								
	1	2	3	4	5	6	7	8	9
1	3.4	4.1	4.7	5.3	3.9	3.5	3.5	3.3	1.7
2	5.5	5.3	3.5	5.3	5.1	4.5	5.1	3.8	4.5
3	4.7	4.8	2.1	5.1	4.9	4.9	4.7	3.1	2.5
4	2.9	2.8	1.2	2.6	2.4	2.5	3.0	6.7	2.1
5	4.5	4.6	3.5	4.6	4.7	4.6	4.7	4.4	3.9
6	4.5	4.3	2.9	4.3	4.2	4.1	4.3	4.1	3.3
7	3.3	3.1	4.5	2.7	2.8	3.1	3.5	5.0	3.1
8	3.5	4.5	3.6	4.5	4.4	4.1	4.2	3.7	2.5
9	5.2	3.9	4.5	3.1	3.3	3.3	3.9	5.1	3.4
10	3.5	3.9	3.3	4.1	4.1	4.2	4.3	3.9	2.6
11	5.8	4.3	4.4	3.7	3.8	4.3	4.4	5.5	3.7
12	4.3	3.8	4.2	3.5	3.6	3.8	3.7	5.0	4.3
13	3.9	4.3	4.2	4.5	4.5	3.7	4.1	4.9	4.7
14	3.9	5.1	3.5	5.3	5.3	4.6	5.3	5.3	5.1
15	3.9	3.9	4.5	3.9	4.2	3.7	4.2	6.5	3.4
16	4.7	4.9	3.5	4.9	4.9	5.0	4.8	3.6	3.3
17	4.1	4.5	3.9	4.4	3.9	3.9	4.5	4.5	2.6
18	4.1	4.8	4.1	4.9	4.3	4.2	5.3	4.2	2.6
19	2.1	1.9	6.5	1.8	2.1	2.1	1.5	7.0	1.7
20	2.5	3.9	3.5	3.9	2.9	2.7	3.6	4.4	3.2
21	4.6	4.6	3.1	4.7	4.4	4.4	4.2	3.2	3.2
22	5.1	5.1	3.7	5.2	4.9	4.5	4.7	5.2	4.7
23	4.7	5.1	3.6	4.9	4.9	4.9	5.9	5.1	3.0
24	5.2	5.2	5.1	4.9	4.9	4.8	5.2	5.5	4.7
25	5.9	5.5	4.2	5.9	5.7	5.5	4.7	5.0	3.3
26	3.4	4.4	5.1	4.0	4.0	4.1	5.0	6.3	5.6
27	4.5	4.5	3.7	4.7	4.5	4.5	4.5	5.6	3.3
28	4.3	4.0	2.7	4.3	4.3	4.1	3.9	3.3	2.3
29	4.3	4.6	3.7	4.6	4.5	4.5	4.5	3.7	3.1
30	4.6	4.3	3.9	4.3	4.3	4.1	4.0	3.9	3.5
31	5.9	5.6	2.5	6.3	6.3	5.6	5.8	2.9	2.5
32	2.2	4.1	3.5	3.7	3.6	3.7	4.3	6.5	6.9
33	3.4	3.1	5.5	3.3	2.6	2.5	3.5	6.3	3.8
34	3.3	4.4	3.3	4.1	3.5	3.5	4.9	5.2	3.7
35	4.1	3.7	3.7	3.9	3.9	4.2	4.1	4.5	4.1
36	2.1	2.5	2.2	2.5	2.8	2.5	3.1	3.9	2.9
37	3.8	3.5	2.3	3.5	3.6	4.1	4.9	5.3	2.8
38	5.5	5.2	3.5	4.9	5.4	5.1	4.9	4.4	4.4
39	3.8	3.1	4.3	3.3	3.6	3.4	4.2	5.4	4.1
40	4.5	4.5	2.9	4.4	4.3	4.1	4.8	3.4	3.3
41	3.3	4.1	4.1	4.1	3.9	4.1	3.9	4.7	3.4
42	3.6	3.5	4.0	3.9	3.9	3.6	3.9	4.1	4.4
43	5.0	5.3	3.9	5.2	5.2	5.0	5.7	4.1	3.5

Table 3.8: Average response, \bar{q}_{ij} , of each subject ($i=1,2,\dots,43$) for each question ($j=1,2,\dots,9$) used to normalize the response data for the fifteen configurations to eliminate question bias

To quantify the steering preferences for the demographic groups, two measures were utilized: the correlation between the preferences of the demographic groups (fun, utility, and car enthusiasts) and the steering characteristics (S_{ratio} and S_{effort}) denoted by r and the p -value. In layman's terms, the latter parameter represents the probability that the given correlation measure is a false positive. Correlation coefficients have associated statistical significance levels. Table 3.9 displays the qualitative scale used in this study to interpret the quantitative measures, r and the p -value. To calculate the correlation coefficients, the means of the demographic and steering configuration preference groups for all subjects were constructed as

$$\bar{D}_L = \frac{1}{43} \sum_{i=1}^{43} D_{iL} \text{ for } (L = 1, 2, 3) \quad (3.9a)$$

$$\bar{S}_{\text{ratio}_p} = \frac{1}{43} \sum_{i=1}^{43} S_{\text{ratio}_{ip}} \text{ for } (p = 1, 2, 3) \quad (3.9b)$$

$$\bar{S}_{\text{effort}_p} = \frac{1}{43} \sum_{i=1}^{43} S_{\text{effort}_{ip}} \text{ for } (p = 1, 2, 3) \quad (3.9c)$$

where D is the demographic metric (D_1 - D_3) from Figure 3.13, and S_{ratio} and S_{effort} are the steering configuration preferences defined by equations (3.7) and (3.8). The variables i , L , and p represent the subject number, demographic group (D_1 - D_3), and roadway ($R1$ - $R3$), respectively. The correlation, r , was formulated as

$$r_{ratio_{Lp}} = \frac{\sum_{i=1}^{43} (D_{iL} - \bar{D}_L)(S_{ratio_{ip}} - \bar{S}_{ratio_p})}{\sqrt{\sum_{i=1}^{43} (D_{iL} - \bar{D}_L)^2} \sqrt{\sum_{i=1}^{43} (S_{ratio_{ip}} - \bar{S}_{ratio_p})^2}} \text{ for } (L = 1, 2, 3) \quad (3.10a)$$

$$r_{effort_{Lp}} = \frac{\sum_{i=1}^{43} (D_{iL} - \bar{D}_L)(S_{effort_{ip}} - \bar{S}_{effort_p})}{\sqrt{\sum_{i=1}^{43} (D_{iL} - \bar{D}_L)^2} \sqrt{\sum_{i=1}^{43} (S_{effort_{ip}} - \bar{S}_{effort_p})^2}} \text{ for } (L = 1, 2, 3) \quad (3.10b)$$

Quantitative Scale	Qualitative Interpretation
$0.0 \leq r < 0.2$	Poor correlation
$0.2 \leq r < 0.4$	Moderate correlation
$0.4 \leq r < 0.6$	Excellent correlation
$0.6 \leq r < 1.0$	Unrealistic
$p \leq 0.05$	Statistically significant correlation

Table 3.9: Qualitative interpretation the of correlation, r, and p-value used to evaluate the strength of results for the demographic study

The most significant test results, which have been determined from the numerous subjective responses, are presented in Table 3.10. A fourth demographic group, D_4 , corresponds to $D_4 = \{10\}$ on the questionnaire. The first column lists the demographic group followed by the steering characteristic to which the group was most sensitive. The second and third columns list the steering characteristic and roadway scenario. The fourth and fifth columns list the correlations and p-values for each entry. To summarize the table of correlations, drivers who used their vehicles for utility/transportation (D_2) preferred quicker steering ratios (C2) and heavier efforts

(C4) in all situations with correlations of $r = 0.341$ and $r = 0.426$, respectively. Next, car enthusiasts (D_3) preferred quick steering ratios (C2) in the residential/country environments ($r = 0.319$, $r = 0.294$) and light steering effort (C5) on the highway ($r = -0.360$). The negative sign denotes that the lighter effort was preferred rather than the heavier effort. The p-values ranged from 0.018 to 0.56 for these entries, which corresponds to statistically significant correlations. Finally, rural drivers (D_4) preferred quicker steering ratios (C2) on country roads ($r = 0.437$). This correlation was the strongest result even though it was not one of the primary demographic categories; the p-value of 0.003 denotes a good statistical correlation.

Demographic Group	Steering Characteristic	Roadway Scenarios	Correlation, r	p-value
Utility (D_2)	Ratio, C2	R1-R3	0.341	0.036
	Effort, C4		0.426	0.008
Car Enthusiast (D_3)	Ratio, C2	Residential (R1)	0.319	0.037
		Country (R2)	0.294	0.056
	Effort, C5	Highway (R3)	-0.360	0.018
Rural Drivers (D_4)	Ratio, C2	Country (R2)	0.437	0.003

Table 3.10: Correlations, r , between the demographic groups and steering systems preferences with related p-measures based on questionnaire data

The important measure to examine is the correlation between the target demographic variable and the preference ratings. The results shown in Table 3.10, and interpretation standard illustrated in Table 3.9, provide additional evidence that the combination of steering characteristics and the steering questionnaire were tapping into the participants' actual steering preferences. No significant correlations

were found for the fun (D₁) demographic, but notice how one of the solo questions resulted in the strongest correlation (D₄ demographic group).

Conclusion

The primary goal of this study was to validate the simulator as a tool for identifying steering preferences associated with demographic groups. The response data was tested to verify that drivers significantly distinguished between steering configurations and environments. Through extensive human subject testing, the steering preferences were correlated with demographic metrics. Both moderate and excellent correlations were found that showed a relationship between the demographic metrics and the steering preferences (refer to Table 3.10). A p-measure was used to determine the significance of the correlations, and proved that these correlations were statistically significant and did not occur by chance. The evidence of strong correlations combined with low p-values was sufficient to validate the steering simulator as a tool for investigating steering preferences with respect to demographic metrics.

One of the outcomes of this study was the recognition that one set of steering system design parameters would not be ideal for all drivers and/or roadway conditions. Clearly, a set of steering parameters should be tuned for the given driver and then applied through an electric power steering system. In this manner, the vehicle steering can be customized for the driver similar to seat and mirror positions. Further, an opportunity may exist to use GPS or vehicle sensors to identify the type of

driving environment and adjust the steering system accordingly. These concepts represent the likely evolution of steering systems in the next decade.

CHAPTER FOUR

CREATION OF A STEERING PREFERENCE OBJECTIVE METRIC FOR INNOVATIVE STEERING FEATURES

A re-occurring problem in ground vehicle steering system development is the identification of a steering setting that is favored by a majority of potential customers. The initial dealership drive is critical to the vehicle purchase process. However, there are two inherent difficulties with steering system parameter selection. First, steering tuning is typically performed by seasoned automotive engineers who may select a setting based on either personal preference or estimation of what the target customer may prefer. Although this may be partially remedied by customer feedback, the difficulty remains in selecting the design parameters given the subjective nature of the task. Second, all drivers are different and each likely has a unique preference for their steering setting. This means that no matter how diligently an engineer tries to obtain an optimal setting, their selection will always be a compromise and a non-optimal selection. However, the emergence of electric power steering systems and customer personalization may lead to unique steering settings for future vehicles.

Previous research (refer to Chapter 3) has been focused on finding an optimal steering setting using a driving simulator and questionnaires aimed at tapping into a driver's steering preference. While successful, it still required the interaction of researchers with drivers to ask about their preferences. Sugita *et al.* (2009) attempted to establish design criteria for an optimal steering configuration for electric power steering. They focused on determining a target level of passivity that felt most

comfortable to the driver. Català *et al.* (2004) attempted to correlate objective steering torque data with kinematics and compliance test results. Jaksch (1979) found that yaw velocity response time was a dominant factor in the subjective rating of a vehicle's handling characteristics during a lane change maneuver. Hearthershaw (2000) developed a variable steering ratio strategy that maximized driver performance in multiple repeatable tests. Yamaguchi and Murakami (2009) used an adaptive control steer-by-wire system to create virtual steering characteristics. In the future, such a system could be used to create personalized steering preferences for drivers. The next logical step in steering preference research should be the development of an objective metric to identify steering preferences without significant driver interactions so that the process may be automated and more scientific.

Through the analysis of the demographics study, the link between objective vehicle response and driver steering preference was investigated. In essence, a hybrid metric of fused vehicle dynamics signals may be used to predict how much drivers enjoyed their steering experience. It should be recognized that many implications associated with this topic exist that may merit further study. First, if questionnaires could be removed from the simulator (or in-vehicle) testing procedure, then the required participation time would decrease. More importantly, the accuracy should improve. One of the biggest challenges the research team faced during laboratory based simulator testing was requesting participants to synthesize their steering experience as a separate entity from the rest of the simulator environment. Simply asking participants about their steering experience likely tainted their response to the

questions. Thus, an objective metric would eliminate this questionnaire bias. Second, the development of an objective steering metric would establish the foundation for an automatically adjusting steering system. It has been assumed that each driver has a unique steering preference. Instead of forcing a driver to adapt to a non-optimal steering setting compromise, the steering setting could instead adapt to the driver. This innovative feature is the basic concept behind developing a steering feedback auto-tuning controller. A steering feedback auto-tuning controller would systematically adjust steering system settings while tracking and optimizing an objective preference metric. After a learning period, the steering system would become optimized for the given driver, eliminating the need to create a compromised steering target. The implementation of an auto-tuning steering algorithm would be a powerful upgrade to the simulator's capabilities. As stated previously, exact steering settings could be matched to a driver instead of using an estimate which was identified based on arbitrary settings. With proper development and maturation, an on-board auto-tuning steering controller could one day become a standard feature on production vehicles.

The first phase of the auto-tuning steering research was the development of an objective steering preference metric. During the demographic driver preference study of Chapter 3, extensive simulated vehicle performance data was collected for each steering configuration. Figure 4.1 displays the steering data for two different configurations. The solid line corresponds to a preferred steering setting while the dotted line denotes a low rated steering setting and subsequent driver behavior. Both

traces were from a single driver (test subject 20) and the only difference between the runs was the steering setting (C7 and C8). The driving environment was a winding road course (R2) with an average vehicle speed of 35 mph (56 kph). While driving the less preferred setting, this driver had a tendency to overshoot their steering input by as much as 86%, often with a subsequent overcorrection as noted in the figure. This steering wheel “sawing” could be pulled out of the data stream through the application of simple statistics (e.g., mean, standard deviation).

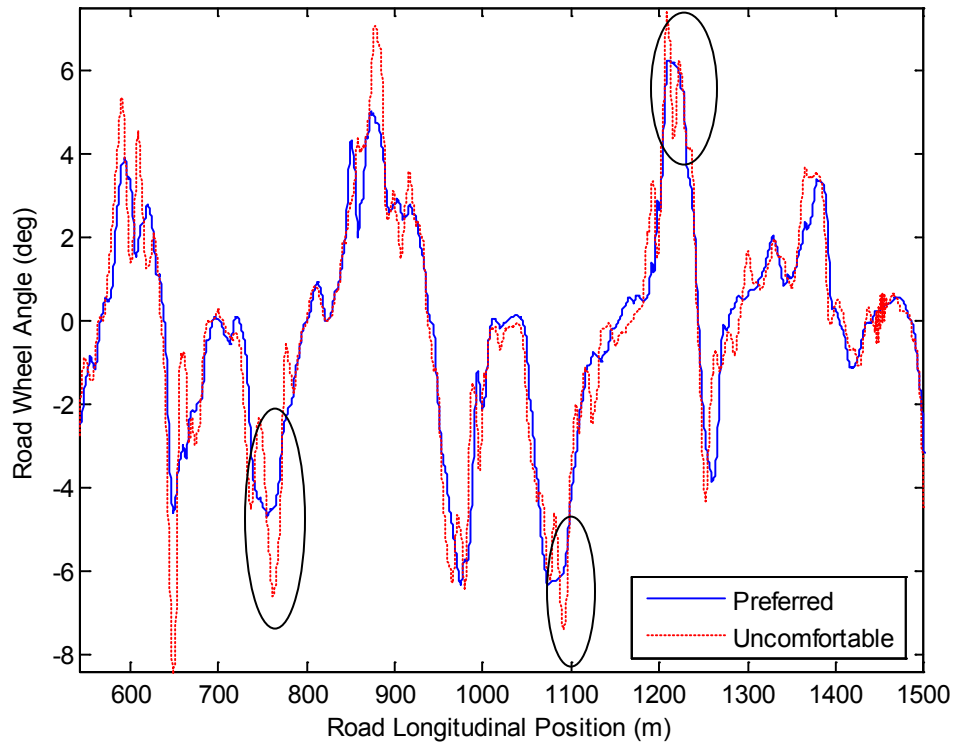


Figure 4.1: Steering angle for test subject 20 driving steering configurations C8 and C7 on road surface R2; the solid line (C8) was identified through questionnaire feedback as the preferred setting while the dotted line (C7) was not preferred

Hypothesis

Based on the initial inspection of the available simulator logged data channels, it was obvious that drivers behaved differently depending on the steering configuration. A hypothesis was formed that states “A metric exists that can predict a driver’s satisfaction with the vehicle’s steering behavior using a normalized numeric value captured from the vehicle operating data”. A combination of metric elements may be considered to create a robust metric. In this manner, the metric may be protected from changing road conditions that may skew a single element. Ideally, the metric would not use impractical vehicle information such as lateral road position or tire slip angles so that the final entity would be valid in both simulator and vehicle applications.

Analysis Method

During simulator human subject testing, thirteen data channels were collected using the output from CarSim. The data channels have been listed in Table 4.1. All driver inputs and the basic vehicle outputs were selected along with the two variables unique to a simulator environment: lateral offset from centerline, and tire slip angles. Even though the goal was to use practical vehicle channels, it was important to be thorough in case an exceptional correlation emerged in this research project.

Number	Description	Symbol	Units
1	lateral offset from centerline	d	m
2-5	tire slip angles for each tire	α	rad
6	yaw rate	$\dot{\psi}$	rad/sec
7	longitudinal acceleration	a_x	m/s ²
8	lateral acceleration	a_y	m/s ²
9	brake position	BP	%
10-11	steering angles of front tires	δ	rad
12	throttle position	TPS	%
13	vehicle velocity	v_x	m/s

Table 4.1: Data channels, H_c , investigated to determine correlation between objective data and subjective human responses

A country road driving scenario (R2 from Table 3.5) was considered for the development of the steering preference metric. This decision was based on the consistent driving profile with a fixed route exhibited by the country road. City and highway environments allow too much creativity from the driver in path selection and traffic demands, leading to unreliable data.

A total of $i = 39$ human subjects evaluated $k = 5$ steering configurations for a total of 195 data sets. Each combination of driver and steering configuration had a matching questionnaire ($j = 9$) result, q_{ik} , with the test subject's opinion on the "fun-to-drive", "controllability", and "ease" of driving for each setting. These questionnaires were completed during the demographics study in Chapter 3. The

results were averaged, \bar{q}_i , and normalized into a single global steering preference, Q_{ik} , for each steering configuration and test subject as

$$\bar{q}_i = \frac{1}{5} \frac{1}{9} \sum_{k=1}^5 \sum_{j=1}^9 q_{ijk} \text{ for } (i = 1, 2, \dots, 39) \quad (4.1)$$

$$Q_{ik} = \frac{\frac{1}{9} \sum_{j=1}^9 q_{ijk}}{\bar{q}_i} \text{ for } (i = 1, 2, \dots, 39), (k = 1, 2, \dots, 5) \quad (4.2)$$

In the expressions, the symbol q denotes the question response on a given questionnaire, and Q is the normalized response for a given driver and steering configuration. The variables i , j , and k represent the human subject number, survey question number, and steering configuration, respectively.

The thirteen data channels from Table 4.1, H_c ($c = 1, 2, \dots, 13$), were processed with future applications in mind. Potential control schemes may require the metric to be positive and reliable after a fixed amount of time. The data channels, H_c , were converted into a metric, J_{ick} , with a single value for each combination of test subject, data channel, and steering configuration for the country road (R2) using the expression

$$J_{ick} = \int_0^{40s} H_{ick}^2 dt \text{ for } (i = 1, 2, \dots, 39), (c = 1, 2, \dots, 13), (k = 1, 2, \dots, 5) \quad (4.3)$$

where c is the number corresponding to the respective data channel. Note that a $t = 40s$ period was selected using a sampling time of $\Delta t = 0.025s$

The metric, J_{ick} , was then normalized for each driver to permit comparison with the subject pool by computing the average of the given metric channel for all steering configurations, \bar{J}_{ic} , and then applying this to the individual metrics, J_{ick} , such that a normalized value, J_{norm} , becomes

$$\bar{J}_{ic} = \frac{1}{5} \sum_{k=1}^5 J_{ick} \text{ for } (i = 1, 2, \dots, 39), (c = 1, 2, \dots, 13) \quad (4.4)$$

$$J_{norm_{ick}} = \frac{J_{ick}}{\bar{J}_{ic}} \text{ for } (i = 1, 2, \dots, 39), (c = 1, 2, \dots, 13), (k = 1, 2, \dots, 5) \quad (4.5)$$

The normalized metrics were then correlated with the normalized questionnaire data for a given human subject and steering configuration. The correlations, r_c , were calculated as

$$\bar{J}_{norm_c} = \frac{1}{39} \frac{1}{5} \sum_{i=1}^{39} \sum_{k=1}^5 J_{norm_{ick}} \text{ for } (c = 1, 2, \dots, 13) \quad (4.6)$$

$$\bar{Q} = \frac{1}{39} \frac{1}{5} \sum_{i=1}^{39} \sum_{k=1}^5 Q_{ik} \quad (4.7)$$

$$r_c = \frac{\sum_{i=1}^{39} \sum_{k=1}^5 (J_{norm_{ick}} - \bar{J}_{norm_c})(Q_{ik} - \bar{Q})}{\sqrt{\sum_{i=1}^{39} \sum_{k=1}^5 (J_{norm_{ick}} - \bar{J}_{norm_c})^2} \sqrt{\sum_{i=1}^{39} \sum_{k=1}^5 (Q_{ik} - \bar{Q})^2}} \text{ for } (c = 1, 2, \dots, 13) \quad (4.8)$$

Once the strongest (i.e., largest absolute value of r_c) correlations were discovered, a computer-based optimization code was applied to identify the strongest

combination and weighting of metrics elements to create a robust metric, $J_{w_{ik}}$. The weighted metric was formulated as

$$J_{w_{ik}} = \sum_{c=1}^{13} w_c \cdot J_{norm_{ick}} \text{ for } (i=1,2,\dots,39), (k=1,2,\dots,5) \quad (4.9)$$

where $w_c = \{w_1, w_2, \dots, w_{13}\}$ is the vector of weighting factors. The weighted metric was correlated with the normalized questionnaire responses, Q_{ik} , to create the weighted correlation, r_w , as

$$\bar{J}_w = \frac{1}{39} \frac{1}{5} \sum_{i=1}^{39} \sum_{k=1}^5 J_{w_{ik}} \quad (4.10)$$

$$r_w = \frac{\sum_{i=1}^{39} \sum_{k=1}^5 (J_{w_{ik}} - \bar{J}_w)(Q_{ik} - \bar{Q})}{\sqrt{\sum_{i=1}^{39} \sum_{k=1}^5 (J_{w_{ik}} - \bar{J}_w)^2} \sqrt{\sum_{i=1}^{39} \sum_{k=1}^5 (Q_{ik} - \bar{Q})^2}} \quad (4.11)$$

The weighting factors, w_c , were allowed any integer value between 0 and 10 with the goal of maximizing the absolute value of the correlation coefficient. The optimization problem was formulated as

$$\max_{w_c \in \{0:10\}} |r_w| \quad (4.12)$$

and solved with a brute force approach that calculated every combination of the thirteen weighting factors (10^{13} cases).

The analysis method has been summarized in Figure 4.2 as a flowchart. In summary, both objective and subjective data was collected from the human test

subjects who drove five steering configurations on a winding road course. The objective data was formulated into positive metrics, and then both the metrics and subjective data were normalized for consistency. Correlations between the metric elements and subjective data were calculated for preliminary consideration. The metric elements were then combined into a single robust metric that was weighted to maximize the correlation with the subjective data. The full results of this analysis will be presented in the next section.

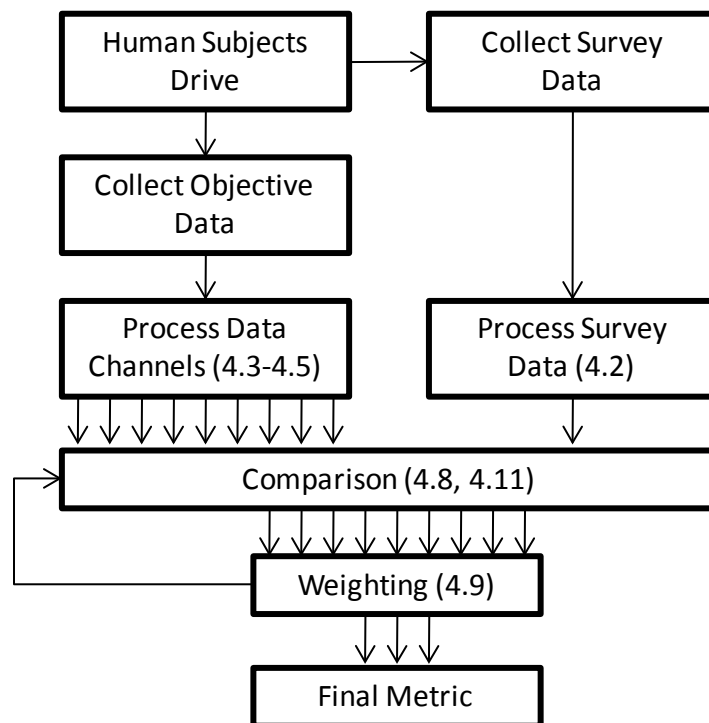


Figure 4.2: Analysis methodology flowchart for creating a weighted objective metric that may predict driver steering preference

Presentation and Discussion of Test Results

All correlations were judged using the standard correlation, r , scale listed in Table 4.2. This table sets the standard for significant correlations to judge the metrics. An ideal metric would lie in the excellent correlation category with $0.4 < |r| < 0.6$. All metrics were correlated with the global normalized questionnaire data shown in Table 4.3. These values were calculated using equations (4.1) and (4.2). The result of the normalization is evident as each row, and subsequently the entire table, averages to a value of 1. At this time, the important connection was between the physical survey and the collected data channels while the steering setting was ignored.

Quantitative Scale	Qualitative Interpretation
$0.0 < r < 0.2$	Poor correlation
$0.2 < r < 0.4$	Moderate correlation
$0.4 < r < 0.6$	Excellent correlation
$0.6 < r < 1.0$	Unrealistic

Table 4.2: Qualitative interpretation of correlation, r , with four categories: poor, moderate, excellent, and unrealistic correlations

The objective metrics were calculated for each data channel, human subject, and steering configuration using equation (4.3) for a total of 2,535 data points. These metrics were normalized with equations (4.4) and (4.5), and the results of this normalization have been included in Appendix J. The normalized metrics were correlated with the global normalized questionnaire data using equations (4.6), (4.7), and (4.8). A single correlation coefficient, r_c , was calculated for each data channel for a total of thirteen correlation coefficients, which have been displayed in Table 4.4.

Note that all correlations were negative, which implied that a smaller metric value corresponded to a more favorable steering setting. The best correlation, $r = -0.32$, occurred with the yaw rate, $\dot{\psi}$. This correlation, along with ten of the remaining twelve correlations, fit in the moderate correlation category of Table 4.2. The normalized yaw rate metric has been plotted against the normalized questionnaire data in Figure 4.3 to visualize the strength of the correlation. For the horizontal axis, $0 < Q \leq 1$ and $1 < Q < 2$ corresponds to “do not like” and “favorable” responses by the subjects, respectively. The vertical axis can be split into $0 < J_{norm_6} \leq 1$ and $1 < J_{norm_6} < 2$ as smooth and aggressive yaw rate responses. Using a standard four quadrant perspective, quadrants II and IV support the negative correlation which reflects that drivers have been recorded to drive more smoothly when they prefer a steering setting and more aggressively when they dislike a setting. In contrast, quadrants I and III are less populated, but support a positive correlation implying that drivers drive more aggressively when they prefer a steering setting and more smoothly when they do not like it.

Subject	Steering Configuration				
	1	2	3	4	5
1	0.84	0.88	0.86	1.15	1.28
2	1.00	1.17	0.97	0.78	1.07
3	0.93	0.95	0.97	0.95	1.21
4	0.98	1.21	0.77	1.08	0.95
5	1.10	1.17	0.80	1.31	0.63
6	1.37	1.20	0.76	0.82	0.85
7	0.85	1.61	1.01	0.89	0.65
8	1.26	0.95	0.90	0.65	1.24
9	0.85	1.05	1.14	1.13	0.83
10	0.98	0.43	0.81	1.53	1.26
11	1.01	1.04	1.07	0.78	1.11
12	0.70	0.56	1.50	1.50	0.74
13	1.03	0.90	0.98	1.13	0.96
14	1.13	0.43	1.17	1.05	1.22
15	1.24	0.77	0.85	0.86	1.29
16	0.88	0.82	1.09	0.80	1.40
17	0.84	0.86	1.57	0.48	1.25
18	1.25	1.06	0.83	0.91	0.96
19	0.84	0.44	1.56	0.77	1.39
20	1.24	1.10	0.93	0.66	1.07
21	0.88	0.83	1.00	1.16	1.13
22	1.30	0.90	1.02	0.60	1.18
23	1.28	1.14	0.89	1.11	0.58
24	1.49	1.12	0.94	0.44	1.01
25	1.03	0.83	1.25	1.18	0.71
26	1.19	0.85	1.33	0.74	0.88
27	0.99	0.91	1.12	0.84	1.14
28	0.65	1.30	1.36	0.48	1.20
29	0.45	1.60	0.84	0.95	1.15
30	0.48	1.69	1.29	0.88	0.65
31	1.18	0.67	1.30	0.58	1.27
32	1.21	0.90	0.71	1.05	1.13
33	1.21	1.00	0.94	1.05	0.79
34	1.06	1.24	0.49	1.20	1.00
35	1.14	0.89	1.20	0.99	0.79
36	0.80	0.97	1.08	1.12	1.03
37	1.11	0.91	1.13	0.76	1.08
38	1.02	0.49	0.94	0.99	1.56
39	1.05	0.55	1.32	0.88	1.19

Table 4.3: Global normalized questionnaire data, Q_{ik} , used for all correlations with objective metrics

Number	Data Channel	Symbol	Correlation, r
1	Lateral offset from centerline	d	-0.22
2	Left front tire slip angle	α_{lf}	-0.28
3	Left rear tire slip angle	α_{lr}	-0.24
4	Right front tire slip angle	α_{rf}	-0.27
5	Right rear tire slip angle	α_{rr}	-0.25
6	Yaw rate	$\dot{\psi}$	-0.32
7	Longitudinal acceleration	a_x	-0.30
8	Lateral acceleration	a_y	-0.31
9	Brake position	BP	-0.15
10	Left front tire angle	δ_{lf}	-0.28
11	Right front tire angle	δ_{rf}	-0.27
12	Throttle position	TPS	-0.31
13	Longitudinal velocity	v_x	-0.18

Table 4.4: Correlation coefficients between objective metrics and questionnaire results with best correlation of $r = -0.32$ for yaw rate, $\dot{\psi}$, metric

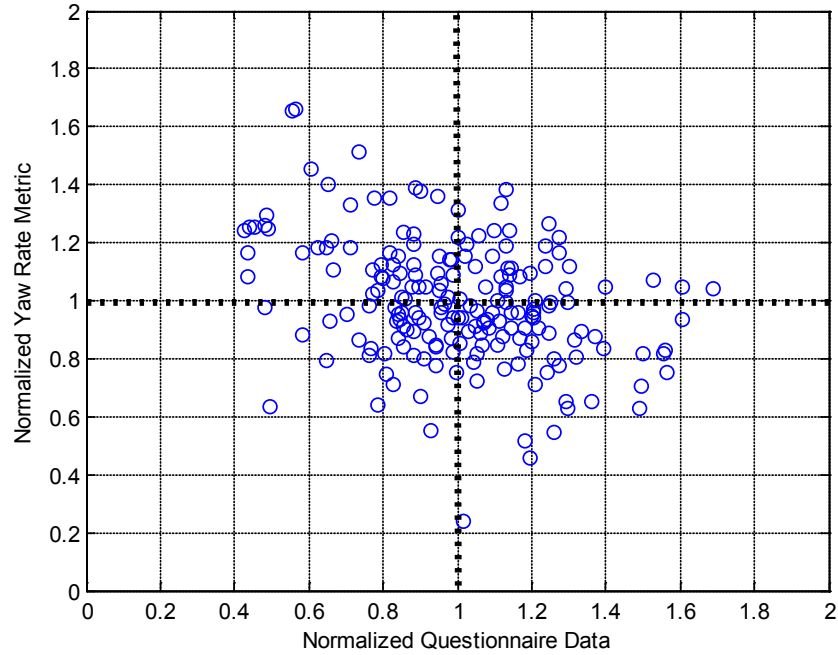


Figure 4.3: Plot of normalized yaw rate metric, J_{norm_6} , vs. normalized questionnaire data, Q , to visualize the moderate correlation of $r = -0.32$

Although eleven data channels produced moderate correlations with the questionnaire data (excluding $c = 9$ and $c = 13$), some channels may have contained similar vehicle response data. For instance, the left and right front tire angles, δ_{lf} and δ_{rf} , should have only differed slightly based on steering linkage compliance and suspension geometry effects. The weighting optimization aimed to eliminate data channels with duplicate information while retaining those channels with unique information that correlated with the questionnaire results. The weighted metric, J_w , was formulated using equation (4.9) and then optimized while maximizing the absolute value of the correlation, r_w .

The optimization resulted in a maximum correlation of $r = -0.39$ for all five steering configurations (global weight) with weighting factors listed in Table 4.5 - column 4 (yaw rate, longitudinal acceleration, lateral acceleration). Although still a moderate correlation, it nearly fell in the excellent correlation range and was significantly stronger than any single metric. Figure 4.4 shows the plot of the correlated data to visually demonstrate the strength of the correlation. In this figure, the vertical axis values of $0 < J_w \leq 19$ and $19 < J_w < 35$ correspond to smooth and aggressive command of the entire vehicle, respectively. The value $J_w = 19$ was selected as the cutoff point representing the mean of the data points. The horizontal axis was partitioned the same as Figure 4.3 with $0 < Q \leq 1$ and $1 < Q < 2$ corresponding to “do not like” and “favorable” responses, respectively. Notice that in

general, smoother driving habits corresponded with preferred steering settings (evident in quadrant IV).

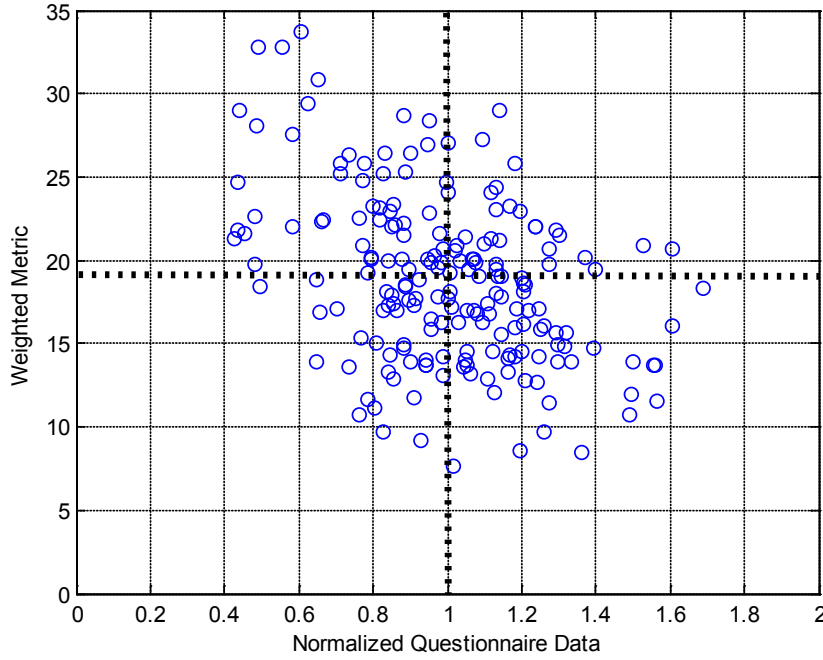


Figure 4.4: Plot of weighted metric, J_w , vs. normalized questionnaire data, Q , to visualize the correlation of $r = -0.39$

To further investigate the weighted metric, the same weighting optimization process was performed while isolating the cases where either the steering ratio ($k = 2, 3$) or steering effort ($k = 4, 5$) was changed. The steering ratio corresponded to configurations 7 and 8, while the steering effort corresponded to configurations 9 and 10 in Table 3.6. The results exposed a surprising conclusion. The maximum correlation for steering ratio changes was $r = -0.55$; however, the maximum correlation for steering effort changes was $r = -0.15$. This result demonstrated that the objective metric may be reliable for discovering an optimal steering ratio, but

insignificant for tuning steering effort settings. The best weighting factors for these two approaches have been summarized in Table 4.5.

#	Data Channel	Symbol	Global Weight, w_c	Ratio Weight, w_c	Effort Weight, w_c
1	Lateral offset	d	0	0	0
2	Left front tire slip angle	α_{lf}	0	0	0
3	Left rear tire slip angle	α_{lr}	0	0	0
4	Right front tire slip angle	α_{rf}	0	0	0
5	Right rear tire slip angle	α_{rr}	0	0	0
6	Yaw rate	$\dot{\psi}$	5	0	0
7	Longitudinal acceleration	a_x	6	3	10
8	Lateral acceleration	a_y	8	0	0
9	Brake position	BP	0	0	0
10	Left front tire angle	δ_{lf}	0	1	5
11	Right front tire angle	δ_{rf}	0	0	0
12	Throttle position	TPS	0	5	0
13	Longitudinal velocity	v_x	0	0	9

Table 4.5: Weighting factors, w_c , for weighted metric, J_w , giving maximum correlations of $r = -0.39$, $r = -0.55$, and $r = -0.15$ for Global ($k = 1-5$), Ratio ($k = 2, 3$), and Effort ($k = 4, 5$) respectively where k denotes the steering configuration

The ratio weighting factors were largely longitudinal dynamics, which may indicate that the drivers misjudge safe cornering speeds when they are unhappy with the steering ratio (safety issue). The plots of the correlated data for the steering ratio and steering effort, independent of each other, have been presented in Figures 4.5 and 4.6 versus the normalized questionnaire data. The significance of a $r = -0.55$ correlation can be clearly seen in Figure 4.5 with a strong linear grouping. In

contrast, Figure 4.6 shows how ambiguous a correlation of $r = -0.15$ appears. Both steering ratio and steering effort data sets have been plotted together in Figure 4.7 to demonstrate the strength of the ratio correlation.

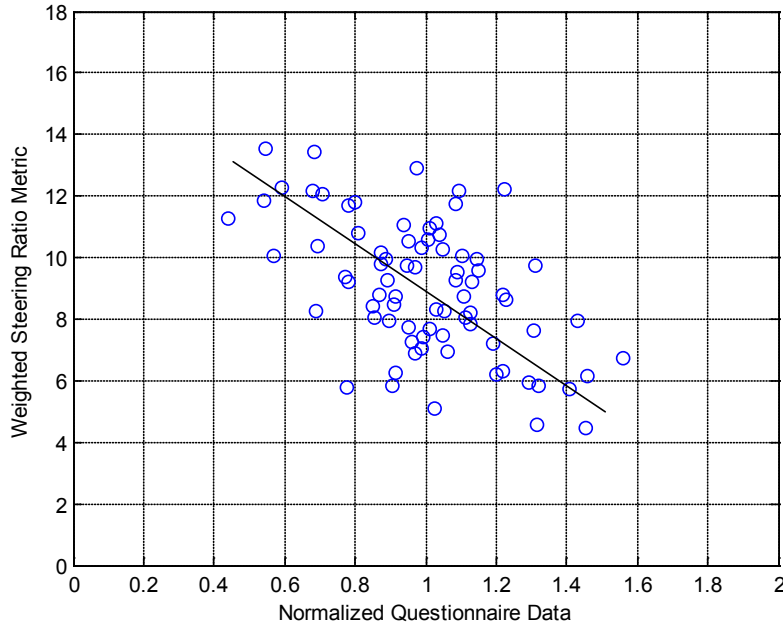


Figure 4.5: Plot of weighted steering ratio metric, J_w , vs. normalized questionnaire data, Q , for changes in steering ratio ($k = 2, 3$) to visualize the correlation of $r = -0.55$

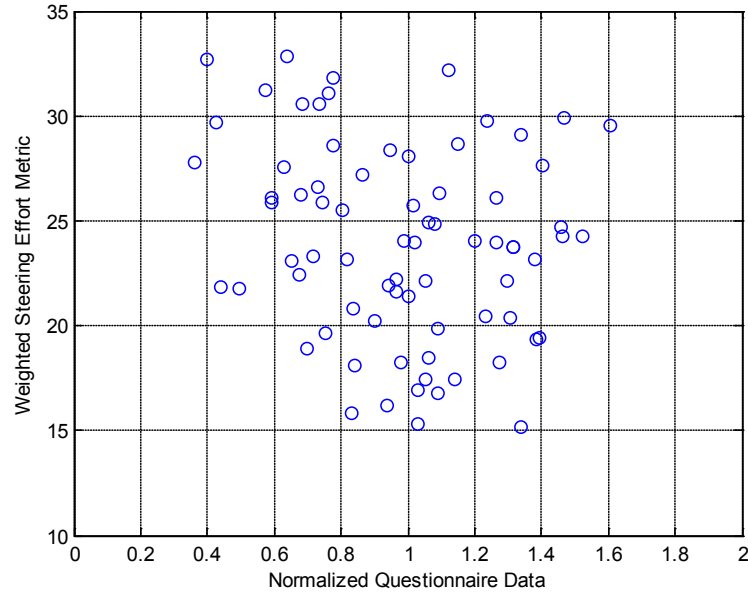


Figure 4.6: Plot of weighted steering effort metric, J_w , vs. normalized questionnaire data, Q , for changes in steering effort ($k = 4, 5$) to visualize the correlation of $r = -0.15$

Summary

Automotive steering system setting targets (i.e., selection of design parameters such as ratio, damping, and assist curve) are an ongoing challenge for automotive engineers. As society moves into an age of personalization, the automotive companies must adapt to win the next generation of car buyers. One area of adaptation may be in the development of an automatic tuning steering control system. Accordingly, the first step in creating an automatic tuning steering system would be the identification of a performance index which captures the driver's steering preferences.

This chapter has investigated an objective steering preference metric through the use of the Clemson University Steering Simulator. Objective data taken from vehicle sensor channels was correlated with questionnaire data completed by human test subjects. A global weighted objective metric was formulated which combined the yaw rate, $\dot{\psi}$, lateral acceleration, a_y , and longitudinal acceleration, a_x , channels according to equations (4.3) and (4.9) while using the weighting factors from Table 4.4. The resulting weighted objective metric produced a correlation with questionnaire data of $r = -0.39$. When steering ratio setting changes were isolated, an even stronger correlation of $r = -0.55$ was discovered using the longitudinal acceleration, a_x , left front tire steer angle, δ_{lf} , and throttle position, TPS. This correlation was in the “excellent” category, $0.4 < |r| < 0.6$. The findings of this investigation suggest that an objective steering preference metric may be able to predict a driver’s steering ratio preference, while steering effort preferences may be transparent to an objective metric.

CHAPTER FIVE

ACTIVE STEERING FOR VEHICLE ROAD RUNOFF

A run-off-road (ROR) accident occurs when one or more tires of a ground vehicle leave the road surface, resulting in the driver losing control and/or colliding with an object. The reasons for road departure can be excessive speed, obstacle avoidance, lack of attention (fatigue, cabin distraction), or other outside influences (alcohol, drugs) (Hadden, 1997). A specific subset of ROR accidents are the result of the driver losing vehicle control while attempting to return to the roadway from a soft shoulder (grass, dirt, gravel). This specific type of event will be identified as a shoulder induced accident (SIA). SIAs may be primarily attributed to the difference in elevation between the paved roadway and the soft road shoulder. An excessive steering angle may be required to negotiate the sharp change in elevation, and this steering input can cause the driver to lose control if the vehicle speed is too high. These accidents are largely attributed to driver error which can be minimized through proper training and/or active steering intervention.

Previous research on ROR has largely focused on road design and construction. Some of the current passive measures to provide driver warnings include roadway rumble strips for lane deviation (Hickey, 1997, Räsänen, 2005). Extended hard shoulders have also been incorporated into road designs, where space allows, giving drivers more time to react before encountering an ROR situation (Zegeer, 1988). To compliment these activities, the circle of safety may be closed

with education and engineering efforts to prevent SIAs after an ROR condition has been reached. This can be accomplished with a mixture of driver training and active steering to eliminate preventable SIAs. The first step towards solving this problem was presented by Black *et al.* (2008) where the concept of driver intention was initially discussed. The availability of an advanced steering system, with accompanying computer intervention, can mitigate the dangerous effects of run-off-road events.

The traditional hydraulic power steering system provides passive torque assistance to the driver while directly channeling the steering input from the steering wheel via the driver to the road wheels. Electric power steering systems, refer to Figure 5.1a, provide similar passive assistance with greater efficiency. However, this steering system can also be programmed with smart algorithms for active torque feedback. The inclusion of a planetary gear set allows an electric power steering system to have limited angular control to improve the driver's steering input as necessary (i.e., active assistance). A steer-by-wire system, refer to Figure 5.1b, offers full torque and road wheel angle intervention. Hence, various levels of active steering can be implemented in either the electric power steering or steer-by-wire configurations depending on the required level of control.

In this Chapter, the SIA scenario will be introduced, mathematically described, and simulated in Sections 5.1 and 5.2 to frame the problem. Potential solutions will be discussed in Section 5.3 including driver training and active braking control. An active steering controller designed to mitigate the dangers of SIAs will

be presented and evaluated in Section 5.4 with representative numerical results for common operating scenarios.

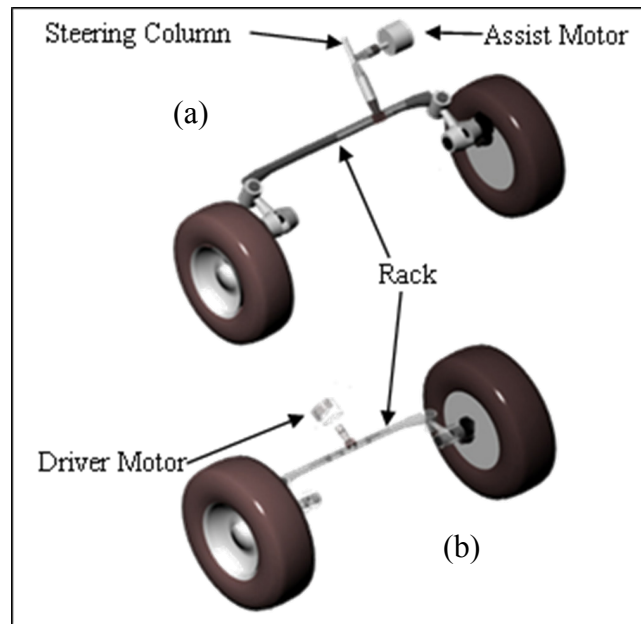


Figure 5.1: Configuration diagrams for an (a) electric power steering, and (b) steer-by-wire system in a ground vehicle

5.1 Description of Vehicle Behavior During a Shoulder Induced Accident

A typical SIA begins with one or more tires leaving the road surface for a number of possible reasons (refer to Figure 5.2). To correct the situation, the driver commands the vehicle back towards the paved road surface. The tire sidewalls catch the lip of the shoulder as they make contact, and the vehicle's lateral motion is suddenly halted due to the elevation difference as shown in Figure 5.3. As the driver increases the steering angle, the sidewalls continue to snag on the shoulder until a sufficient steering angle is provided to overcome the elevation difference and return to the road surface. The front wheels are now steered at a high angle, and if the

vehicle speed is high enough, then the vehicle will dart across the road with a minimal window for the driver to react (refer to Figure 5.4).



Figure 5.2: Passenger vehicle with two tires off the road surface



Figure 5.3: Front tire caught against the road shoulder prior to the vehicle's return to the road surface



Figure 5.4: Vehicle immediately after re-entry onto the road surface with a large commanded front wheel steer angle

What happens beyond this point depends on the driver's reaction time, operating skills, experience, and road conditions. If the driver's reaction is too slow or insufficient, the vehicle will likely strike an oncoming vehicle or an object on the far side of the road (refer to Figure 5.5). More likely, the driver will overreact, sending the vehicle into a skid and/or leaving the road surface once again. Since the vehicle will be in an unstable mode, the driver has a much greater chance of colliding with an object once the vehicle leaves the road surface. Furthermore, the vehicle runs a high risk of overturning either from the skid (high CG vehicles) or from tripping once the vehicle leaves the road surface (all vehicles).



Figure 5.5: Vehicle less than one second after re-entry with large yaw angle and approaching roadway double solid line

The primary factors that turn this seemingly mild event into a dangerous possible loss of vehicle control situation are the high steering angle, often excessive vehicle speed during the maneuver, and slow/improper driver reaction just after the vehicle returns to the road surface. The high steering angle is unavoidable in this scenario; however, it can be reduced with some countermeasures. For example, two possible methods include slower vehicle speeds and “getting a run” at the shoulder lip rather than approaching it gradually. Both require a smaller steering wheel angle to return all tires to the road surface. The proper procedure for returning to the road in this scenario is to slow down to a near stop before attempting to traverse the elevation difference. Although this sounds logical, due to shock, impatience, ignorance, and/or necessity (e.g., imminent obstacles), drivers attempt to return to the road surface at excessive speeds. While requiring a larger steering angle, higher speeds also reduce the driver’s reaction time while increasing the risk of losing vehicle control.

Once the vehicle returns to the road surface at speed, the driver is typically surprised by the sudden yaw rate (due to the high steering angle) and may have a delayed reaction due to human response characteristics. The vehicle is now in a state that is typically outside the driver's realm of vehicular experience. This is a dangerous vehicle operating condition since the driver can become a destabilizing disturbance within the human-machine system. The key to mitigating these accidents is to prevent the vehicle's response from departing the typical safety region. This can be accomplished through active steering/speed intervention during the incident and/or increasing the driver's experience through focused classroom, simulator, and test track training.

5.2 Shoulder Induced Accident Vehicle Dynamics

To establish a basis to understand run-off-road events and active steering intervention, the governing equations of motion for a reduced-order chassis platform will be presented. It shall be assumed that the vehicle's behavior immediately following the return to the roadway can be modeled as a J-turn steering event (i.e., fixed steering wheel input applied quickly and held until vehicle reaches steady state). To demonstrate the severity of this steering maneuver, a two degree-of-freedom chassis model (refer to Figure 5.6) has been selected similar to the formulation by Yih *et al.* (2005) except with the cornering stiffnesses defined on a per tire basis rather than per axle. The front and rear slip angle, α_f and α_r , can be expressed as

$$\alpha_f = \delta - \frac{v_y + a\dot{\psi}}{v_x}, \quad \alpha_r = \frac{b\dot{\psi} - v_y}{v_x} \quad (5.1)$$

where v_x and v_y denote the longitudinal and lateral velocities. The variable $\dot{\psi}$ represents the vehicle yaw rate. The parameters a and b correspond to the distances from the front and rear axles to the center of gravity (CG) at point O, and δ is the steered front road wheel angle.

Using a linear approximation to express the tire cornering stiffnesses, $C_{\alpha f}$ and $C_{\alpha r}$, the front and rear lateral tire forces, F_{yf} and F_{yr} , become

$$F_{yf} = 2C_{\alpha f}\alpha_f, \quad F_{yr} = 2C_{\alpha r}\alpha_r \quad (5.2)$$

The lateral force and moment equations for the platform may be written using Newton's Law about the center of gravity at point O in Figure 5.6 as

$$m(\dot{v}_y + \dot{\psi}v_x) = F_{yf} + F_{yr} \quad (5.3a)$$

$$I\ddot{\psi} = aF_{yf} - bF_{yr} \quad (5.3b)$$

where m and I represent the vehicle's mass and moment of inertia, respectively.

The expressions in equations (5.1), (5.2), and (5.3) may be combined and then substitute the angular side-slip angle, $\beta = \tan^{-1}\left(\frac{v_y}{v_x}\right) \cong \left(\frac{v_y}{v_x}\right)$, to eliminate v_y . The substitution for \dot{v}_y may be continued with $\dot{v}_y \cong \dot{v}_x\beta + v_x\dot{\beta} \cong v_x\dot{\beta}$ since $\dot{v}_x = 0$ as the

longitudinal velocity was assumed to be constant. The differential equations for the vehicle's yaw and side slip angles may now be rewritten as

$$m\dot{\beta} + \frac{2\beta}{v_x}(C_{\alpha f} + C_{\alpha r}) + \dot{\psi} \left[m + \frac{2}{v_x^2}(aC_{\alpha f} - bC_{\alpha r}) \right] = \frac{2C_{\alpha f}}{v_x} \delta \quad (5.4a)$$

$$I\ddot{\psi} + \frac{2\dot{\psi}}{v_x}(a^2C_{\alpha f} + b^2C_{\alpha r}) + 2\beta(aC_{\alpha f} - bC_{\alpha r}) = 2aC_{\alpha f}\delta \quad (5.4b)$$

The equations (5.4) can be rewritten in state space form as

$$\begin{bmatrix} \dot{\beta} \\ \ddot{\psi} \end{bmatrix} = \begin{bmatrix} \frac{2}{mv_x}(C_{\alpha f} + C_{\alpha r}) & 1 + \frac{2}{mv_x^2}(aC_{\alpha f} - bC_{\alpha r}) \\ \frac{2}{I}(aC_{\alpha f} - bC_{\alpha r}) & \frac{2}{Iv_x}(a^2C_{\alpha f} + b^2C_{\alpha r}) \end{bmatrix} \begin{bmatrix} \beta \\ \dot{\psi} \end{bmatrix} + \begin{bmatrix} \frac{2C_{\alpha f}}{mv_x} \\ \frac{2aC_{\alpha f}}{I} \end{bmatrix} \delta \quad (5.5)$$

As a two degree of freedom handling model, the velocity, v_x , was assumed to be constant ($\dot{v}_x = 0$) in equation (5.5) which suggests no change in vehicle speed during the short duration event. To transform the state variables β and ψ into the global X and Y coordinate system, the following equations were used

$$\dot{X} = v_x \cos(\beta + \psi), \quad X(t) = \int_{t_o}^t \dot{X} d\tau + X(t_o) \quad (5.6a)$$

$$\dot{Y} = v_x \sin(\beta + \psi), \quad Y(t) = \int_{t_o}^t \dot{Y} d\tau + Y(t_o) \quad (5.6b)$$

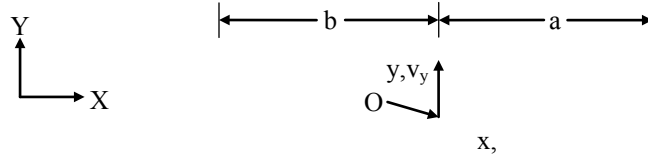


Figure 5.6: Low order vehicle model with front and rear tire slip angles, yaw angle, and sideslip angle with commanded speed and steer angle

To investigate a sudden return to the road surface in a shoulder induced accident, these dynamics were used to simulate a standard J-turn step steering input maneuver. The model parameters corresponded to a generic 4-door sedan traveling at $v_x = 72$ kph with a step steering input of $\delta_{sw} = 90^\circ$ (1.57 rad) at $t = 0$ seconds. Using a steering gearbox ratio of 18:1 ($\bar{K} = 0.055$), the front road wheel angle was $\delta = 5^\circ$ (0.087 rad). The vehicle's longitudinal-lateral trajectory, shown in Figure 5.7, demonstrates the severity of the incident without driver correction. The vehicle quickly darts for the centerline, reaching it after only $\Delta t = 1$ second and $X = 20m$ of longitudinal distance traveled. To emphasize the small window that the driver has to react in a potential SIA, the lateral position of the vehicle is plotted against time in Figure 5.8. The correction window is less than a second in duration. The vehicle attains a large yaw angle of $\psi = 21^\circ$ (0.37 rad) at $t = 1$ second as shown in Figure 5.9 with a yaw rate of $\dot{\psi} = 23$ deg/sec (0.44 rad/sec).

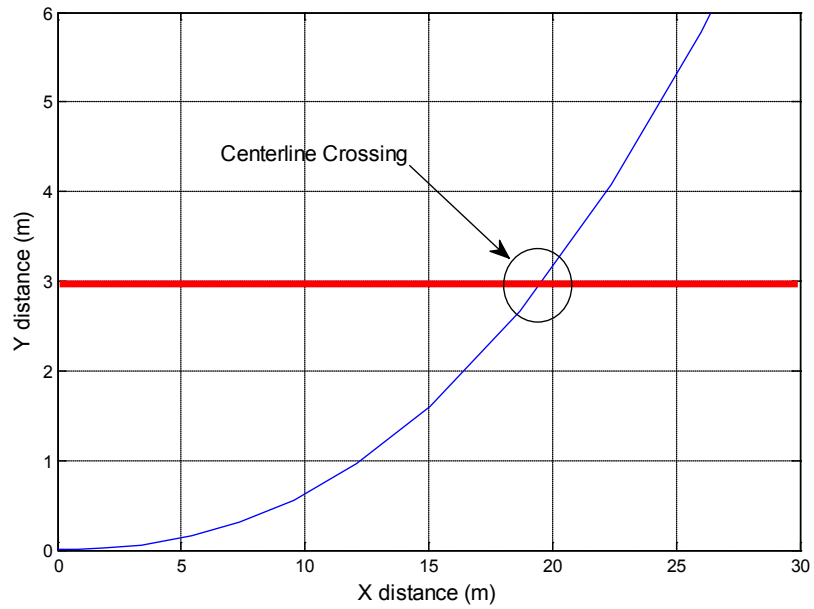


Figure 5.7: Vehicle trajectory during an emulated shoulder induced accident (simulated J-turn); roadway double solid line at 3 meters crossed by vehicle traveling at 72 kph

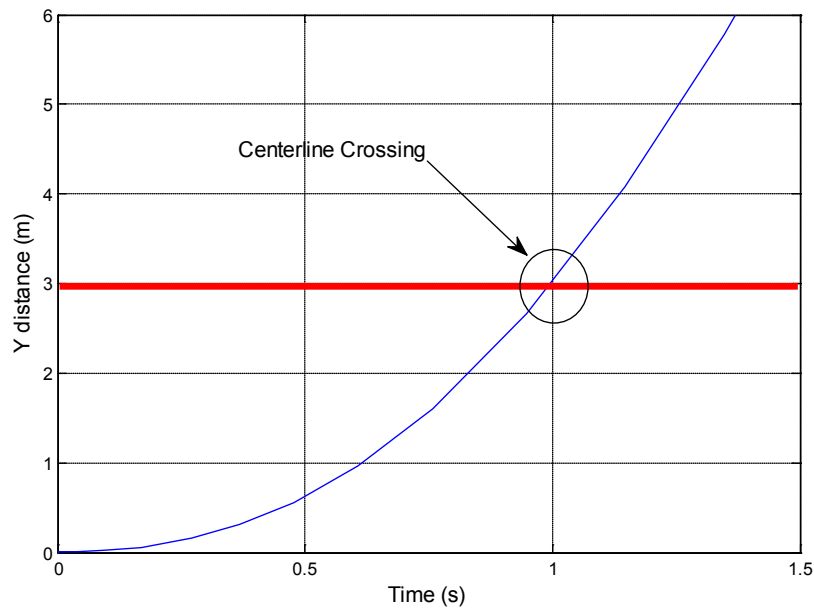


Figure 5.8: Lateral vehicle position versus time for shoulder induced accident; roadway double solid line crossed within one second for vehicle traveling at 72 kph

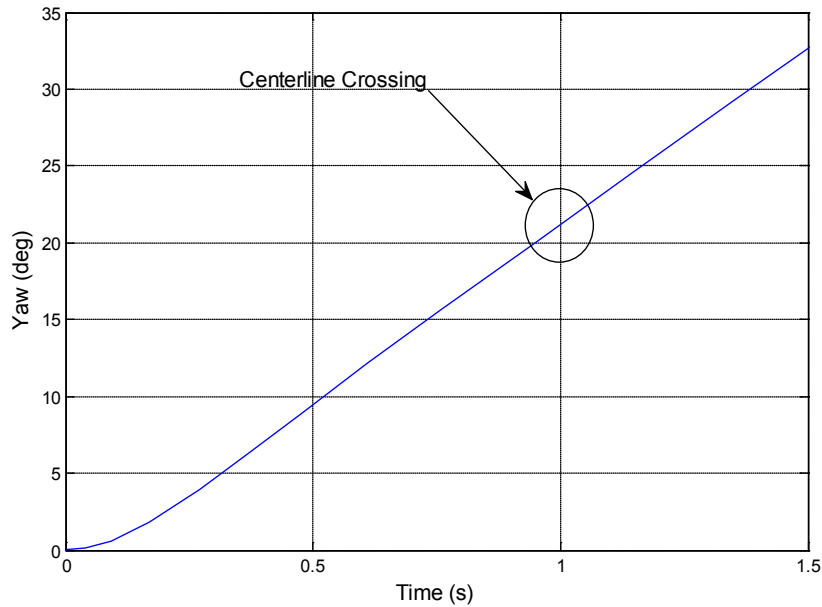


Figure 5.9: Yaw versus time for shoulder induced accident; roadway centerline crossed at $t = 1$ second for vehicle traveling at 72 kph

Now that the cause and severity of a SIA is known, potential steps to mitigate the danger of these accidents can be investigated. The following section will examine the three potential phases of intervention and several paths that can be taken to address them.

5.3 Training and Active Control for SIA Mitigation

A number of opportunities exist to intervene in a likely shoulder induced accident (SIA). In descending order of attractiveness they are: (i) before the vehicle first leaves the road surface, (ii) while the vehicle's tires are off the road surface, and (iii) the short window immediately after the vehicle returns to the road surface. Although important, the first opportunity is not the focus of this research because it is

in the realm of human factors and standard electronic stability control systems. In the second intervention window (one or more tires off the road surface), there are opportunities to slow the vehicle down either through an active braking system and/or driver education training. Active steering intrusion is not recommended in the window since the driver's intention cannot be fully identified at this point.

The third intervention window has the greatest potential for active steering to mitigate SIAs. This window requires an immediate reaction from the driver to straighten the steering wheel and avoid losing control of the vehicle after returning to the roadway. With proper training and experience, a driver can do this maneuver unassisted. However, the current driver education infrastructure does not typically support this level of training through driving simulator and/or real world driving time on a closed track. Instead of requiring an experienced response from the driver, an active braking or steering system could intervene and make the necessary corrections before the driver realizes that life threatening danger is imminent. The education and braking approaches will now be examined briefly, followed by active steering in the next section.

Run-Off-Road Driver Training

Driver training can be effectively implemented with “hands on” hardware-in-the-loop simulator and/or closed course vehicle exercises. Classroom driver education already exists in many high schools to provide a medium for increasing awareness of

driving dangers including ROR incidents. Although this may be covered lightly in the current system, the severity is often not fully realized by licensed drivers. The two major problems in ROR crashes from the standpoint of human factors are overconfidence combined with inexperience. Effective classroom education cannot typically provide drivers with extensive experience, but it could make drivers more cautious in a ROR event. Classroom instruction should offer drivers a greater respect for the potential dangers along with a mental procedure for responding in the safest manner possible. Although driver education is not specifically an engineering problem, it must be taken into account and properly researched.

The most effective training approach requires automotive simulators and/or in-vehicle experience in a safe, controlled, closed track environment. Special equipment (private roadways, outriggers, instructors) could help to duplicate the primary factors involved in returning to the road safely. Drivers would experience the excessive steering angles required to return to the road followed by the sudden yaw of the vehicle as it clears the obstruction. This would offer drivers more respect for potential dangers and provide them with valuable experience. Further, ROR training could be combined with other car control training programs to increase the overall skill and experience of drivers.

Active Braking Control

During the second intervention phase (wheels off the road surface), there is a potential for braking control to be utilized to reduce the vehicle's speed to make the return maneuver safer. This control system would apply a uniform deceleration through the antilock brake system and illuminate a dashboard warning light to notify the driver of danger. Yi and Chung (2001) developed a braking control law for collision avoidance that could be adapted for this situation. Their control law used a vehicle braking model to optimize safety and comfort in an automatic braking situation. A future research contribution would be the identification of situations in which the vehicle has unintentionally left the road surface. Tire vertical travel sensors could be employed so that the road surface may be evaluated, and the control algorithm triggered when a differential road surface has been detected.

5.4 Active Steering Control

An active steering control strategy may be developed to mitigate the danger of a shoulder induced accident after it has been initiated. A schematic of the proposed strategy has been displayed in Figure 5.10. The determination of driver intent requires an understanding of the perceived road conditions. All drivers will have an inherent delay in sensing changing road conditions. Although an active steering controller could quickly adjust to changing road conditions, the supplied input may not reflect the output desired by the driver. Consequently, two sets of parameters

must be calculated for the tire/road interface's lateral handling characteristics: (a) the estimated vehicle parameters, \hat{C}_{af} and \hat{C}_{ar} , and (b) the driver's perceived vehicle parameters, \tilde{C}_{af} and \tilde{C}_{ar} . The variables C_{af} and C_{ar} are the front and rear tire cornering stiffnesses. The symbol $\hat{}$ denotes the estimate of the cornering stiffness, while the symbol $\tilde{}$ represents the driver's perceived cornering stiffness. One method to predict the driver's perceived parameters is through a time delay, τ , of the vehicle parameters, $\tilde{C}_{af} = \hat{C}_{af}(t - \tau)$ and $\tilde{C}_{ar} = \hat{C}_{ar}(t - \tau)$. The current steering wheel input, δ_{sw} , may be combined with the perceived vehicle parameters, \tilde{C}_{af} and \tilde{C}_{ar} , to determine the driver's intention. This becomes the steering controller's target to track through the commanded front wheel angle, δ , to realize a stable vehicle.

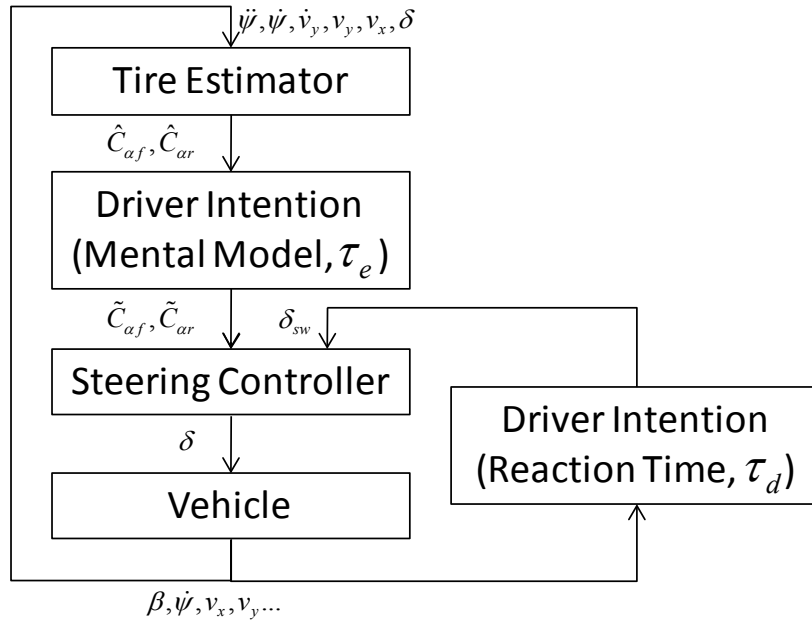


Figure 5.10: Schematic diagram of active steering controller with driver steering input angle δ_{sw} being supplemented by the steering controller to create the front wheel angle δ

Cornering Stiffness Estimation

The success of an active steering controller required the accurate estimation of the lateral tire/road force, F_y . The longitudinal capability of the tires, F_x , was not estimated since the recovery event was assumed to occur at a constant velocity ($\dot{v}_x = 0$), and lateral motion was deemed critical. To be compatible with the two degree-of-freedom chassis model in Section 5.2, the cornering stiffnesses, $C_{\alpha f}$ and $C_{\alpha r}$, were chosen as the vehicle parameters to estimate since they predominantly dictate the vehicle's lateral response. The selected estimation technique was based on Sierra *et al.* (2006) who compared multiple cornering stiffness estimation techniques to demonstrate their strengths and weaknesses, including the accuracy, operating range, and required sensors.

The expressions for the front and rear cornering stiffnesses may be written by substituting equation (5.2) into equation (5.3) so that

$$m(\dot{v}_y + \dot{\psi}v_x) = 2C_{\alpha f}\alpha_f + 2C_{\alpha r}\alpha_r \quad (5.7a)$$

$$I\ddot{\psi} = 2aC_{\alpha f}\alpha_f - 2bC_{\alpha r}\alpha_r \quad (5.7b)$$

Next, equation (5.1) may be substituted into equation (5.7) to obtain

$$m(\dot{v}_y + \dot{\psi}v_x) = 2C_{\alpha f} \left(\delta - \frac{v_y + a\dot{\psi}}{v_x} \right) + 2C_{\alpha r} \left(\frac{b\dot{\psi} - v_y}{v_x} \right) \quad (5.8a)$$

$$I\ddot{\psi} = 2aC_{\alpha f} \left(\delta - \frac{v_y + a\dot{\psi}}{v_x} \right) - 2bC_{\alpha r} \left(\frac{b\dot{\psi} - v_y}{v_x} \right) \quad (5.8b)$$

The cornering stiffnesses, $C_{\alpha f}$ and $C_{\alpha r}$, may be isolated by solving for these two unknowns in equations (5.8a) and (5.8b) such that

$$C_{\alpha f} = \frac{1}{2} \frac{(b\dot{v}_y m + b\dot{\psi} m v_x + I\ddot{\psi})v_x}{(-v_y - \dot{\psi}a + \delta v_x)(a+b)} \quad (5.9a)$$

$$C_{\alpha r} = \frac{1}{2} \frac{(a\dot{\psi} m v_x + a\dot{v}_y m - I\ddot{\psi})v_x}{(\dot{\psi}b - v_y)(a+b)} \quad (5.9b)$$

Note that these two expressions require knowledge of the simulated vehicle model states $(\dot{\psi}, \ddot{\psi})$ and (v_y, \dot{v}_y) .

Sierra *et al.* (2006) noted that this technique was unreliable when the front and rear slip angles approached zero, $\alpha_f = \alpha_r \cong 0$. Therefore, estimation was not performed when the steering was on-center, $\delta_{sw} \cong 0$, which corresponds to “no commanded” lateral motion. For a shoulder induced accident scenario, the driver typically commands a large steering wheel angle, $\delta_{sw} \neq 0$, and maintains this posture even once the vehicle returns to the road surface. Therefore, this constraint does not present a limitation to the target application.

The front and rear tire cornering stiffnesses, $C_{\alpha f}$ and $C_{\alpha r}$, were predicted using a Kalman filter approach to obtain the estimated variables $\hat{C}_{\alpha f}$ and $\hat{C}_{\alpha r}$. To ensure accurate and stable estimation, two specific thresholds were implemented. The estimation was only activated with front road wheel angles and angular velocities of $|\delta| \geq 0.833^\circ$ (0.015 rad), $|\delta_{sw}| \geq 15^\circ$ (0.26 rad), and $|\dot{\delta}| \leq 2.222 \text{ deg/s}$ (0.078 rad/s),

$|\dot{\delta}_{sw}| \leq 40 \text{ deg/s}$ (1.40 rad/s), respectively. Specifically, the front road wheel angle threshold was set to ensure that the vehicle was not traveling in a straight line during estimation. Further, the road wheel angular velocity threshold was set to temporarily ignore transient steering maneuvers with large magnitudes. In general, the bicycle model approach loses accuracy during rapid steering inputs.

The basis to estimate the tire cornering stiffnesses will now be presented. The continuous and discrete Kalman filter problems were reviewed by Brown and Hwang (1997). First, the discrete Kalman filter, originally formulated by Kalman (1960), will be presented. Consider the discrete dynamic system description

$$x_k = Ax_{k-1} + w_{k-1} \quad (5.10a)$$

$$z_k = Hx_k + v_k \quad (5.10b)$$

where the system state and measurement vectors are $x_k \in \mathfrak{R}^n$ and $z_k \in \mathfrak{R}^m$. The $n \times n$ state matrix A relates x_{k-1} to x_k , and the $m \times n$ output matrix H relates the state x_k to the measurement vector z_k . The parameters w_k and v_k represent the white process noise on the state and the white measurement noise, respectively. The covariance matrices for w_k and v_k become

$$E[w_k w_i^T] = \begin{cases} Q_k, & i = k \\ 0, & i \neq k \end{cases} \quad (5.11a)$$

$$E[v_k v_i^T] = \begin{cases} R_k, & i = k \\ 0, & i \neq k \end{cases} \quad (5.11b)$$

$$E[w_k v_i^T] = 0, \text{ for all } k \text{ and } i \quad (5.11c)$$

where Q ($n \times n$) is the process noise covariance and R ($m \times m$) is the measurement noise covariance. The *a priori* and *a posteriori* estimation errors, e_k^- and e_k , may be defined as

$$e_k^- = x_k - \hat{x}_k^- \quad (5.12a)$$

$$e_k = x_k - \hat{x}_k \quad (5.12b)$$

where $\hat{x}_k^- \in \mathfrak{R}^n$ is the *a priori* state estimate and $\hat{x}_k \in \mathfrak{R}^n$ is the *a posteriori* state estimate. These lead to the *a priori* and *a posteriori* error covariances

$$P_k^- = E[e_k^- e_k^{-T}] = E[(x_k - \hat{x}_k^-)(x_k - \hat{x}_k^-)^T] \quad (5.13b)$$

$$P_k = E[e_k e_k^T] = E[(x_k - \hat{x}_k)(x_k - \hat{x}_k)^T] \quad (5.13b)$$

The state estimate, \hat{x}_k , is then combined with the noisy measurement and previous estimate so that

$$\hat{x}_k = \hat{x}_k^- + K_k (z_k - H_k \hat{x}_k^-) \quad (5.14)$$

where $(z_k - H_k \hat{x}_k^-)$ is the measurement error weighted by K_k . The error covariance matrix, P_k , may be obtained by substituting equation (5.10b) into equation (5.14), and then this result into equation (5.13b) so that

$$P_k = E\{[(x_k - \hat{x}_k^-) - K_k (H_k x_k + v_k - H_k \hat{x}_k^-)] [(x_k - \hat{x}_k^-) - K_k (H_k x_k + v_k - H_k \hat{x}_k^-)]^T\} \quad (5.15)$$

With equations (5.12) and (5.13) in mind, the expected value of equation (5.15) may be determined as

$$P_k = (I - K_k H_k) P_k^- (I - K_k H_k)^T + K_k R_k K_k^T \quad (5.16)$$

This expression can be expanded using standard mathematical operations into

$$P_k = P_k^- - K_k H_k P_k^- - P_k^- H_k^T K_k^T + K_k (H_k P_k^- H_k^T + R_k) K_k^T \quad (5.17)$$

The trace of P_k may be differentiated with respect to K_k to obtain

$$\frac{d(\text{Tr}(P))}{dK_k} = -2(H_k P_k^-)^T + 2K_k (H_k P_k^- H_k^T + R_k) \quad (5.18)$$

The optimal gain may be computed by setting $\frac{d(\text{Tr}(P))}{dK_k} = 0$ so that

$$K_k = P_k^- H_k^T (H_k P_k^- H_k^T + R_k)^{-1} \quad (5.19)$$

The covariance matrix in equation (5.16) may be rewritten for the optimal gain as

$$P_k = (I - K_k H_k) P_k^- \quad (5.20)$$

The discrete Kalman filter will now be converted to continuous space. To transition to continuous space, consider the process and measurement models given in Brown and Hwang (1997) as

$$\dot{x} = Fx + Gu \quad (5.21a)$$

$$z = Hx + v \quad (5.21b)$$

where the state matrix F is $n \times n$, input vector G is $n \times 1$, and output matrix H is $m \times n$. The system state, x , and measurement vectors, z , are $x \in \mathfrak{R}^n$ and $z \in \mathfrak{R}^m$. The parameters u and v represent the white state noise and the white measurement noise, respectively with zero cross-correlation. The covariances of u and v are defined similar to equation (5.11), using Q ($n \times n$) and R ($m \times m$) as

$$E[u(t)u^T(\tau)] = Q\delta(t - \tau) \quad (5.22a)$$

$$E[v(t)v^T(\tau)] = R\delta(t - \tau) \quad (5.22b)$$

$$E[v(t)u^T(\tau)] = 0 \quad (5.22c)$$

To convert Q_k and R_k from discrete to continuous, first consider that Q_k can be written as

$$Q_k \approx \iint G(\xi)E[u(\xi)u^T(\eta)]G^T(\eta)d\xi d\eta \approx \iint G(\xi)Q\delta(t - \tau)G^T(\eta)d\xi d\eta \quad (5.23)$$

Integrating over a small Δt leads to

$$Q_k = GQG^T\Delta t \quad (5.24)$$

For R_k , the conversion to R begins with formulating v_k starting with the measurement z_k as

$$z_k = \frac{1}{\Delta t} \int_{t_{k-1}}^{t_k} z(t)dt = \frac{1}{\Delta t} \int_{t_{k-1}}^{t_k} [Hx(t) + v(t)]dt \quad (5.25)$$

and x can be considered to be constant over Δt , so that

$$z_k \approx Hx(t) + \frac{1}{\Delta t} \int_{t_{k-1}}^{t_k} v(t) dt \quad (5.26)$$

Comparing equation (5.26) with equation (5.10b) leads to the relationship which maps continuous into discrete for the measurement noise as

$$v_k = \frac{1}{\Delta t} \int v(t) dt \quad (5.27)$$

Using equation (5.11b) and equation (5.27), the discrete R_k becomes

$$R_k = E[v_k v_k^T] = \frac{1}{\Delta t^2} \iint E[v(u) v^T(v)] du dv \quad (5.28)$$

The relationship in equation (5.22b) may be substituted into equation (5.28) and integrated to obtain

$$R_k = \frac{R}{\Delta t} \quad (5.29)$$

Finally, the discrete gain K_k may be converted to continuous time by starting with equation (5.19) and substituting equation (5.29) so that

$$K_k = P_k^- H_k^T (H_k P_k^- H_k + R / \Delta t)^{-1} \approx P_k^- H_k^T R^{-1} \Delta t \quad (5.30)$$

since $R / \Delta t \gg H_k P_k^- H_k^T$. The notation for continuous time can be revised by dropping the subscripts and “-” superscripts on the right hand side

$$K_k = (P H^T R^{-1}) \Delta t \quad (5.31)$$

and let $K \equiv P H^T R^{-1}$.

The discrete error covariance, P_{k+1}^- , will now be examined with

$$\begin{aligned}
P_{k+1}^- &= A_k P_k^- A_k^T + Q_k \\
&= A_k (I - K_k H_k) P_k^- A_k^T + Q_k \\
&= A_k P_k^- A_k^T - A_k K_k H_k P_k^- A_k^T + Q_k
\end{aligned} \tag{5.32}$$

Approximating A_k as $I + F\Delta t$ and expanding equation (5.32) while ignoring the Δt^2 terms, the expression becomes

$$P_{k+1}^- = P_k^- + F P_k^- \Delta t + P_k^- F^T \Delta t - K_k H_k P_k^- + Q_k \tag{5.33}$$

Substituting equations (5.31) for K_k and (5.24) for Q_k into equation (5.33) leads to

$$\left(\frac{P_{k+1}^- - P_k^-}{\Delta t} \right) = F P_k^- + P_k^- F^T - P_k^- H_k^T R^{-1} H_k P_k^- + G Q G^T \tag{5.34}$$

Finally, taking the limit as $\Delta t \rightarrow 0$ while dropping the discrete notation and superscripts to obtain the differential equation for P as

$$\begin{aligned}
\dot{P} &= F P + P F^T - P H^T R^{-1} H P + G Q G^T \\
P(0) &= P_o
\end{aligned} \tag{5.35}$$

To form the differential equation for the state estimator, start with equation (5.14) and apply $\hat{x}_k^- = A_{k-1} \hat{x}_{k-1}$ so that

$$\hat{x}_k = \hat{x}_k^- + K_k (z_k - H_k \hat{x}_k^-) \tag{5.14}$$

$$\hat{x}_k = A_{k-1} \hat{x}_{k-1} + K_k (z_k - H_k A_{k-1} \hat{x}_{k-1}) \tag{5.36}$$

Note that $A \cong I + F\Delta t$ and neglect higher order terms so that

$$\hat{x}_k - \hat{x}_{k-1} = F\hat{x}_{k-1}\Delta t + K\Delta t(z_k - H_k\hat{x}_{k-1}) \quad (5.37)$$

Divide by Δt and take the limit as $\Delta t \rightarrow 0$ leads to the differential equation for the estimate \hat{x} given as

$$\dot{\hat{x}} = F\hat{x} + K(z - H\hat{x}) \quad (5.38)$$

The equations (5.31), (5.35), and (5.38) form the continuous Kalman filter.

For this investigation, the cornering stiffnesses, C_{af} and C_{ar} , will be estimated using the continuous Kalman filter to accommodate the inherent noise and uncertainty in the calculation technique. The state space description in this problem formulation may be stated as

$$\dot{x} = Fx + Gu \quad (5.21a)$$

$$z = Hx + v \quad (5.21b)$$

where $\hat{x} = \begin{bmatrix} \hat{C}_{af} \\ \hat{C}_{ar} \end{bmatrix}$, $F = \begin{bmatrix} 1 & 0 \\ 0 & 1 \end{bmatrix}$, $G = \begin{bmatrix} 1 & 0 \\ 0 & 1 \end{bmatrix}$, $H = \begin{bmatrix} 1 & 0 \\ 0 & 1 \end{bmatrix}$, $Q = \begin{bmatrix} Q_f & 0 \\ 0 & Q_r \end{bmatrix}$,

$R = \begin{bmatrix} R_f & 0 \\ 0 & R_r \end{bmatrix}$, and $P_0 = \begin{bmatrix} P_{01} & 0 \\ 0 & P_{02} \end{bmatrix}$. The assumption of white state and measurement

noise has again been imposed. Expanding into longhand matrix format, the equations (5.38), (5.31), and (5.35) become

$$\begin{bmatrix} \dot{\hat{C}}_{af} \\ \dot{\hat{C}}_{ar} \end{bmatrix} = \begin{bmatrix} 1 & 0 \\ 0 & 1 \end{bmatrix} \begin{bmatrix} \hat{C}_{af} \\ \hat{C}_{ar} \end{bmatrix} + \begin{bmatrix} K_f & 0 \\ 0 & K_r \end{bmatrix} \begin{bmatrix} C_{af} - \hat{C}_{af} \\ C_{ar} - \hat{C}_{ar} \end{bmatrix} \quad (5.39a)$$

$$\begin{aligned}
\begin{bmatrix} K_f & 0 \\ 0 & K_r \end{bmatrix} &= \begin{bmatrix} P_1 & 0 \\ 0 & P_2 \end{bmatrix} \begin{bmatrix} 1 & 0 \\ 0 & 1 \end{bmatrix}^T \begin{bmatrix} R_f & 0 \\ 0 & R_r \end{bmatrix}^{-1} \\
&= \begin{bmatrix} P_1 & 0 \\ 0 & P_2 \end{bmatrix} \begin{bmatrix} R_f & 0 \\ 0 & R_r \end{bmatrix}^{-1} = \begin{bmatrix} \frac{P_1}{R_f} & 0 \\ 0 & \frac{P_2}{R_r} \end{bmatrix}
\end{aligned} \tag{5.39b}$$

$$\begin{aligned}
\begin{bmatrix} \dot{P}_1 & 0 \\ 0 & \dot{P}_2 \end{bmatrix} &= \begin{bmatrix} 1 & 0 \\ 0 & 1 \end{bmatrix} \begin{bmatrix} P_1 & 0 \\ 0 & P_2 \end{bmatrix} + \begin{bmatrix} P_1 & 0 \\ 0 & P_2 \end{bmatrix} \begin{bmatrix} 1 & 0 \\ 0 & 1 \end{bmatrix} - \\
&\quad \begin{bmatrix} P_1 & 0 \\ 0 & P_2 \end{bmatrix} \begin{bmatrix} 1 & 0 \\ 0 & 1 \end{bmatrix} \begin{bmatrix} R_f & 0 \\ 0 & R_r \end{bmatrix}^{-1} \begin{bmatrix} 1 & 0 \\ 0 & 1 \end{bmatrix} \begin{bmatrix} P_1 & 0 \\ 0 & P_2 \end{bmatrix} + \\
&\quad \begin{bmatrix} 1 & 0 \\ 0 & 1 \end{bmatrix} \begin{bmatrix} Q_f & 0 \\ 0 & Q_r \end{bmatrix} \begin{bmatrix} 1 & 0 \\ 0 & 1 \end{bmatrix} \\
&= \begin{bmatrix} 2P_1 & 0 \\ 0 & 2P_2 \end{bmatrix} - \begin{bmatrix} \frac{P_1^2}{R_f} & 0 \\ 0 & \frac{P_2^2}{R_r} \end{bmatrix} + \begin{bmatrix} Q_f & 0 \\ 0 & Q_r \end{bmatrix}
\end{aligned} \tag{5.39c}$$

Equation (5.39a) leads to the set of equations

$$\dot{\hat{C}}_{\alpha f} = \hat{C}_{\alpha f} + K_f(C_{\alpha f} - \hat{C}_{\alpha f}) \tag{5.40a}$$

$$\dot{\hat{C}}_{ar} = \hat{C}_{ar} + K_r(C_{ar} - \hat{C}_{ar}) \tag{5.40b}$$

where $C_{\alpha f}$ and C_{ar} are constructed from equation (5.9) using measured vehicle operating variables including $\ddot{\psi}, \dot{\psi}, \dot{v}_y, v_y, v_x, \delta$. The K values may be simplified from equation (5.39b) to

$$K_f = \frac{P_1}{R_f} \tag{5.41a}$$

$$K_r = \frac{P_2}{R_r} \quad (5.41b)$$

The equation for P in (5.39c) becomes

$$\dot{P}_1 = 2P_1 - \frac{P_1^2}{R_f} + Q_f \quad (5.41a)$$

$$\dot{P}_2 = 2P_2 - \frac{P_2^2}{R_r} + Q_r \quad (5.41b)$$

The solutions to the Riccati equations in (5.41a) and (5.41b) were calculated numerically in Matlab/Simulink (refer to Appendix I) during the vehicle simulation.

The cornering stiffness estimator was evaluated using the CarSim version 6 software package which generated the simulated unknown vehicle dynamic behavior $(\dot{\psi}, v_y, v_x, \beta)$. A generic small sedan was selected for the vehicle database. During real-time applications, the estimated cornering stiffnesses, $\hat{C}_{\alpha f}$ and $\hat{C}_{\alpha r}$, based on the measured variables, stiffness expressions and Kalman filter, were fed into the simplified bicycle model described by equation (5.5). The output of this bicycle model, $\hat{\psi}$ and $\hat{\beta}$, was compared to the CarSim output to verify the accuracy of the estimation in terms of tire cornering stiffnesses and yaw rate.

The vehicle was driven with a $f = 0.25Hz$ sinusoidal steering input with an amplitude of $\delta_{sw} = 90^\circ$ as shown in Figure 5.11. The velocity was kept constant at $v_x = 60kph$ while the vehicle drove across a road surface with the friction coefficient

abruptly changing from $\mu = 0.85$ to $\mu = 0.3$ to $\mu = 0.85$ at $X = 300m$ and $X = 600m$, respectively. The estimator was manually tuned to $P_{01} = P_{02} = 100$, $R_f = R_r = 100$, and $Q_f = Q_r = 0.01$ to ensure a reliable estimation during static road conditions without compromising the quick response to new conditions. The initial guess for the cornering stiffness was set to $C_{\alpha_0} = [0 \ 0]^T$ as a worst case scenario, but in a practical application this would be set based on testing results.

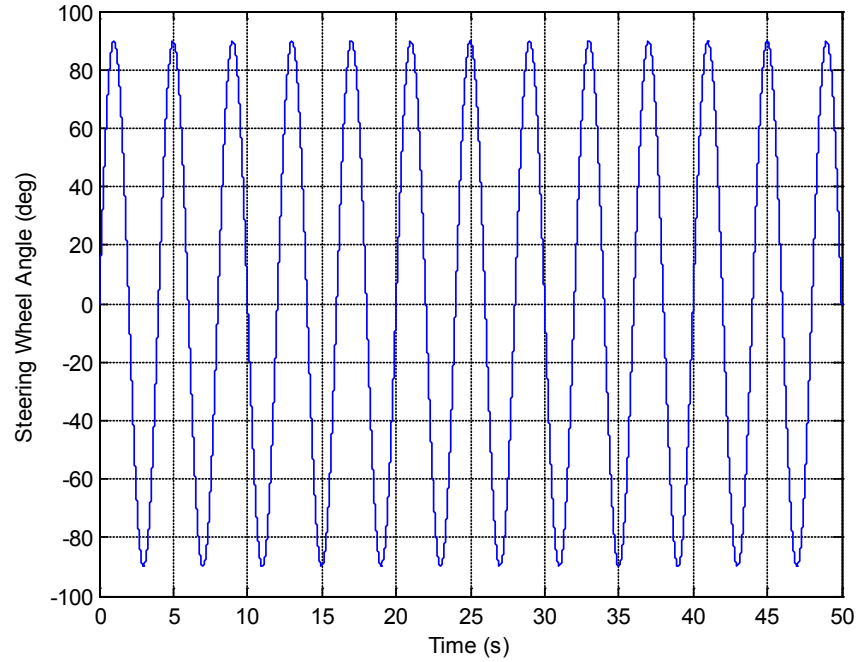


Figure 5.11: The input steering wheel angle to validate the estimation strategy for tire cornering stiffness with frequency and amplitude of $f = 0.25Hz$ and $\delta_{sw} = 90^\circ$

The estimated front and rear cornering stiffnesses have been shown in Figures 5.12 and 5.13; the subsequent yaw rate estimation and error are displayed in Figures 5.14 and 5.15. The vehicle transitioned to the $\mu = 0.3$ surface at $t \approx 19$ seconds and

returned to the $\mu = 0.85$ surface at $t \approx 38$ seconds. The transition was promptly detected by the cornering stiffness estimator within 150ms, as displayed in Figures 5.12 and 5.13. The lower cornering stiffness values may be attributed to the reduced yaw rate, yaw acceleration, lateral speed, and lateral acceleration as a result of less road friction. The effect of the road surface coefficient of friction transition on the vehicle dynamics can be observed in Figure 5.14 where the peak yaw rate, $\dot{\psi}$, was reduced by 0.15 rad/s from $\dot{\psi} = 0.39$ rad/sec to $\dot{\psi} = 0.23$ rad/sec. A reduced yaw rate was experienced due to the decreased lateral forces per lower road friction. The general agreement between the simplified and CarSim models is evident by the 6.9% maximum error on the $\mu = 0.85$ surface. Although the error in the yaw rate between the two models (refer to Figure 5.15) jumps to a significant 0.1 rad/s, this can be attributed to a time lag in the response rather than a failure in estimation. During the sample maneuver, the lateral accelerations reached as high as 0.6g as shown in Figure 5.16. This was well outside the linear range of the tires (0.3g) and was effectively a worst case scenario for the estimator.

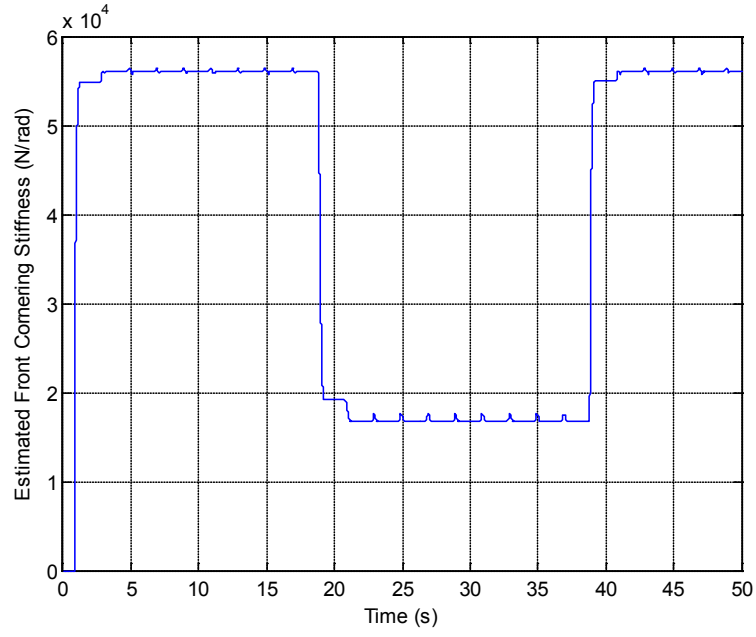


Figure 5.12: Estimated front cornering stiffness, $\hat{C}_{\alpha f}$, on a road surface changing from $\mu = 0.85$ to $\mu = 0.3$ and back with $v_x = 60kph$

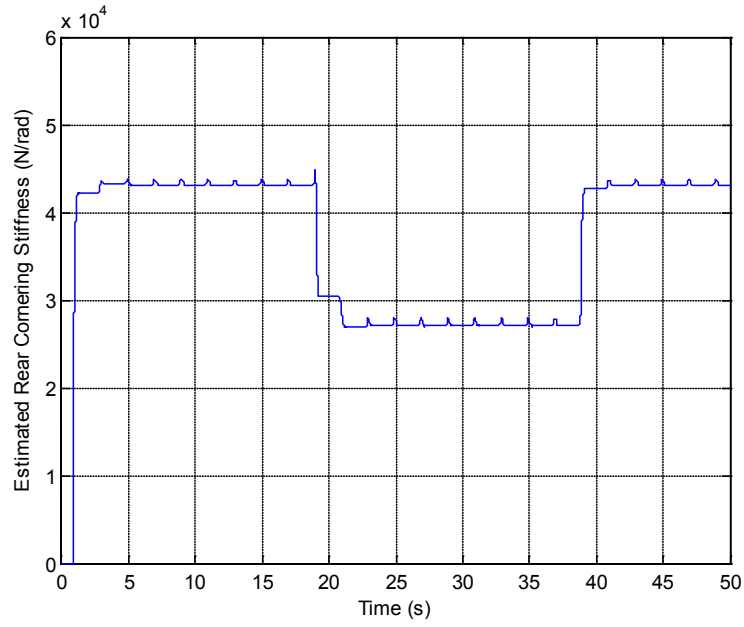


Figure 5.13: Estimated rear cornering stiffness, $\hat{C}_{\alpha r}$, on a road surface changing from $\mu = 0.85$ to $\mu = 0.3$ and back with $v_x = 60kph$

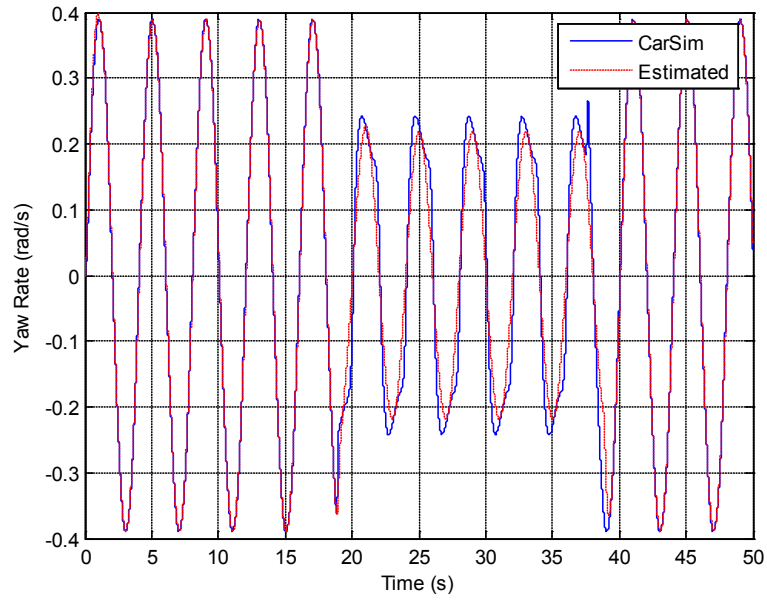


Figure 5.14: Yaw rate for the CarSim vs. estimated chassis model on a road surface changing from $\mu = 0.85$ to $\mu = 0.3$ and back with $v_x = 60kph$

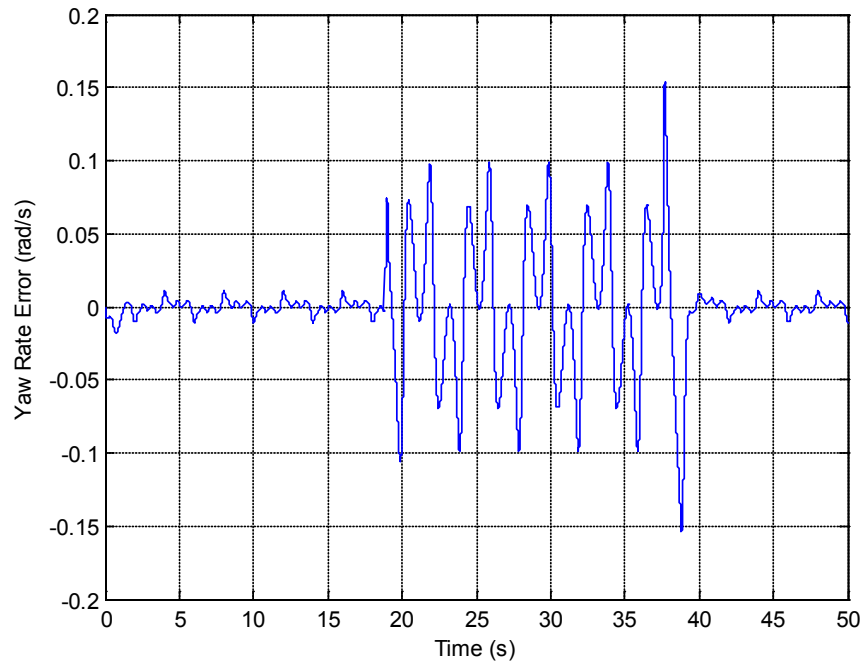


Figure 5.15: Error in yaw rate between CarSim and bicycle model on a road surface changing from $\mu = 0.85$ to $\mu = 0.3$ and back with $v_x = 60kph$

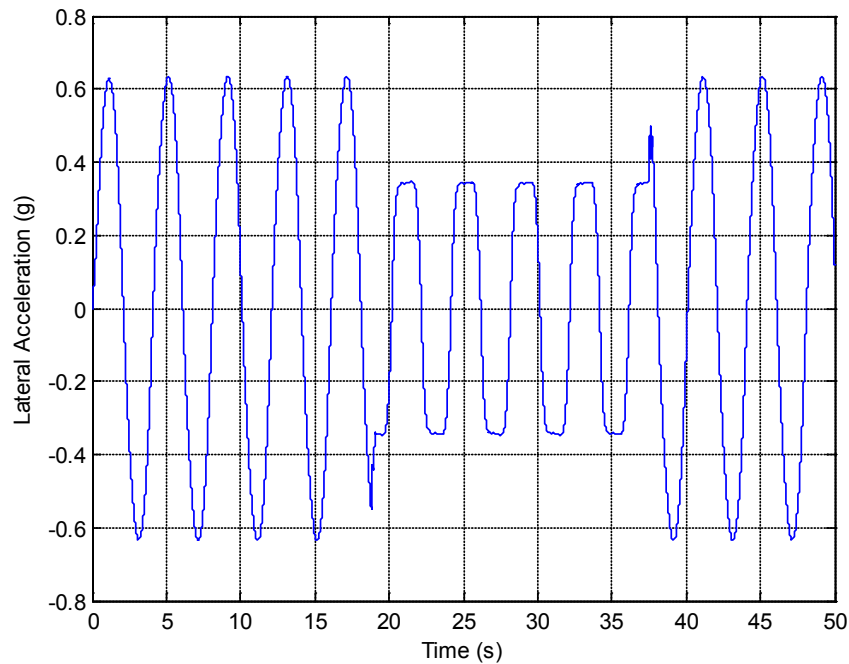


Figure 5.16: Lateral acceleration for the CarSim vehicle model on a road surface changing from $\mu = 0.85$ to $\mu = 0.3$ and back with $v_x = 60kph$

Driver Intention

The key to accident prevention is the concept of “driver intention”. What does the driver wish to accomplish? Once an onboard control system knows this, it can then determine the “best” vehicle command(s) to achieve the desired output. This tends to be a critical and difficult task given that driving remains a dynamic process with overlapping maneuvers and human judgment. For example, consider a vehicle swerving to miss a dog in the road versus swerving accidentally due to sudden changes in the road conditions. Without context, the vehicle responses may appear similar, but one swerve is desired by the driver and the other is not. To be safe and

successful, an active steering system must be able to determine the driver's intention before intervening.

In this project, the implemented approach for driver intention addresses the latter case of changing road conditions. The primary assumption (A.1) is that the road surface may change suddenly due to a run-off-road incident; however, the driver does not immediately recognize the change and continues to operate in a nominal manner. In this case, the driver's inputs will not result in the intended vehicle response. Until the driver recognizes this change in conditions, they will be driving as if the road surface has not changed. It is further assumed (A.2) that the driver supplies vehicle commands based on a mental model that lags behind the instantaneous conditions by a time, τ_e (Green, 2000). The driver intention module attempts to emulate this approach by storing the estimated $\hat{C}_\alpha(t)$ from a prior time, $t = \tau_e$.

A model for the driver's expected lateral tire stiffness value, \tilde{C}_α , may be constructed as

$$\tilde{C}_{\alpha f}(t) = \hat{C}_{\alpha f}(t - \tau_e) \quad (5.42a)$$

$$\tilde{C}_{\alpha r}(t) = \hat{C}_{\alpha r}(t - \tau_e) \quad (5.42b)$$

These values are constantly updated and represent a guess at what the driver perceives to be the road conditions. A start point does not exist; however, the controller has been formulated such that intervention only occurs when $\tilde{C}_\alpha(t) \neq \hat{C}_\alpha(t)$

(i.e., immediately following a road surface transition) as shown in Figure 5.17. During the times $t_b < t < t_c$ and $t_d < t < t_e$, the delayed cornering stiffness, \tilde{C}_α , differs from the real time estimated cornering stiffness, \hat{C}_α , so intervention occurs. The intervention continues for $\Delta t = \tau_e$, during which time the controller aims to replicate the driving conditions from the prior time period. After the $\Delta t = \tau_e$ time period, it may be assumed that the driver has recognized the changing road conditions and intervention ceases.

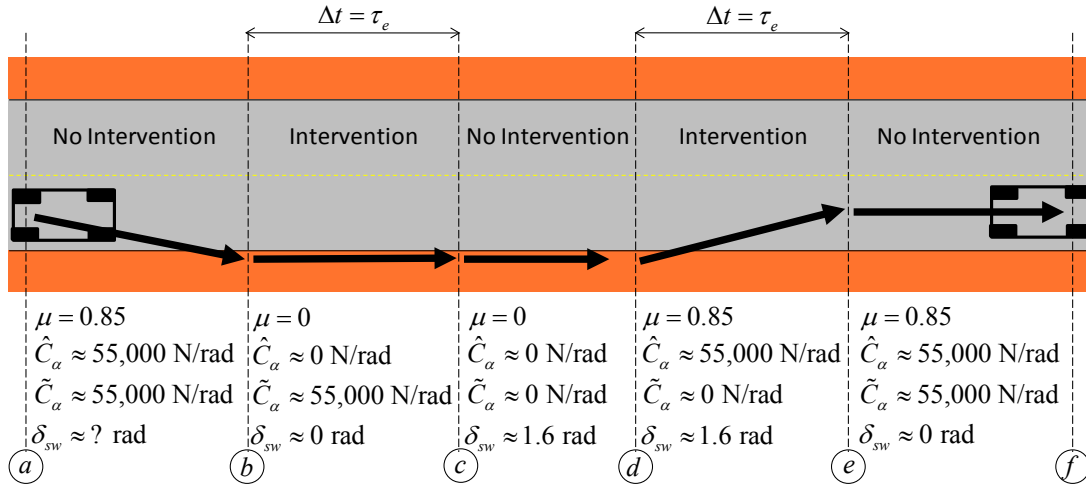


Figure 5.17: Visual representation of driver intention module showing intended intervention intervals of steering controller; controller designed to assist during the $\Delta t = \tau_e$ time period following a tire/road equivalent friction transition

Steering Control

The full state feedback control strategy, based on the bicycle model, follows the concepts proposed by Yih and Gerdes (2005). The authors created a controller which forced the vehicle to behave as if it had higher, or lower, tire cornering

stiffnesses. Specifically, the controller allowed the vehicle to be driven in low grip conditions as if it were operated on dry asphalt. For this research investigation, a similar type of functionality was desired except only during brief moments (e.g., road surface transitions such as points b and d in Figure 5.17). The Yih and Gerdes approach has been adapted to use the percent difference in driver's expected cornering stiffness, \tilde{C}_α , compared to the real-time current cornering stiffness, \hat{C}_α , to scale the steering control gains.

Consider the bicycle model from equation (5.5). Now substitute in the delayed estimated cornering stiffness, $\tilde{C}_{\alpha f}$ and $\tilde{C}_{\alpha r}$, for the front and rear cornering stiffnesses, $C_{\alpha f}$ and $C_{\alpha r}$, to realize the perceived sideslip and yaw rate derivatives as

$$\begin{bmatrix} \dot{\hat{\beta}} \\ \ddot{\hat{\psi}} \end{bmatrix} = \begin{bmatrix} \frac{2}{mv_x}(\tilde{C}_{\alpha f} + \tilde{C}_{\alpha r}) & 1 + \frac{2}{mv_x^2}(a\tilde{C}_{\alpha f} - b\tilde{C}_{\alpha r}) \\ \frac{2}{I}(a\tilde{C}_{\alpha f} - b\tilde{C}_{\alpha r}) & \frac{2}{Iv_x}(a^2\tilde{C}_{\alpha f} + b^2\tilde{C}_{\alpha r}) \end{bmatrix} \begin{bmatrix} \hat{\beta} \\ \dot{\hat{\psi}} \end{bmatrix} + \begin{bmatrix} \frac{2\tilde{C}_{\alpha f}}{mv_x} \\ \frac{2a\tilde{C}_{\alpha f}}{I} \end{bmatrix} \delta(t) \quad (5.43)$$

The parameters used for both estimation and control are given in Table 5.1 and correspond to the small sedan previously simulated in CarSim 6.

Symbol	Value	Units	Symbol	Value	Units
a	0.948	m	m	940	kg
b	1.422	m	τ_d	{1,2}	s
I	1152	kg m ²	τ_e	{1,2}	s
\bar{K}	0.55	-	v_x	60	kph

Table 5.1: Table of parameter values for a small sedan simulated in CarSim 6

Yih and Gerdes (2005) defined the variable η as the desired fixed percent change in the front tire cornering stiffness, $C_{\alpha f}$. Their stated objective was to adjust the real vehicle's front cornering stiffness, $C_{\alpha f}$, to the selected value $\tilde{C}_{\alpha f}$ through adjustment of η as

$$\tilde{C}_{\alpha f} = C_{\alpha f}(1 + \eta) \quad (5.44)$$

For this project, the variable η was adapted to represent the percent change in road conditions as evident by the front and rear tire cornering stiffnesses, $C_{\alpha f}$ and $C_{\alpha r}$, from a prior time τ_e when compared to the current time, t , so that

$$\eta = \frac{\tilde{C}_{\alpha f} + \tilde{C}_{\alpha r}}{\hat{C}_{\alpha f} + \hat{C}_{\alpha r}} - 1 \quad (5.45)$$

The steering control gains, K_β , K_ψ , and K_{sw} reflect contributions from the vehicle slip angle, yaw rate, and commanded steering angle. The full state feedback control may be defined (Yih and Gerdes, 2005) as

$$\delta = K_\psi \dot{\psi} + K_\beta \hat{\beta} + K_{sw} (\delta_{sw} \bar{K}) \quad (5.46)$$

where the individual gains become

$$K_\beta = -\eta \quad (5.47)$$

$$K_\psi = -\frac{a}{v_x} \eta \quad (5.48)$$

$$K_{sw} = (1 + \eta) \quad (5.49)$$

The parameters a and v_x represent the distance from the front axle to the CG and the longitudinal speed. The term δ is the augmented steering angle, and δ_{sw} is the driver commanded steering angle. The main advantage of full state feedback resides in the control of the slip angle, β , which increases stability over a pure yaw rate, $\dot{\psi}$, controller.

Results and Discussion

The control algorithm of equations (5.43), (5.45), (5.46), (5.47), (5.48), and (5.49) produced the variables $\hat{\beta}, \dot{\psi}, \eta, K_\beta, K_{\dot{\psi}}, K_{sw}$, and δ which were implemented in Matlab/Simulink. Concurrently, the CarSim 6 software package was applied to simulate the vehicle dynamics and generate the required system information ($\dot{\psi}, \ddot{\psi}, v_y, \dot{v}_y, v_x$). The CarSim software utility is a commercial vehicle dynamics modeling package developed by the Mechanical Simulation Corporation (Ann Arbor, MI). CarSim generates the complete vehicle dynamics (similar to in-vehicle applications with accompanying sensors) while the on-board controller design utilizes the reduced-order chassis (bicycle) model. To ensure compatibility, the parameters for the chassis model have been listed in Table 5.1.

The shoulder induced accident (SIA) event (refer to Section 5.1) was modeled as a ramp steering input, $\delta_{sw} = 0.524t$ rad/sec, with a road friction coefficient of

$\mu = 0$ to describe the tire sidewalls attempting to climb and catching on the road shoulder (i.e., wheels off road surface). When the driver commanded steering angle reached $\delta_{sw} = 1.57$ rad, the road return event occurred (i.e., the road friction coefficient was instantaneously set to $\mu = 0.85$ and all four wheels assumed to be on the road surface). The friction profile can be viewed in Figure 5.18. Points b and d represent the run off and return events, respectively, labeled in Figure 5.17. The variable τ_d was used to describe the reaction time of the driver independent from the controller assistance time, τ_e , used in the controller. These variables are summarized in Table 5.2. This approach was based on the perception and reaction delay presented by Green (2000). After the road return event transpired, the steering angle was held constant for a time τ_d , and then returned to $\delta_{sw} = 0$ within 0.5s afterwards. In other words, once the theoretical driver recognized the road surface change, they responded by returning the steering wheel to the center position without taking any further evasive maneuvers. However, the range of potential evasive maneuvers may be viewed as unlimited; consequently, this basic and repeatable response was selected for initial study.

Symbol	Description and Units	Values	Cases
τ_d	Driver reaction time (s) – Time period it takes for driver to recognize and respond to driving event	2	#1-#3
		1	#4-#6
τ_e	Controller assistance time (s) – Time period during which controller intervenes after road transition is detected	2	#2, #5
		1	#3, #6

Table 5.2: Summary of driver and controller time variables showing symbol, unit, and case values

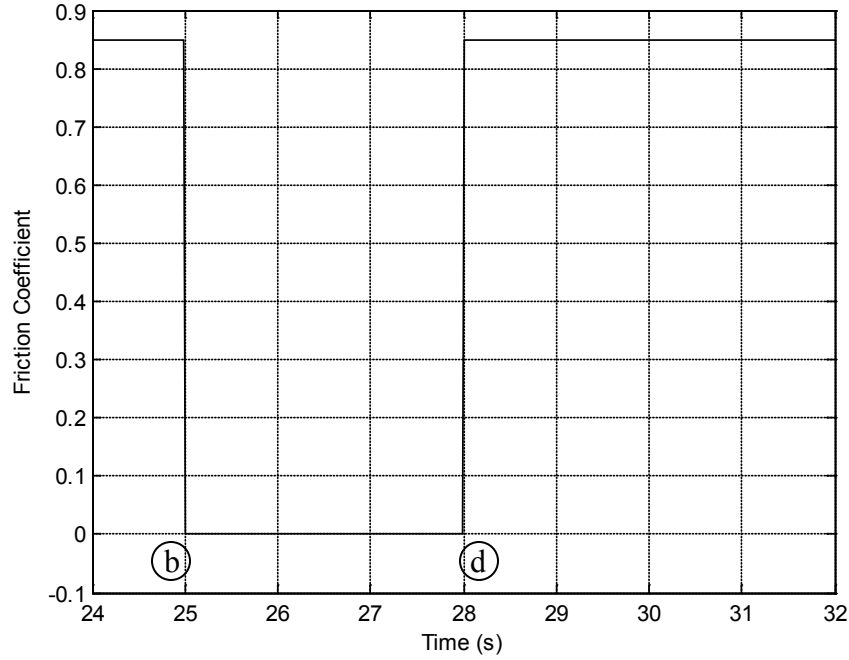


Figure 5.18: Friction coefficient during simulated shoulder induced maneuver stepping from $\mu = 0.85$ to $\mu = 0$ (wheels off road surface) at $t = 25s$ and back to $\mu = 0.85$ (wheels on road surface) at $t = 28s$

The numerical results were divided into six cases and grouped into two subsets. The first set of results (Cases #1-#3) represented an “inattentive driver” with a slow reaction time of $\tau_d = 2s$. The results for Cases #1-#3 have been shown in Figures 5.19-5.24. The first case, Case #1, was the baseline result without controller intervention; the following two cases were the results available with the controller tuned to $\tau_e = 2s$ (Case #2) and $\tau_e = 1s$ (Case #3). Figure 5.19 shows the road wheel angle with and without controller intervention. The points b, d, and e represent the run off, return, and driver correction points corresponding to the same points in Figure 5.17. The solid line is the untouched steering input from the driver, which

stayed constant between points d and e for a time $\Delta t = \tau_d$ representing the delay before the driver recognized a change in road conditions. The duration of intended controller interventions, τ_e , have been labeled for the time period between points d and e. For the $\tau_e = 1s$ case, the road wheel angle intervened for approximately $\Delta t = 1s$ and then began to return to the commanded angle just after $t = 29s$. The $\tau_e = 2s$ case intervened for the full $\Delta t = 2s$ between points d and e. The controller also intervened between points b and d following the initial transition to the low friction road surface. The controller compensated in the opposite direction during this transition, which would be expected upon inspection of equations (5.45) and (5.46). However, the low friction road surface coefficient minimized the vehicle's lateral response.

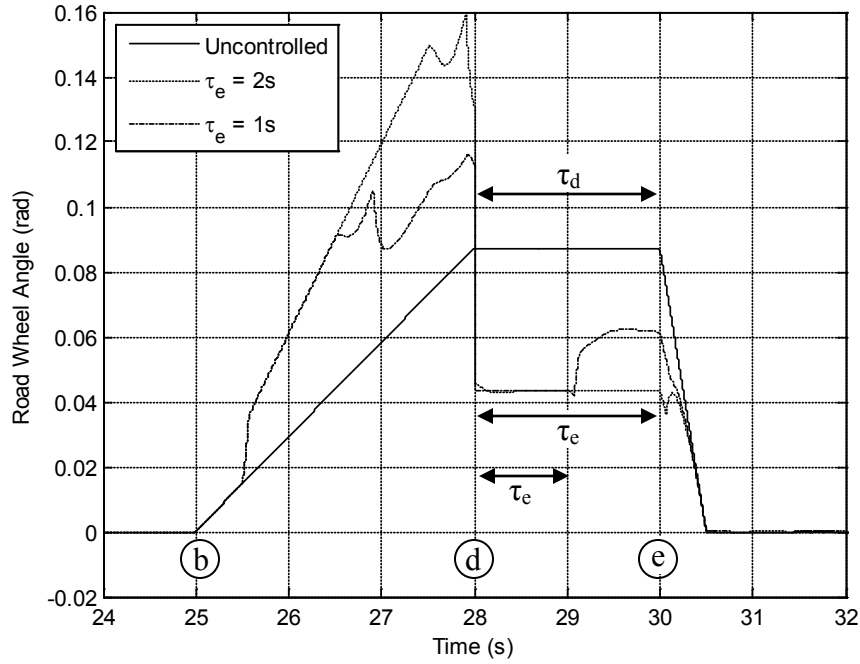


Figure 5.19: Road wheel angle, δ , during SIA event with driver reaction time of $\tau_d = 2s$ and controller settings of $\tau_e = 0s$ (Case #1 - uncontrolled baseline), $\tau_e = 2s$ (Case #2), and $\tau_e = 1s$ (Case #3)

In Figure 5.20, the baseline (Case #1) offered a peak yaw rate of $\dot{\psi} = 0.42$ rad/sec, while Cases #2 and #3 reduced the peak yaw rate to $\dot{\psi} = 0.21$ rad/sec and $\dot{\psi} = 0.28$ rad/sec, respectively. The controller in Case #2 was tuned to match the worst case inattentive driver scenario, so it was expected to have the best response. The intervention lasted for the full duration of the event (from point d to point e or $t = 2s$). The vehicle's final heading angle was reduced from $\psi = 0.86$ rad for Case #1 to $\psi = 0.47$ rad for Case #2; a 45% reduction. Case #3 was tuned for a more attentive driver, which resulted in a one second shorter duration intervention interval. This approach offered a higher peak yaw rate, $\dot{\psi}$, than Case #2. However, the

mitigating effects of Case #3 cannot be overlooked since the severity of the maneuver was reduced similarly to Case #2 with half the intervention time. The final yaw angle of Case #3 was $\psi = 0.52$ rad, a reduction of 40% from the baseline. Figures 5.21 and 5.22 show the vehicle slip angle, β , and the vehicle lateral velocity, v_y , during the maneuvers to demonstrate that the directional stability of the vehicle was not compromised to improve a single variable response. The consistent directional stability was largely attributed to the use of full state feedback instead of pure yaw rate feedback. Figures 5.23 and 5.24 display the lateral position of the vehicle with respect to time and longitudinal position, respectively. The two controlled cases resulted in nearly identical lane crossing times of $\Delta t_c = 1.30s$ and $\Delta t_c = 1.31s$ for Case #2 and Case #3. These results were improvements of approximately 0.3s (30%) over the baseline (Case #1) of $\Delta t_c = 1.01s$.

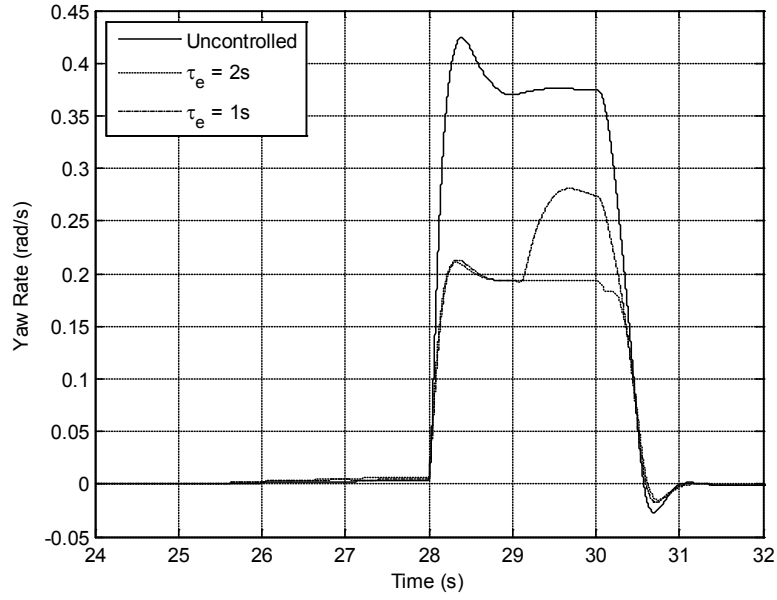


Figure 5.20: Yaw rate, $\dot{\psi}$, during SIA event with driver reaction time of $\tau_d = 2s$ and controller settings of $\tau_e = 0s$ (Case #1 - uncontrolled baseline), $\tau_e = 2s$ (Case #2), and $\tau_e = 1s$ (Case #3)

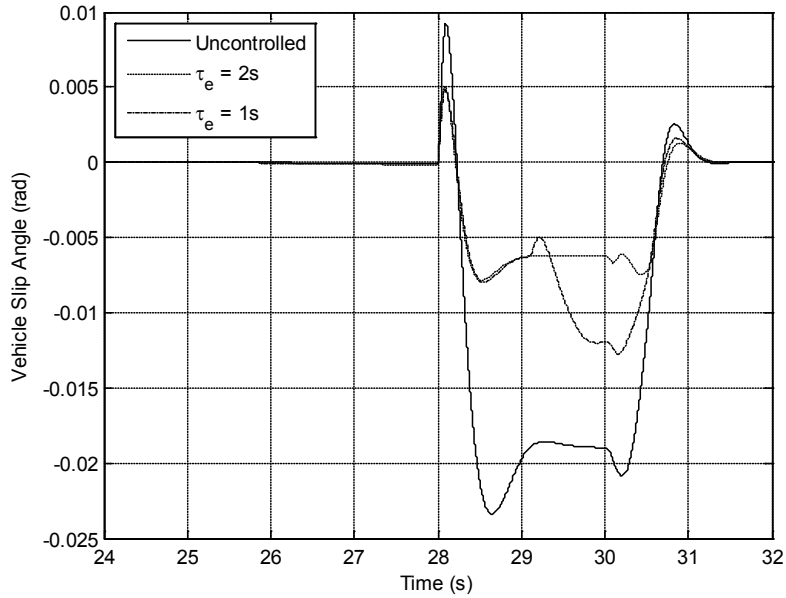


Figure 5.21: Vehicle slip angle, β , during SIA event with driver reaction time of $\tau_d = 2s$ and controller settings of $\tau_e = 0s$ (Case #1 - uncontrolled baseline), $\tau_e = 2s$ (Case #2), and $\tau_e = 1s$ (Case #3)

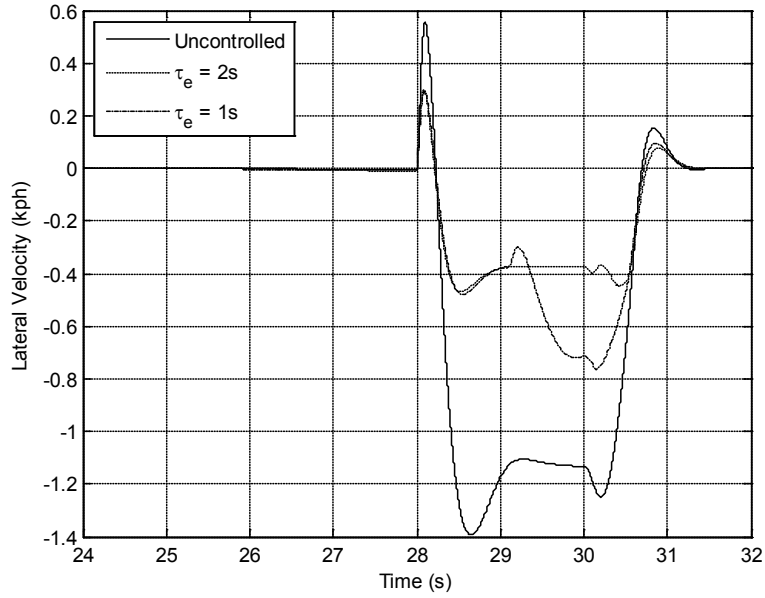


Figure 5.22: Lateral velocity, v_y , during SIA event with driver reaction time of $\tau_d = 2s$ and controller settings of $\tau_e = 0s$ (Case #1 - uncontrolled baseline), $\tau_e = 2s$ (Case #2), and $\tau_e = 1s$ (Case #3)

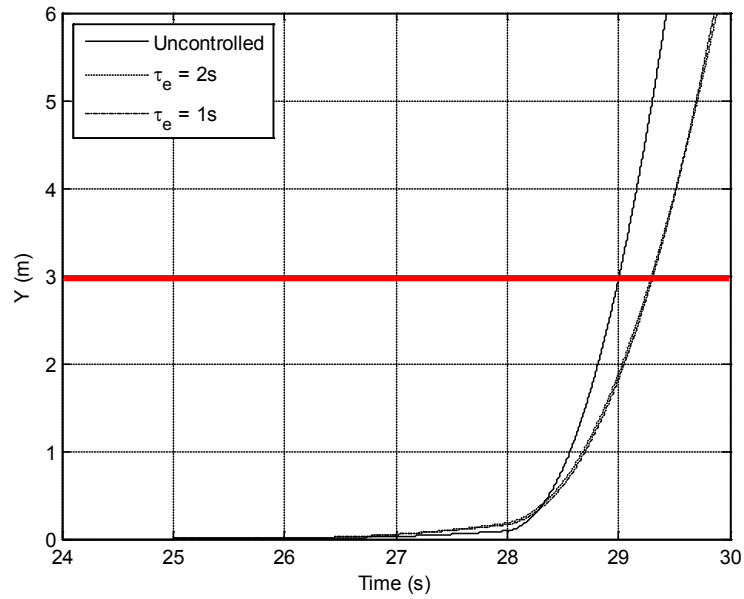


Figure 5.23: Lateral position, Y , during SIA event with driver reaction time of $\tau_d = 2s$ and controller settings of $\tau_e = 0s$ (Case #1 - uncontrolled baseline), $\tau_e = 2s$ (Case #2), and $\tau_e = 1s$ (Case #3)

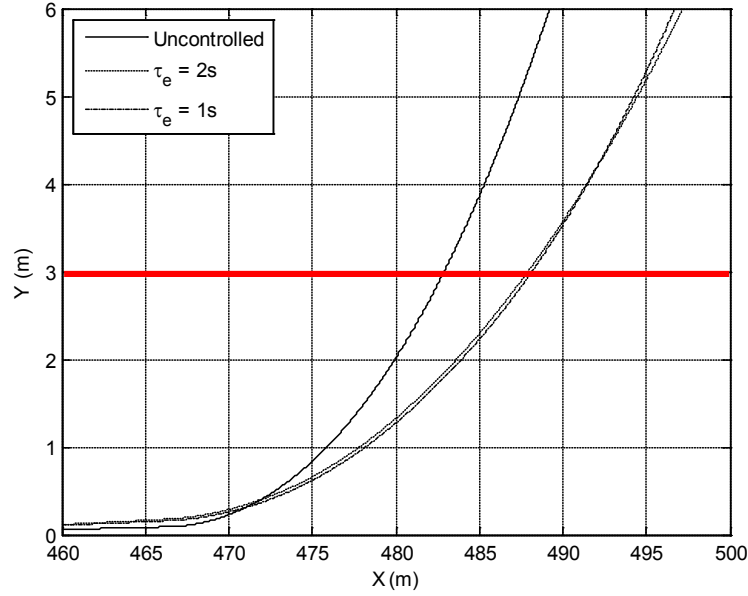


Figure 5.24: Vehicle trajectory during SIA event with driver reaction time of $\tau_d = 2s$ and controller settings of $\tau_e = 0s$ (Case #1 - uncontrolled baseline), $\tau_e = 2s$ (Case #2), and $\tau_e = 1s$ (Case #3)

Consider the situation in which the driver was paying attention and had a reaction time of $\tau_d = 1s$. This was the scenario used for Cases #4-#6 shown in Figures 5.25-5.30. Figure 5.25 displays road wheel angular results for the shorter driver reaction time, τ_d , which has been labeled between points d and e. Case #4 was the baseline situation without intervention from the controller, and resulted in a peak yaw rate (refer to Figure 5.26) of $\dot{\psi} = 0.42$ rad/sec; the final heading angle was $\psi = 0.48$ rad. Before examining the controlled cases (Cases #5 and #6), it is important to note that the final heading angle for Case #4 was similar to the controlled cases for the inattentive driver (Cases #2 and #3). Essentially, the controller transformed the inattentive driver (Cases #1-#3) into an uncontrolled

attentive driver (Case #4). Cases #5 and #6 assigned the controller values of $\tau_e = 2s$ and $\tau_e = 1s$, respectively. As shown in Figure 5.25, these two cases produced similar steering responses between $28 < t < 30s$. The only difference was for $\tau_e = 1s$ (Case #6) full control was returned to the driver soon after correction took place at $t = 29s$; however, $\tau_e = 2s$ (Case #5) continued to intervene even after the driver returned the steering angle to $\delta_{sw} = 0$ rad. Simply put, a driver reaction time of $\tau_d > 1s$ would have been required to see a significant difference in controller response.

The vehicle response will be investigated for these three scenarios. Case #5 had a peak yaw rate of $\dot{\psi} = 0.21$ rad/sec and a final heading angle of $\psi = 0.28$ rad; Case #6 offered a peak yaw rate and final heading angle of $\dot{\psi} = 0.21$ rad/sec and $\psi = 0.26$ rad. These values represent reductions in the final heading angle of 42% and 46% for Case #5 and Case #6 when compared to Case #4. The similarity between Case #5 and Case #6 was expected since the driver did not attempt any further evasive action. However, the controller would continue to intervene during an evasive maneuver in Case #5. Figures 5.27 and 5.28 display the slip angle, β , and lateral velocity, v_y , of the vehicle during the maneuvers to demonstrate that vehicle stability was not compromised to produce favorable results. Figures 5.29 and 5.30 indicate the improvements in lateral position, Y , for the controlled cases when compared to the uncontrolled case. The centerline crossing times for Case #5 and Case #6 were $\Delta t_c = 1.30s$ and $\Delta t_c = 1.31s$ respectively. They were a similar

improvement over the baseline of $\Delta t_c = 1.00s$ (Case #4) by approximately 0.3s (30%).

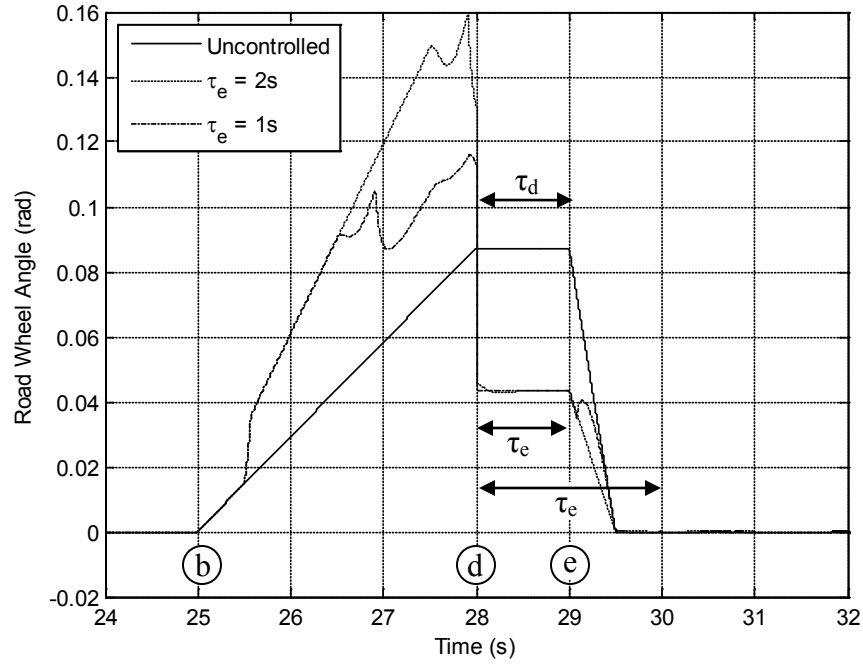


Figure 5.25: Steering angle, δ , during SIA event with driver reaction time of $\tau_d = 1s$ and controller settings of $\tau_e = 0s$ (Case #4 - uncontrolled baseline), $\tau_e = 2s$ (Case #5), and $\tau_e = 1s$ (Case #6)

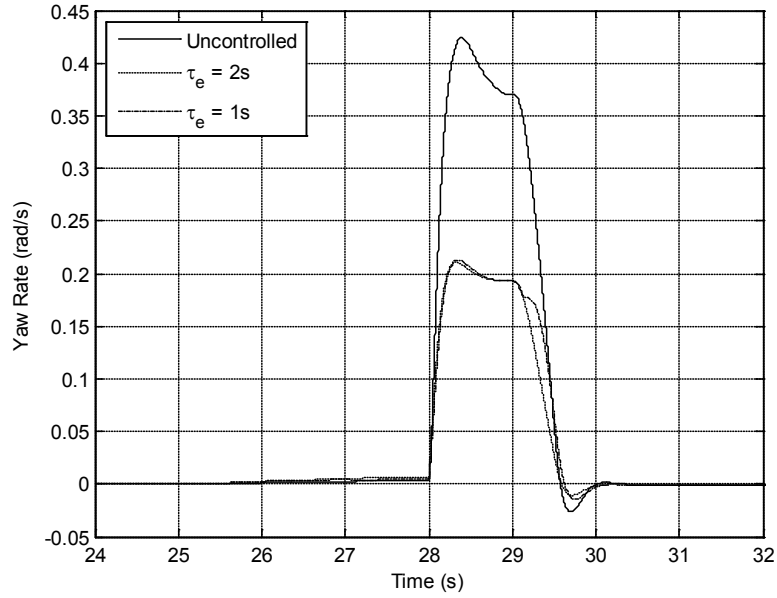


Figure 5.26: Yaw rate, $\dot{\psi}$, during SIA event with driver reaction time of $\tau_d = 1$ s and controller settings of $\tau_e = 0$ s (Case #4 - uncontrolled baseline), $\tau_e = 2$ s (Case #5), and $\tau_e = 1$ s (Case #6)

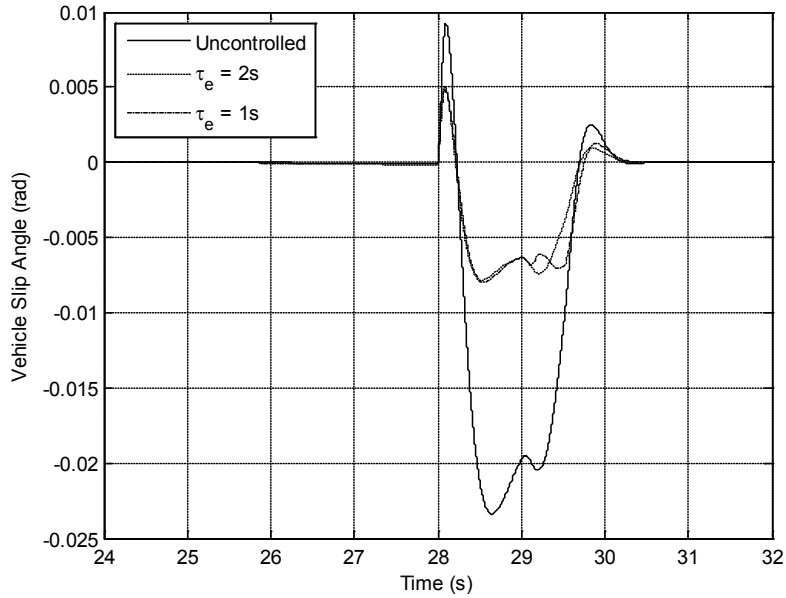


Figure 5.27: Vehicle slip angle, β , during SIA event with driver reaction time of $\tau_d = 1$ s and controller settings of $\tau_e = 0$ s (Case #4 - uncontrolled baseline), $\tau_e = 2$ s (Case #5), and $\tau_e = 1$ s (Case #6)

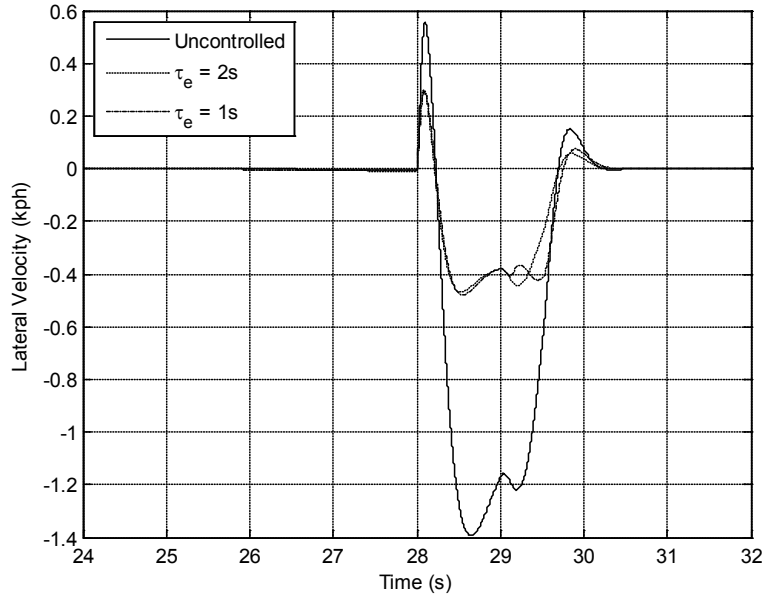


Figure 5.28: Lateral velocity, v_y , during SIA event with driver reaction time of $\tau_d = 1$ s and controller settings of $\tau_e = 0$ s (Case #4 - uncontrolled baseline), $\tau_e = 2$ s (Case #5), and $\tau_e = 1$ s (Case #6)

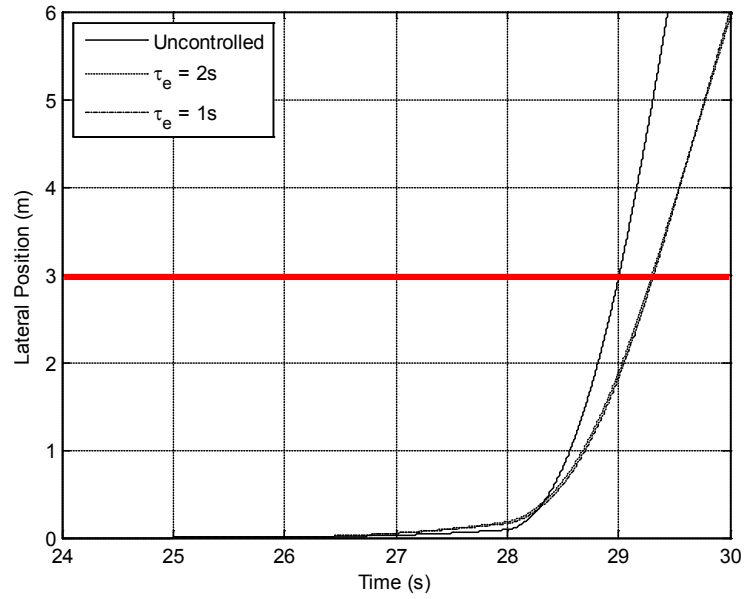


Figure 5.29: Lateral position, Y , during SIA event with driver reaction time of $\tau_d = 1$ s and controller settings of $\tau_e = 0$ s (Case #4 - uncontrolled baseline), $\tau_e = 2$ s (Case #5), and $\tau_e = 1$ s (Case #6)

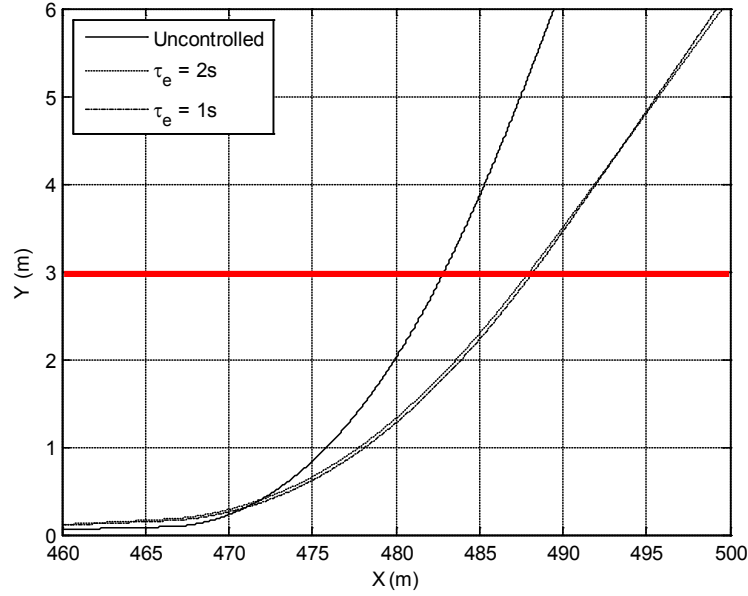


Figure 5.30: Vehicle trajectory during SIA event with driver reaction time of $\tau_d = 1s$ and controller settings of $\tau_e = 0s$ (Case #4 - uncontrolled baseline), $\tau_e = 2s$ (Case #5), and $\tau_e = 1s$ (Case #6)

A summary of the numerical results has been presented in Table 5.3. The performance of the driver/controller combination was characterized as a final vehicle heading angle with respect to the road direction, ψ_f , the time to the centerline crossing, Δt_c , maximum yaw rate, $\dot{\psi}_{\max}$, peak lateral velocity, $v_{y_{\max}}$, and maximum vehicle sideslip angle, β_{\max} . In addition, the driver behavior and intervention type has been recorded. The final heading angle was highly dependent on the driver response time, τ_d . However, with controller intervention the final heading angle for $\tau_d = 2s$ was reduced from $\psi_f = 0.857$ rad (Case #1) to $\psi_f = 0.472$ rad (Case #2), which was equivalent to the uncontrolled $\tau_d = 1s$ final heading angle of

$\psi_f = 0.480$ rad (Case #4). In all other categories, Case #2 was an improvement over Case #4, so it was given a rank of 3. Case #3 was an improvement over Case #4 in all categories except final heading angle; therefore, Cases #3 and #4 were given a tie for rank 4. Cases #5 and #6 tied for rank 1 with best performance in all categories, including final heading angles of $\psi_f = 0.276$ rad and $\psi_f = 0.255$ rad, respectively. The centerline crossing values show surprising similarity across all controlled cases. Regardless of controller assistance time, τ_e , or driver reaction time, τ_d , the controller gave the driver an extra $\Delta t = 0.3s$ before crossing the centerline. This accomplished the design goal of the controller in that a potential shoulder induced accident could be mitigated with the assistance of the controller without otherwise interfering in the daily operation of the vehicle. Assuming the driver was paying attention ($\tau_d = 1s$), a situation may exist where a centerline crossing of $\Delta t_c = 1.30s$ may be enough to avoid a crash.

Considering that a controller assistance time of $\tau_e = 1s$ produced similar results to $\tau_e = 2s$ while simultaneously being the more conservative and unobtrusive setting, it was recommended as the starting point for the controller. Further tuning in a driving simulator or real vehicle would be necessary to discover an optimal setting for the full range of potential drivers.

Case	τ_d (sec)	τ_e (sec)	ψ_f (rad)	Δt_c (s)	$\dot{\psi}_{\max}$ (rad/s)
1	2	0	0.857	1.01	0.42
2	2	2	0.472	1.30	0.21
3	2	1	0.522	1.31	0.28
4	1	0	0.480	1.00	0.42
5	1	2	0.276	1.30	0.21
6	1	1	0.255	1.31	0.21
Case	$v_{y_{\max}}$ (kph)	β_{\max} (rad)	Driver Behavior	Intervene	Rank
1	-1.39	-0.023	Inattentive	No	6
2	-0.47	-0.008	Inattentive	Long	3
3	-0.76	-0.013	Inattentive	Short	4 (tie)
4	-1.39	-0.023	Attentive	No	4 (tie)
5	-0.47	-0.008	Attentive	Long	1 (tie)
6	-0.48	-0.008	Attentive	Short	1 (tie)

Table 5.3: Summary of test cases for shoulder induced accident control system with driver reaction times, τ_d , controller reaction times, τ_e , final vehicle heading angle, ψ_f , time to lane crossing, Δt_c , peak yaw rate, $\dot{\psi}_{\max}$, peak lateral velocity, $v_{y_{\max}}$, peak slip angle, β_{\max} , driver behavior, intervention time period, and performance rank in terms of vehicle safety

Summary

Run-off-road incidents are a significant problem in the realm of vehicle crashes. A variety of measures may be being taken to decrease the opportunity of a vehicle leaving the road surface. However, the circle of safety must be closed to mitigate accidents that occur once the vehicle leaves the road. This can be accomplished through improvements in driver training and active steering technology.

In this chapter, an innovative approach to active steering was presented. The concept of driver intention was introduced to ensure that the controller only intervened when the vehicle was behaving different from what the driver would expect. For this controller, it was assumed that the driver expected the road conditions to be the same as they were a time τ_e prior. This way the controller only intervened during quickly changing road conditions. The controller did not make any attempts to improve vehicle performance during static road conditions.

During the scenario of returning to the road after a runoff, the controller performed exceptionally well in mitigating the associated dangers. Figures 5.18-29 show the improvement of the controller over a baseline condition. The controller only intervened during these brief changes in road conditions. In standard driving situations on a static road surface, the vehicle behaved the same with and without the controller enabled. This type of steering intervention can already be realized with the variable steering ratio technology available on high end commercial vehicles. More importantly, the results show how small the correction window is during a road return. Even with controller intervention, a driver must be prepared for the event to completely avoid a dangerous lane crossing situation.

CHAPTER SIX

CONCLUSION AND FUTURE RESEARCH

6.1 Summary

The availability of ground transportation offers mobility to millions of people throughout the world. The work presented in this dissertation establishes a foundation for steering preference research centered on the development and usage of the Clemson University steering simulator. The custom hardware-in-the-loop steering simulator was developed and refined over three generations. Through the course of the upgrades, the steering feel was brought to realistic levels while being fully adjustable in real-time. With this real-time adjustability, the simulator is not only a powerful tool for human subject research, but also as a pure engineering tool that allows steering engineers to evaluate steering settings back-to-back to help make design decisions. A laboratory procedure was developed to use the simulator to determine the steering preferences of human test subjects placed into demographic groups. Utility drivers preferred quicker steering ratios and heavier steering efforts on residential, country, and highway roadways with correlations between the utility demographic and steering preference of $r = 0.341$ (ratio) and $r = 0.426$ (effort). In contrast, car enthusiasts favored quick steering ratios in residential/country environments ($r = 0.319$, $r = 0.294$) and light steering effort on the highway ($r = -0.360$). Finally, rural drivers desired quicker steering ratios on country roads

($r = 0.437$). The impact of this study is the demonstration that the correlations should allow steering system engineers to faithfully cater to target demographic groups.

The data collected during the demographics steering preference study was also investigated to discover any connections between driver steering preferences and vehicle sensor data. A robust steering preference metric was developed based on the collected vehicle data channels (variables). For example, changes to the vehicle's steering ratio resulted in an excellent correlation, $r = -0.55$, between the subjective steering preference and the objective vehicle data. However, changes to the vehicle's steering effort did not produce a reliable correlation. The connection between steering ratio and vehicle response likely supports the conclusion that drivers steer vehicles using angular inputs rather than torque inputs.

To compliment the steering preference research, steering safety was addressed through the development of an active steering controller to mitigate shoulder induced accidents. Run-off-road crashes are dangerous because they typically involve striking oncoming traffic, stationary objects, or result in a vehicle rollover. While active steering controllers have been developed, none consider the idea of “driver intention” to insure the intervention is appropriate and noninvasive to normal daily driving. An active steering controller was developed with the concept of “driver intention” in mind. A cornering stiffness estimation technique, using a Kalman filter, was coupled with a full state feedback controller through a “driver intention” module to create a limited window of intervention after a measurable road surface change. For the shoulder induced accident scenario, the centerline crossing time was increased from

1.0s to 1.3s for a 30% improvement. The final vehicle heading angle was reduced by approximately 45% across multiple scenarios resulting in a smaller required corrective steering input from the driver. While not designed to remove the danger completely, the steering controller can provide precious assistance to the driver so that evasive maneuvers may be performed to avoid a crash.

6.2 Future Research Challenges

Current steering research hinges on two factors: safety and driver preference. From a safety perspective, control algorithms can be developed to intervene or warn the driver in hazardous situations. However, from a more fundamental standpoint, safety can be improved by ensuring that the driver's intended commands are obeyed by the vehicle. A worst case steering intervention algorithm was presented in Chapter 5 to compensate for a driver's reaction time in quickly changing road conditions. Although useful and relevant to steering safety, it was designed for an occasional dangerous event - road runoff. The other side of safety is controllability in everyday driving situations; ensuring that the vehicle behaves and provides feedback in a predictable manner. On a broad scale, this may be achieved with careful tuning of the understeer coefficient and the power steering system. However, each driver's desire for feedback and responsiveness varies considerably. At this point, safety merges with driver preference. For instance, driver preference may be traditionally considered to apply to a driver's happiness, but in this case, it can be expanded to include a driver's ability to control the vehicle. This illustrates the core problem:

How can a vehicle's steering be tuned to give each driver optimal control and happiness? All drivers are different, so no single setting will ever be able to accomplish this. A smart steering system would be required to adapt to the driver's preferences.

With this problem identified, the next stage focuses on examining the major problem of developing a steering system that adapts to the driver. The major hurdle here is the knowledge that humans are remarkable control systems. Drivers will likely adapt to any reasonable steering setting whether they prefer it or not. Furthermore, even if a setting is moved in a favorable direction for the driver, the driver may react poorly to the initial change due to the prior adaptation to the previous setting. The problems faced in developing this controller will be vastly different from typical control theory. Setting changes will need to be performed in discrete increments, and a subsequent unweighted learning time (i.e., grace period during which a driver may adapt to the new setting) will always be required.

The completion of the objective steering metric research in Chapter 4 offers an opportunity for an auto-tuning steering controller. The auto-tuning steering research would focus on the development of a controller that can learn a driver's steering preference and adapt the steering setting to match it. With a potentially long time delay in receiving a reliable feedback signal, the controller would need to be designed with built in “patience”. The largest obstacle with this controller would be determining the exact point when the feedback signal can be trusted to make a tuning decision. Even with an ideal objective metric, the driver will always be fighting the

control authority to some degree as his/her natural adaptive system tries to take over. If successful, this auto-tuning steering controller would become a valuable module in the steering simulator. No longer would discrete steering tests with tedious questionnaires be required. A subject would simply be able to drive the simulator for a set amount of time, and upon completion the subject's optimal steering setting would be known.

An active steering controller to mitigate shoulder induced accidents was presented in Chapter 5. The goal of the controller was to intervene when the driver was unaware of road surface changes. Although validated for a generic steering input, the controller should be tuned and validated in a simulator environment with human test subjects. This approach would help demonstrate the nonintrusive nature of the controller during standard driving conditions and also provide insight into the response time of drivers during these deadly scenarios. The true value of the active steering controller could then be evaluated to set the target for future research.

APPENDICES

Appendix A

Pilot Study 1 and 2 Scenario Questionnaire

The first questionnaire developed featured sixteen questions that asked the drivers to evaluate the steering system in terms of fun, control, ease, and safety. These questionnaires were administered after each steering configuration experienced by the drivers during the two pilot studies.

- Q1 I had good control over the vehicle.
1 - 2 - 3 - 4 - 5 - 6 - 7
Strongly Agree *Strongly Disagree*
- Q2 It was easy to drive this vehicle.
1 - 2 - 3 - 4 - 5 - 6 - 7
Strongly Agree *Strongly Disagree*
- Q3 The vehicle went where I wanted it to go.
1 - 2 - 3 - 4 - 5 - 6 - 7
Strongly Agree *Strongly Disagree*
- Q4 I felt that I could drive this vehicle safely at low speeds.
1 - 2 - 3 - 4 - 5 - 6 - 7
Strongly Agree *Strongly Disagree*
- Q5 I was able to steer the vehicle accurately.
1 - 2 - 3 - 4 - 5 - 6 - 7
Strongly Agree *Strongly Disagree*
- Q6 Driving this vehicle for a long distance would make me tired.
1 - 2 - 3 - 4 - 5 - 6 - 7
Strongly Agree *Strongly Disagree*
- Q7 I felt in control of the vehicle at all times.
1 - 2 - 3 - 4 - 5 - 6 - 7
Strongly Agree *Strongly Disagree*

- Q8 The steering on my vehicle makes it fun to drive.
1 - 2 - 3 - 4 - 5 - 6 - 7
Strongly *Strongly*
Agree *Disagree*
- Q9 I felt that I could drive this vehicle safely at high speeds.
1 - 2 - 3 - 4 - 5 - 6 - 7
Strongly *Strongly*
Agree *Disagree*
- Q10 I was comfortable driving this vehicle.
1 - 2 - 3 - 4 - 5 - 6 - 7
Strongly *Strongly*
Agree *Disagree*
- Q11 I had to apply lots of steering corrections to get the vehicle to go where I wanted.
1 - 2 - 3 - 4 - 5 - 6 - 7
Strongly *Strongly*
Agree *Disagree*
- Q12 I felt that I could drive this vehicle safely if I had to swerve around an object on the road.
1 - 2 - 3 - 4 - 5 - 6 - 7
Strongly *Strongly*
Agree *Disagree*
- Q13 I felt that I could drive this vehicle safely if I had to make a sudden stop in an emergency.
1 - 2 - 3 - 4 - 5 - 6 - 7
Strongly *Strongly*
Agree *Disagree*
- Q14 I had pay close attention to keep the vehicle where I wanted it on the road.
1 - 2 - 3 - 4 - 5 - 6 - 7
Strongly *Strongly*
Agree *Disagree*
- Q15 I had to apply a lot of physical effort to get the vehicle to go where I wanted.
1 - 2 - 3 - 4 - 5 - 6 - 7
Strongly *Strongly*
Agree *Disagree*
- Q16 The steering seemed too sensitive on this vehicle.
1 - 2 - 3 - 4 - 5 - 6 - 7
Strongly *Strongly*
Agree *Disagree*

Appendix B

Pilot Study 1 Raw Data

The raw data for Pilot Study 1 has been presented for the eleven test subjects, six configurations, and sixteen questions.

Subject	Configurations	Survey Question #															
		1	2	3	4	5	6	7	8	9	10	11	12	13	14	15	16
1	C1	4	4	5	5	7	6	2	6	6	2	6	4	2	7	5	4
1	C2	5	5	6	6	7	7	2	6	6	5	6	2	5	7	4	5
1	C3	6	6	6	6	7	6	2	5	6	5	6	3	6	7	3	6
1	C4	6	6	7	6	7	7	2	6	6	6	6	2	6	7	4	6
1	C5	5	5	6	5	6	5	2	5	6	4	6	6	4	6	5	3
1	C6	5	5	5	4	6	4	2	4	6	2	6	5	2	6	4	2
2	C1	5	5	5	5	5	5	5	5	5	5	5	4	3	2	4	4
2	C2	5	5	5	5	5	5	5	5	5	5	5	2	4	4	5	5
2	C3	6	6	6	6	6	6	6	6	6	6	5	2	5	6	4	4
2	C4	5	6	6	6	6	6	5	5	5	5	5	3	5	5	4	5
2	C5	5	6	5	5	6	5	6	5	5	4	5	4	4	4	5	5
2	C6	5	4	5	4	7	5	6	5	5	4	5	5	5	5	6	5
3	C1	6	5	6	5	7	5	4	5	5	6	5	1	4	5	6	5
3	C2	7	7	7	6	5	7	1	7	7	7	5	5	5	6	4	4
3	C3	4	4	4	3	5	3	5	3	2	2	3	5	3	4	7	2
3	C4	5	5	3	2	6	3	6	4	1	4	3	3	1	2	6	1
3	C5	6	6	6	5	5	5	4	5	5	5	4	4	4	5	5	4
3	C6	6	6	6	6	7	7	2	6	6	7	5	1	5	6	5	7
4	C1	6	6	6	6	7	7	1	6	7	6	6	3	5	6	4	6
4	C2	4	4	5	4	6	5	4	2	3	2	4	3	2	6	5	4
4	C3	5	6	4	5	7	3	3	5	3	3	5	5	5	5	4	6
4	C4	5	5	5	5	7	6	2	5	5	4	5	3	5	4	3	4
4	C5	5	4	5	3	6	3	2	2	2	2	5	6	2	2	6	4
4	C6	5	6	5	4	7	5	2	4	7	6	5	4	6	5	5	6
5	C1	7	7	7	6	7	6	3	6	6	5	6	2	3	3	2	6
5	C2	7	7	6	6	7	6	4	6	6	6	7	1	5	4	2	6
5	C3	7	6	6	6	7	6	5	6	6	5	6	3	4	5	4	5
5	C4	7	7	6	5	7	6	6	6	6	4	5	3	4	5	4	5
5	C5	7	7	6	7	7	6	2	6	6	5	6	2	4	3	1	7
5	C6	7	7	6	7	7	6	5	6	6	6	6	2	6	5	3	6

Table B.1: Raw questionnaire data for Pilot Study 1 for subjects 1-5

Subject	Configurations	Survey Question #															
		1	2	3	4	5	6	7	8	9	10	11	12	13	14	15	16
6	C1	4	4	3	4	5	5	6	5	3	4	3	5	3	5	5	3
6	C2	6	6	6	6	7	6	5	6	5	6	5	5	6	5	5	6
6	C3	1	1	1	2	2	2	6	1	1	1	1	7	1	2	6	3
6	C4	6	5	4	5	5	5	5	6	4	6	6	5	5	5	4	6
6	C5	6	5	5	6	6	5	6	5	3	3	4	3	4	5	5	3
6	C6	4	3	3	4	5	4	6	4	3	3	4	4	4	5	4	4
7	C1	7	6	6	6	7	6	6	5	5	6	6	6	5	5	6	6
7	C2	6	6	6	5	7	6	6	4	5	6	6	6	5	5	6	7
7	C3	7	7	7	6	7	6	7	6	6	6	6	6	5	5	6	5
7	C4	5	5	6	5	7	5	6	4	5	5	6	6	5	5	6	5
7	C5	3	4	4	3	6	1	6	4	3	4	4	6	5	4	7	4
7	C6	4	4	5	3	7	5	6	3	4	3	4	7	5	5	7	4
8	C1	7	7	6	6	6	6	1	7	7	7	7	1	7	7	1	7
8	C2	4	3	3	2	5	2	7	3	3	2	2	6	2	2	6	4
8	C3	6	6	5	6	7	7	2	6	6	6	6	1	6	6	2	6
8	C4	4	5	4	5	6	5	7	4	3	4	4	3	4	4	6	3
8	C5	7	7	7	7	7	6	1	5	7	7	6	2	7	6	2	6
8	C6	2	4	3	3	5	2	6	2	2	2	2	7	3	3	7	3
9	C1	4	5	4	5	6	5	4	5	4	4	5	2	3	4	3	4
9	C2	6	6	6	5	7	6	5	6	5	6	5	1	5	7	2	5
9	C3	5	5	4	5	7	5	3	4	3	4	4	3	3	2	4	4
9	C4	4	2	3	3	4	3	5	4	4	3	4	6	2	4	3	4
9	C5	7	6	7	6	7	6	4	5	5	6	6	1	6	7	1	7
9	C6	3	4	3	4	5	4	5	3	2	2	3	4	2	2	5	4
10	C1	5	4	4	5	6	5	2	4	2	3	5	3	3	3	5	6
10	C2	4	5	4	4	6	5	3	5	2	3	5	3	3	3	5	6
10	C3	5	5	5	5	5	4	2	4	2	3	4	3	2	3	5	6
10	C4	6	5	5	5	7	5	4	4	3	4	5	2	4	2	4	6
10	C5	6	5	6	5	7	5	3	5	3	5	5	2	4	4	3	5
10	C6	5	5	5	6	5	5	1	3	3	3	5	3	2	1	4	7
11	C1	4	4	4	4	6	6	3	4	5	5	4	3	3	6	3	5
11	C2	3	4	4	4	6	4	4	3	4	3	3	5	3	6	3	4
11	C3	2	3	2	2	5	2	6	2	3	2	2	6	1	6	5	6
11	C4	1	1	2	2	7	3	4	2	4	1	3	6	3	6	6	4
11	C5	4	5	4	5	7	4	4	4	5	4	5	2	6	6	3	5
11	C6	4	4	3	6	6	6	3	3	5	6	4	2	5	2	3	2

Table B.2: Raw questionnaire data for Pilot Study 1 for subjects 6-11

Appendix C

Pilot Study 2 Raw Data

The raw data for Pilot Study 2 has been presented for the nine test subjects, six configurations, and sixteen questions.

Subject	Configuration	Survey Question #															
		1	2	3	4	5	6	7	8	9	10	11	12	13	14	15	16
1	C1	5	5	5	6	6	3	5	6	6	5	3	6	7	3	3	6
1	C2	3	4	3	2	2	4	1	1	1	4	7	1	7	5	5	1
1	C3	2	2	5	1	2	1	3	5	5	5	6	4	4	3	2	5
1	C4	4	4	4	5	4	2	5	5	6	6	5	6	5	1	7	5
1	C5	5	5	4	4	4	1	5	4	6	5	6	2	5	3	3	4
1	C6	5	5	4	5	4	3	5	4	5	5	5	3	4	3	5	5
2	C1	5	5	4	4	4	5	4	3	5	4	2	3	4	5	2	3
2	C2	5	5	4	4	4	5	4	3	5	4	2	2	3	5	2	3
2	C3	5	5	4	5	5	4	5	3	5	4	2	3	4	4	2	3
2	C4	4	4	4	5	5	5	5	3	4	4	3	3	3	5	2	3
2	C5	4	4	4	4	4	3	3	3	4	4	2	2	3	4	2	4
2	C6	2	2	2	3	2	3	2	2	2	2	4	2	4	3	4	2
3	C1	4	4	4	5	5	2	4	4	3	4	4	3	5	2	3	4
3	C2	5	5	5	6	6	4	5	4	6	5	3	4	3	2	3	5
3	C3	4	5	5	4	4	3	5	4	4	4	5	4	4	2	4	4
3	C4	5	4	5	5	4	3	4	4	5	4	3	5	3	3	2	5
3	C5	6	6	6	7	6	2	6	4	6	5	2	5	3	3	3	6
3	C6	6	6	6	6	5	2	6	4	5	6	2	5	3	3	2	6
4	C1	5	4	6	7	6	2	7	7	6	7	2	6	2	2	3	5
4	C2	6	5	7	7	7	2	6	7	6	6	2	5	3	3	2	6
4	C3	6	6	6	6	6	2	6	7	7	7	5	6	3	5	2	7
4	C4	6	6	6	6	6	2	6	7	7	7	5	6	2	4	1	7
4	C5	4	4	4	4	4	4	4	5	4	4	5	4	5	5	5	5
4	C6	6	6	6	6	6	2	5	6	6	6	3	5	3	3	2	6
5	C1	5	5	5	5	5	1	5	5	5	5	2	4	3	4	4	4
5	C2	6	6	6	6	6	7	6	6	6	6	4	5	3	2	4	6
5	C3	5	5	5	6	4	7	5	5	6	5	6	5	3	2	4	4
5	C4	5	5	5	5	5	2	6	5	6	5	2	6	4	2	4	5
5	C5	6	6	5	5	6	1	6	6	6	5	3	4	3	2	4	5
5	C6	5	6	6	6	5	1	5	5	5	5	3	3	3	3	4	5

Table C.1: Raw questionnaire data for Pilot Study 2 for subjects 1-5

Subject	Configuration	Survey Question #															
		1	2	3	4	5	6	7	8	9	10	11	12	13	14	15	16
6	C1	6	6	6	6	4	5	6	4	6	6	5	5	3	5	3	4
6	C2	6	6	6	6	4	4	6	4	6	6	5	5	3	4	3	4
6	C3	6	6	6	6	4	4	6	4	6	6	5	5	3	4	3	4
6	C4	6	6	6	6	5	5	6	5	6	6	5	5	3	5	3	5
6	C5	4	4	6	6	3	2	4	5	5	6	6	4	4	2	3	6
6	C6	5	6	5	4	2	5	5	1	6	5	6	2	4	5	1	2
7	C1	6	6	7	6	6	2	7	7	5	7	1	4	5	1	2	7
7	C2	4	3	4	3	3	3	2	2	2	3	6	2	7	3	6	3
7	C3	6	6	7	6	6	3	5	6	5	6	5	4	5	2	2	6
7	C4	5	6	6	5	6	2	4	6	4	6	3	4	5	2	4	5
7	C5	5	5	5	4	5	2	5	5	4	6	3	4	5	1	2	5
7	C6	5	5	4	6	4	6	4	4	5	4	5	3	5	5	1	4
8	C1	3	4	3	3	3	6	1	2	2	2	5	2	4	5	4	1
8	C2	3	3	2	3	2	6	2	4	2	5	6	2	6	6	2	2
8	C3	2	2	2	3	3	7	2	4	2	5	6	2	6	6	4	1
8	C4	6	6	5	6	6	2	6	6	6	6	1	4	3	4	2	6
8	C5	3	4	3	3	3	6	1	2	2	2	5	2	4	5	4	1
8	C6	3	4	3	3	3	6	1	2	2	2	5	2	4	5	4	1
9	C1	4	4	4	4	4	5	4	4	4	4	4	3	5	3	3	3
9	C2	4	4	4	4	4	5	3	3	2	3	4	2	4	3	3	3
9	C3	4	4	3	5	5	5	3	3	3	3	5	3	6	4	3	3
9	C4	4	4	3	4	3	3	4	3	4	4	4	2	5	4	3	3
9	C5	4	4	4	4	4	5	3	3	3	3	5	3	5	4	3	2
9	C6	4	4	4	3	3	4	4	3	2	3	3	3	6	3	3	3

Table C.2: Raw questionnaire data for Pilot Study 2 for subjects 6-9

Appendix D

Final Demographics Questionnaire

Prior to driving the simulator, test subjects were required to read the following letter as well as fill out the subsequent questionnaire. The survey was used to classify each driver in various demographic categories.

Informational Letter - **Evaluating reactions to various automobile steering systems**

The purpose of this study is to evaluate the characteristics of various types of automobile steering systems. Approximately 20 licensed drivers over the age of 18 will be invited to participate. As part of the research procedures, you will be asked to drive a route on our driving simulator, then fill out a short questionnaire. This procedure will be repeated several times. Information from this survey will allow us to know more about what drivers think about various types of steering. There are no risks involved.

This study should take less than 1 hour to complete. This study is anonymous so no one will know how you drove in the simulator or responded to any of the questionnaire items.

Participation is voluntary. You can refuse to answer any questions at any time and can withdraw without any penalty. Return of the questionnaire is deemed consent to participate in the research study.

The Principal Investigator on this research study is Dr. John Wagner and the co-investigator is Dr. Fred Switzer. Dr. Switzer may be contacted at *switzef@clemson.edu*. If you have any questions regarding your rights as a research participant, you may contact the Office of Research Compliance at 864-656-6460.

Thank you for your assistance in this study.

Q1,Q2 Your age _____ Your gender (M or F) _____
{sec. A}

Q3 How long have you been driving (how long since you got your driver's license)?
(Feel free to use portions of years, for example: 3.5 years)
_____ years

Q4 Have you ever purchased your own car? (Y or N) _____

Q5 What is your profession (or your major if you're in college)?

Q6 If you have any children, what are their ages? _____

Q7 About how many miles do you put on your primary vehicle each year?

For the next question please tell us what percentage of your time driving you spend in each type of driving (note that the percentages should add up to 100%):

Q8	City/urban driving	_____
Q9	Small town/suburban driving	_____
Q10	Rural/country road driving	_____
Q11	Intercity highway driving	_____
		100%

Q12 Do you use your vehicle for towing (utility trailer, boat, etc.)?

Q13 How much of your driving time (what percentage) do you spend towing?
_____ %

- Q14 I see my car primarily as means of getting from one place to another.
1 - 2 - 3 - 4 - 5 - 6 - 7
Strongly Disagree Strongly Agree
- Q15 My car is source of pride for me.
1 - 2 - 3 - 4 - 5 - 6 - 7
Strongly Disagree Strongly Agree
- Q16 I consider myself someone who is interested in cars, a “car person”.
1 - 2 - 3 - 4 - 5 - 6 - 7
Strongly Disagree Strongly Agree
- Q17 I play lots of driving video games.
1 - 2 - 3 - 4 - 5 - 6 - 7
Strongly Disagree Strongly Agree
- Q18 I pay attention to what kinds of cars my friends have.
1 - 2 - 3 - 4 - 5 - 6 - 7
Strongly Disagree Strongly Agree
- Q19 It’s important to me that my vehicle is fun to drive.
1 - 2 - 3 - 4 - 5 - 6 - 7
Strongly Disagree Strongly Agree
- Q20 I play lots of video games.
1 - 2 - 3 - 4 - 5 - 6 - 7
Strongly Disagree Strongly Agree
- Q21 I have fun driving.
1 - 2 - 3 - 4 - 5 - 6 - 7
Strongly Disagree Strongly Agree
- Q22 I spend a lot of my time taking care of my car.
1 - 2 - 3 - 4 - 5 - 6 - 7
Strongly Disagree Strongly Agree
- Q23 How a vehicle steers plays a big role in whether or not I want to buy it.
1 - 2 - 3 - 4 - 5 - 6 - 7
Strongly Disagree Strongly Agree

If you've ever purchased your own car or had a substantial amount of input or control over ^{sec. B} the purchase of a car, please answer the following questions (if not, then please skip this section):

- Q24 What make (Chrysler, Honda, Ford etc.) was it? _____
- Q25 What model (PT Cruiser, Accord, Explorer etc.) was it? _____
- Q26 What model year (year it was made) was it? _____
- Q27 What was the approximate cost of that car? \$ _____

Rate the following factors on how important they were in the purchase of the car:

- Q28 a) The looks/appearance of the car.

	1	-	2	-	3	-	4	-	5	-	6	-	7	
<i>Not at all</i>														<i>Extremely</i>
<i>important</i>														<i>important</i>

- Q29 b) The cost of the car.

	1	-	2	-	3	-	4	-	5	-	6	-	7	
<i>Not at all</i>														<i>Extremely</i>
<i>important</i>														<i>important</i>

- Q30 c) How much fun the car was to drive.

	1	-	2	-	3	-	4	-	5	-	6	-	7	
<i>Not at all</i>														<i>Extremely</i>
<i>important</i>														<i>important</i>

- Q31 d) The practicality/utility of the car.

	1	-	2	-	3	-	4	-	5	-	6	-	7	
<i>Not at all</i>														<i>Extremely</i>
<i>important</i>														<i>important</i>

- Q32 e) The gas mileage.

	1	-	2	-	3	-	4	-	5	-	6	-	7	
<i>Not at all</i>														<i>Extremely</i>
<i>important</i>														<i>important</i>

- Q33 How long did it take for you to become comfortable driving your new car? _____
- Q34 Do you have (or did you have) a repair manual for this car?
(Y or N) _____
- Q35 Do you know approximately how much horsepower this car has/had?
(Y or N) _____
- Q36 If yes, about how much? _____ hp
- Q37 Do you know approximately how much torque this car has/had?
(Y or N) _____
- Q38 If yes, about how much? _____ lb/ft

Appendix E

Demographics Questionnaire Data

The following tables contain the demographic data collected for all 43 human.

The data corresponds with the 38 question survey in Appendix D.

Subject	Age	Gender	Driving Time	Purchased	Profession
1	23	m	8	y	Mech Eng
2	42	m	24	y	Mech Eng
3	25	m	9	y	Mech Eng
4	25	f	11	y	student services
5	24	m	8	y	Mech Eng
6	19	m	3.5	n	Psych
7	22	f	6	n	Sociology
8	22	f	7	y	Psych
9	24	f	8.5	y	Sociology
10	22	f	4	y	Electrical Eng
11	23	f	7	y	Psych
12	22	f	5.5	y	Psych
13	20	f	4.75	n	Education
14	21	f	5	n	Psych
15	18	f	3	n	Biology
16	19	f	4	n	Health Science
17	20	m	5	y	Electrical Eng
18	21	m	6	n	Psych
19	20	f	3.5	n	Psych
20	45	f	28	y	THRD
21	21	f	0	n	Wildlife Biology
22	20	f	4.5	n	Psych
23	19	f	4	y	Economics
24	21	m	4	n	Comp Eng
25	23	m	6	n	Sociology
26	18	f	2.5	n	communications
27	18	m	2	n	English
28	18	m	4	y	Business
29	18	m	2	n	Graphic Communications
30	18	f	2.5	y	Biology
31	18	m	3.5	n	Business
32	18	f	2.5	n	Business
33	18	f	2	n	communications
34	18	f	3.5	n	Packaging Science
35	18	f	3	n	Travel & Tourism
36	20	f	5	y	Psych
37	18	f	3.5	n	Packaging Science
38	18	m	2	y	Biology
39	18	f	3	y	Graphic Communications
40	18	m	2.5	n	Forest Resource Management
41	18	f	3	n	Nursing
42	20	f	3	n	Psych
43	20	f	4	y	Psych

Table E.1: Raw data from demographics questionnaire for questions 1-5

Subject	Children Age	Miles	city	small town	rural	highway
1	0	20000	5	30	15	50
2	3, 5	12000	0	60	20	20
3	0	5000	20	30	30	20
4	0	25000	15	45	40	0
5	0	10000	10	60	20	10
6	0	15000	50	20	20	10
7	0	15000	20	40	20	20
8	0	50000	15	50	20	15
9	0	8000	10	60	20	10
10	0	20000	20	40	10	30
11	0	6000	25	25	25	25
12	0	10000	25	50	10	15
13	0	5000	5	25	10	60
14	0	5000	50	20	5	25
15	0	15000	50	20	5	25
16	0	15000	15	25	10	50
17	0	7000	10	40	30	20
18	0	10000	2.5	80	2.5	15
19	0	5000	2	3	20	75
20	0	12000	0	94	6	0
21	0	15000	10	20	10	60
22	0	15000	10	50	20	20
23	0	11000	15	50	10	25
24	0	4000	5	15	15	65
25	0	3000	20	60	10	10
26	0	15000	15	60	10	15
27	0	2000	5	45	15	30
28	0	50000	25	25	25	25
29	0	15000	50	45	0	5
30	0	25000	5	5	20	70
31	0	15000	80	5	5	10
32	0	25000	5	80	5	10
33	0	20000	25	25	25	25
34	0	15000	0	70	20	10
35	0	15000	50	20	15	15
36	0	20000	50	10	5	35
37	0	3500	5	90	3	2
38	0	15000	25	15	25	35
39	0	15000	10	80	5	5
40	0	1000	10	60	20	10
41	0	15000	10	50	15	25
42	0	15000	10	70	10	10
43	0	12000	0	25	25	50

Table E.2: Raw data from demographics questionnaire for questions 6-11

Subject	% Tow	1	2	3	4	5	6	7	8	9	10
1	1	2	6	6	4	6	7	3	7	5	6
2	0	6	5	3	1	2	7	1	6	5	5
3	5	5	5	6	2	4	5	2	6	6	3
4	5	7	2	3	1	4	2	1	4	1	5
5	0	7	4	7	3	6	7	7	7	1	7
6	1	7	7	7	5	7	7	7	7	7	7
7	0	6	4	2	1	5	4	1	5	3	5
8	0	7	3	2	2	4	4	2	6	3	4
9	0	6	3	1	2	4	6	1	6	4	4
10	0	4	4	6	3	5	5	2	6	3	5
11	5	6	1	3	1	1	4	1	4	6	7
12	0	6	2	2	1	3	2	1	3	2	4
13	0	6	4	1	1	2	5	1	6	3	6
14	0	7	4	3	1	3	5	1	6	3	4
15	0	7	4	2	1	5	3	1	3	1	4
16	0	7	5	3	2	3	6	2	7	5	5
17	0	5	4	3	4	5	5	5	5	3	5
18	0	5	5	3	2	5	6	2	4	3	5
19	0	7	2	2	1	2	2	1	5	4	4
20	0	7	2	2	1	4	6	1	6	2	7
21	0	5	4	3	1	5	5	1	4	4	5
22	0	7	7	6	2	7	6	1	5	5	6
23	0	7	5	2	3	6	5	2	5	3	4
24	0	6	6	3	5	6	6	7	7	5	6
25	0	7	5	2	2	2	5	4	4	3	6
26	0	5	1	1	1	2	6	1	5	3	7
27	0	6	5	3	5	6	4	6	4	2	6
28	10	3	6	5	5	6	6	6	5	6	6
29	0	7	7	5	3	4	5	5	4	5	4
30	0	4	6	6	1	6	7	1	7	7	7
31	5	5	4	5	5	3	7	7	7	5	7
32	0	7	7	5	3	3	4	2	7	4	5
33	10	6	6	7	4	6	6	2	6	6	7
34	0	5	4	3	1	6	5	4	6	2	6
35	0	6	5	4	1	6	6	1	6	5	5
36	0	7	5	2	1	4	6	3	6	5	7
37	0	5	4	5	2	4	5	1	5	6	6
38	5	6	5	4	3	6	5	4	7	5	4
39	0	6	4	3	2	4	3	1	7	3	5
40	0	6	5	4	4	6	6	5	5	4	6
41	0	7	3	5	1	6	4	1	5	4	6
42	0	6	4	3	2	5	3	1	4	3	5
43	0	7	5	4	1	4	6	2	5	6	5

Table E.3: Raw data from demographics questionnaire for questions 12-23

Subject	Make	Model	Year	Cost
1	BMW	M Roadster	2001	25500
2	Honda	Civic	1989	1500
3	Ford	Mustang	1992	4000
4	Honda	Accord	1997	2500
5	Toyota	Corolla	1994	3000
6	Hyundai	Tiburon	2006	26000
7				
8	Nissan	Maxima	1995	4500
9	Mercedes	C Class	2007	27000
10	Honda	Accord	1999	8000
11	Toyota	Camry	2002	
12	Chevrolet	Cavalier	2000	5000
13	Chevrolet	Blazer	2000	
14				
15	Honda	Civic	2001	11000
16	Honda	Accord	1997	6500
17	Acura	RSX-Type S	2004	23000
18				
19	Ford	Focus	2001	
20	Honda	Accord	2001	16000
21				
22	Ford	Mustang	2002	18000
23	Honda	Civic	2005	20000
24	Volvo	S40	2000	12000
25	Dodge	Durango	2003	
26				
27	Volvo	S70	1998	5000
28	Jeep	Cherokee	1999	6500
29	Jeep	Cherokee	2005	26500
30	Lexus	IS 300	2003	40000
31	Jeep	Grand Cherokee	1998	6000
32	Land Rover	Discovery	2004	35000
33	Chevrolet	Tahoe	2006	40000
34	Honda	CR-V	2000	
35				
36	Hyundai	Sonata	2006	18700
37	Toyota	4 Runner	2007	28500
38	Toyota	4 Runner	1998	8500
39	Toyota	Camry	1995	3000
40	Jeep	Wrangler	2005	18000
41	Mitsubishi	Eclipse	2000	10500
42	Ford	Focus	2001	15000
43	Toyota	4 Runner	2000	15000

Table E.4: Raw data from demographics questionnaire for questions 24-27

Subject	a	b	c	d	e	Comfort	Repair	HP	Torque
1	6	5	7	2	3	12 hr	n	315	0
2	6	6	5	7	7	1 week	y	60	0
3	3	6	6	2	2	1 week	y	230	300
4	2	7	4	6	6	2 weeks	y	0	0
5	7	1	7	7	7	1 week	y	76	80
6	7	5	5	5	7	3 weeks	y	196	0
7						1 month	n	0	0
8	6	6	2	4	6	immediately	y	0	0
9	7	6	7	7	6	2 days	n	0	0
10	7	7	5	7	6	1 week	y	0	0
11	6	5	4	4	7	1 week	y	0	0
12	3	6	3	4	5	immediately	y	0	0
13	5	6	5	7	6	1 week	y	0	0
14									
15	6	5	5	1	7	1 day	y	0	0
16	7	7	5	7	6	2 weeks	n	0	0
17	5	5	4	3	5	6 months	n	200	0
18	6	7	5	6	7		y	0	0
19	3	6	3	7	7	1 week	y	0	0
20	6	3	6	6	7	3 weeks	y	0	0
21									
22	7	7	7	3	5	1 week	y	185	0
23	6	3	5	7	7	1 month	y	0	0
24	5	5	6	7	6	2 weeks	n	0	0
25	5	3	6	6	5	2 weeks	y	0	0
26									
27	6	7	3	7	6	3 days	y	0	0
28	5	5	5	6	3	2 days	y	210	0
29	6	5	4	5	5	1 week	n	0	0
30	7	2	7	7	7	2 weeks	y	0	0
31	6	5	7	6	7	1 week	n	0	0
32	5	4	4	7	4	1 week	y	0	0
33	7	6	5	7	4	2 weeks	y	0	0
34	6	5	6	5	6	1 month	y	0	0
35									
36	7	6	6	6	7	3 weeks	y	0	0
37	6	3	5	6	4	1 week	y	0	0
38	6	6	6	6	3	1 week	y	250	0
39	2	7	5	7	7	1 week	n	0	0
40	7	6	6	5	6	1 month	n	0	0
41	7	5	5	6	4	2 weeks	y	0	0
42	3	6	4	7	7	1 day	y	0	0
43	5	7	5	7	5	1 week	y	0	0

Table E.5: Raw data from demographics questionnaire for questions 28-38

Appendix F

Final Scenario Questionnaire

The Pilot Study questionnaire was streamlined based on the results of the two studies to a nine question survey. Questions pertaining to vehicle safety were removed. The following questionnaire was completed by test subjects after each of fifteen driving scenarios experienced during the demographics study.

Think about the scenario in which you just drove.

Circle the number below each question that best represents how you felt while you were driving that vehicle.

Q1 The steering on this vehicle makes it fun to drive.

1 - 2 - 3 - 4 - 5 - 6 - 7

Strongly

Strongly

Disagree

Agree

Q2 I had good control over this vehicle.

1 - 2 - 3 - 4 - 5 - 6 - 7

Strongly

Strongly

Disagree

Agree

Q3 I had to apply a lot of physical effort to get this vehicle to go where I wanted.

1 - 2 - 3 - 4 - 5 - 6 - 7

Strongly

Strongly

Disagree

Agree

Q4 I felt confident in my ability to drive the vehicle safely.

1 - 2 - 3 - 4 - 5 - 6 - 7

Strongly

Strongly

Disagree

Agree

Q5 I was comfortable driving this vehicle.

1 - 2 - 3 - 4 - 5 - 6 - 7

Strongly

Strongly

Disagree

Agree

Q6 It was easy to drive this vehicle.

1 - 2 - 3 - 4 - 5 - 6 - 7

Strongly

Strongly

Disagree

Agree

Q7 The vehicle went where I wanted it to go.

1 - 2 - 3 - 4 - 5 - 6 - 7

Strongly Disagree *Strongly Agree*

Q8 I had to pay close attention to keep the vehicle where I wanted it on the road.

1 - 2 - 3 - 4 - 5 - 6 - 7

Strongly Disagree Strongly Agree

Q9 The steering seemed too sensitive on this vehicle.

 1 - 2 - 3 - 4 - 5 - 6 - 7

Strongly Disagree *Strongly Agree*

Appendix G

Demographics Study Raw Data

The data from the nine item questionnaires have been presented here. Each of the 43 subjects completed the questionnaire fifteen times, once after each scenario.

Subject	Scenario	Question								
		1	2	3	4	5	6	7	8	9
1	C1	5	5	4	6	5	5	5	3	2
1	C2	5	5	5	6	4	3	5	3	2
1	C3	1	2	7	5	2	2	1	3	1
1	C4	2	3	6	5	3	2	2	3	1
1	C5	4	4	5	6	3	3	3	3	2
1	C6	3	3	5	5	4	3	2	3	1
1	C7	3	4	5	5	4	3	3	3	2
1	C8	3	4	5	5	4	3	3	4	2
1	C9	4	5	3	5	5	5	4	3	2
1	C10	5	5	3	6	5	5	5	3	3
1	C11	2	3	5	5	3	3	2	5	1
1	C12	3	4	6	4	3	4	5	3	2
1	C13	4	5	3	6	5	4	5	3	2
1	C14	3	4	5	5	4	3	3	5	1
1	C15	4	5	3	6	5	5	5	3	2
2	C1	6	6	3	6	6	6	5	3	5
2	C2	6	6	3	6	6	5	6	4	5
2	C3	5	3	5	4	3	3	4	5	3
2	C4	4	5	4	6	4	4	5	4	4
2	C5	5	5	3	5	5	5	6	3	4
2	C6	6	5	5	5	4	3	5	5	4
2	C7	6	6	2	5	5	5	4	3	5
2	C8	5	5	4	5	5	3	4	4	5
2	C9	4	3	6	3	3	4	5	6	4
2	C10	5	5	4	5	6	4	5	4	5
2	C11	7	7	2	7	7	6	6	2	4
2	C12	5	5	3	5	6	4	6	4	5
2	C13	6	6	3	6	5	5	6	3	5
2	C14	7	6	3	6	6	6	4	3	4
2	C15	6	6	3	6	6	4	6	4	5

Table G.1: Raw demographics study data for subjects 1 and 2

Subject	Configuration	Question								
		1	2	3	4	5	6	7	8	9
3	C1	5	5	2	5	5	5	5	3	3
3	C2	5	5	2	5	5	5	5	3	2
3	C3	4	5	2	5	5	5	5	4	3
3	C4	4	5	3	5	4	5	5	3	2
3	C5	5	6	1	6	6	5	5	2	2
3	C6	4	3	1	4	4	5	4	4	3
3	C7	4	4	3	5	4	4	4	3	3
3	C8	4	4	3	4	5	4	5	4	3
3	C9	4	4	2	4	4	5	4	4	3
3	C10	5	6	2	6	6	5	5	3	2
3	C11	6	6	2	6	6	5	5	2	2
3	C12	5	5	2	6	5	5	5	3	2
3	C13	5	5	2	5	5	5	5	3	2
3	C14	4	3	3	4	4	4	4	3	3
3	C15	6	6	2	6	6	6	5	2	2
4	C1	3	4	1	3	4	3	4	6	2
4	C2	3	3	1	3	3	3	3	7	2
4	C3	3	3	1	2	2	2	3	7	3
4	C4	3	3	1	3	3	3	3	6	2
4	C5	4	3	1	3	2	2	3	6	2
4	C6	3	2	1	2	2	2	2	7	2
4	C7	3	3	1	2	3	3	3	7	2
4	C8	2	2	2	2	1	2	2	7	2
4	C9	3	3	1	3	2	2	3	7	2
4	C10	2	3	2	3	2	2	3	7	2
4	C11	3	3	1	2	3	2	3	7	2
4	C12	4	4	1	4	4	4	4	6	2
4	C13	3	3	1	3	2	2	3	7	2
4	C14	2	1	2	2	1	2	3	7	2
4	C15	3	2	1	2	2	3	3	7	2

Table G.2: Raw demographics study data for subjects 3 and 4

Subject	Configuration	Question								
		1	2	3	4	5	6	7	8	9
5	C1	4	4	2	5	3	4	4	4	5
5	C2	4	5	4	5	5	5	5	3	3
5	C3	6	5	4	5	6	5	5	4	3
5	C4	5	4	3	5	5	5	6	5	2
5	C5	5	4	4	5	5	5	4	5	3
5	C6	5	5	5	5	5	5	5	5	5
5	C7	5	6	3	5	5	6	6	5	3
5	C8	4	3	5	3	4	3	4	6	7
5	C9	5	6	2	6	6	6	7	2	1
5	C10	3	2	6	3	4	2	2	6	7
5	C11	5	5	3	5	5	5	5	3	3
5	C12	4	6	2	5	4	5	5	5	3
5	C13	4	4	4	3	4	4	4	6	6
5	C14	4	5	3	5	5	5	5	3	4
5	C15	4	5	3	4	5	4	4	4	4
6	C1	4	3	2	1	3	1	2	1	2
6	C2	7	7	1	7	7	7	7	1	1
6	C3	4	2	5	4	4	2	2	7	1
6	C4	4	4	3	5	3	5	5	3	3
6	C5	6	6	2	6	6	6	6	2	2
6	C6	7	6	1	7	7	7	7	3	4
6	C7	6	6	2	6	7	6	6	5	6
6	C8	4	4	2	3	3	4	4	4	3
6	C9	5	5	5	5	5	1	6	7	7
6	C10	5	5	2	1	3	5	2	2	7
6	C11	5	5	3	5	5	5	4	2	4
6	C12	2	3	6	3	3	3	4	7	1
6	C13	2	1	1	1	1	1	1	7	1
6	C14	1	3	5	5	3	3	5	6	3
6	C15	5	5	3	6	3	5	4	4	4

Table G.3: Raw demographics study data for subjects 5 and 6

Subject	Configuration	Question								
		1	2	3	4	5	6	7	8	9
7	C1	2	2	5	2	3	3	2	5	5
7	C2	5	5	3	4	4	4	5	3	3
7	C3	1	1	7	1	1	1	2	6	7
7	C4	5	5	3	4	4	5	5	2	2
7	C5	2	2	2	1	2	3	2	4	2
7	C6	2	1	6	2	2	2	2	6	2
7	C7	4	4	2	3	3	4	4	5	2
7	C8	3	2	5	1	1	3	3	6	3
7	C9	2	2	6	2	2	2	2	6	5
7	C10	2	2	7	1	1	1	2	7	2
7	C11	5	5	3	4	4	4	5	6	3
7	C12	4	3	5	3	3	3	5	5	4
7	C13	4	3	6	2	2	3	4	7	2
7	C14	6	6	3	6	6	5	5	2	1
7	C15	3	4	5	4	4	4	4	5	4
8	C1	3	4	4	5	4	4	4	4	3
8	C2	3	5	4	5	4	3	3	3	2
8	C3	5	5	3	5	6	6	5	4	3
8	C4	4	6	3	6	6	5	4	3	3
8	C5	5	4	2	4	5	5	5	4	3
8	C6	5	5	3	5	5	6	5	4	3
8	C7	3	5	4	4	5	4	4	4	2
8	C8	3	3	3	4	4	5	4	5	5
8	C9	2	4	5	3	3	2	3	4	2
8	C10	5	5	3	5	6	5	4	4	3
8	C11	3	4	5	4	2	2	4	4	2
8	C12	2	2	5	3	3	3	3	4	2
8	C13	5	6	2	6	6	6	6	2	2
8	C14	2	4	4	4	3	3	4	3	2
8	C15	2	5	4	4	4	2	5	3	1

Table G.4: Raw demographics study data for subjects 7 and 8

Subject	Configuration	Question								
		1	2	3	4	5	6	7	8	9
9	C1	5	6	5	4	4	4	5	4	3
9	C2	6	4	4	3	4	4	4	5	4
9	C3	4	5	3	4	4	5	5	4	3
9	C4	5	4	4	3	3	3	3	5	4
9	C5	5	5	3	4	4	4	5	5	4
9	C6	5	2	6	1	2	2	1	6	2
9	C7	6	3	6	2	2	2	3	6	5
9	C8	5	3	6	3	3	3	3	6	1
9	C9	6	2	6	2	3	2	3	5	6
9	C10	6	2	7	1	1	1	2	6	3
9	C11	4	5	5	4	4	4	7	5	2
9	C12	4	6	3	4	4	5	5	4	3
9	C13	6	3	3	3	2	2	3	6	4
9	C14	5	5	2	5	5	5	6	4	3
9	C15	6	4	4	3	4	4	4	5	4
10	C1	2	2	5	3	3	3	2	5	3
10	C2	3	5	2	5	4	5	6	3	3
10	C3	3	4	4	5	5	4	5	3	3
10	C4	3	5	3	4	5	5	5	3	3
10	C5	4	5	2	5	5	5	5	2	2
10	C6	3	3	5	2	3	3	3	4	5
10	C7	1	1	6	1	1	2	2	6	2
10	C8	2	2	5	3	3	3	3	6	2
10	C9	5	5	3	4	4	5	5	4	3
10	C10	3	4	3	5	5	4	5	5	3
10	C11	5	5	3	4	3	4	3	5	2
10	C12	5	5	2	6	6	6	6	2	2
10	C13	2	2	3	2	3	2	3	6	2
10	C14	5	5	2	6	6	6	6	2	2
10	C15	6	6	2	6	6	6	6	2	2

Table G.5: Raw demographics study data for subjects 9 and 10

Subject	Configuration	Question								
		1	2	3	4	5	6	7	8	9
11	C1	6	4	6	3	4	5	5	5	2
11	C2	5	2	4	2	3	2	3	7	7
11	C3	5	6	3	5	5	5	5	6	3
11	C4	6	3	6	2	4	3	5	7	4
11	C5	7	7	2	7	6	6	6	3	2
11	C6	6	6	3	3	3	4	5	5	3
11	C7	6	4	4	4	4	6	5	7	4
11	C8	6	4	3	4	4	5	3	4	4
11	C9	4	4	5	4	2	4	4	6	6
11	C10	6	6	4	4	4	5	5	5	2
11	C11	7	6	4	3	4	4	3	5	3
11	C12	5	1	6	1	2	3	4	6	4
11	C13	7	4	6	6	6	5	4	4	2
11	C14	6	6	4	5	4	6	6	6	3
11	C15	5	2	6	2	2	2	3	7	6
12	C1	4	3	5	3	2	3	3	5	5
12	C2	2	2	4	2	2	3	5	5	5
12	C3	3	5	4	4	3	5	4	5	6
12	C4	5	6	4	5	6	5	5	4	3
12	C5	6	6	2	5	6	5	5	3	4
12	C6	3	2	5	1	2	3	2	5	5
12	C7	4	1	6	1	1	1	1	6	3
12	C8	6	5	3	6	5	5	6	5	2
12	C9	6	5	4	4	6	5	5	4	3
12	C10	4	2	5	1	3	2	1	6	5
12	C11	5	4	4	4	4	4	4	5	3
12	C12	6	6	3	6	6	6	6	2	2
12	C13	2	2	7	2	1	3	2	7	7
12	C14	4	4	5	5	4	4	3	6	6
12	C15	5	4	2	3	3	3	3	7	5

Table G.6: Raw demographics study data for subjects 11 and 12

Subject	Configuration	Question								
		1	2	3	4	5	6	7	8	9
13	C1	4	4	4	5	5	4	5	5	5
13	C2	5	6	2	6	6	4	6	3	4
13	C3	4	5	3	5	5	4	5	3	4
13	C4	3	3	5	4	4	4	3	5	5
13	C5	5	5	3	5	5	4	5	3	4
13	C6	3	3	5	4	4	3	3	6	5
13	C7	3	3	7	3	3	3	2	7	7
13	C8	3	4	5	3	3	3	3	6	5
13	C9	4	3	6	3	3	4	3	6	6
13	C10	3	3	5	3	3	3	3	6	4
13	C11	4	4	4	4	4	3	3	6	6
13	C12	5	6	4	6	6	5	5	4	4
13	C13	5	6	3	6	6	4	6	4	4
13	C14	4	5	4	5	5	5	5	5	4
13	C15	4	5	3	5	5	3	5	4	4
14	C1	4	5	3	5	5	4	5	5	5
14	C2	5	6	4	7	6	6	6	5	4
14	C3	4	5	3	5	6	4	6	6	5
14	C4	2	4	2	5	5	4	3	5	5
14	C5	4	6	4	6	6	5	6	5	5
14	C6	4	5	4	5	6	5	6	6	6
14	C7	2	2	3	2	1	1	2	6	6
14	C8	4	5	4	6	6	5	5	5	6
14	C9	4	4	2	5	5	4	5	5	5
14	C10	4	5	5	6	6	6	6	5	5
14	C11	4	5	4	6	6	6	6	4	4
14	C12	4	6	4	5	5	4	6	6	5
14	C13	5	6	4	6	6	6	6	6	5
14	C14	4	6	4	5	5	4	5	6	5
14	C15	5	7	3	6	6	5	6	4	5

Table G.7: Raw demographics study data for subjects 13 and 14

Subject	Configuration	Question								
		1	2	3	4	5	6	7	8	9
15	C1	5	3	3	4	5	5	4	7	5
15	C2	2	2	7	3	3	1	3	7	5
15	C3	7	7	3	7	7	6	6	6	4
15	C4	1	1	6	1	3	2	3	7	4
15	C5	7	7	1	7	7	7	7	4	1
15	C6	2	2	2	1	2	2	5	7	1
15	C7	2	2	7	3	3	2	3	7	5
15	C8	5	5	4	5	5	5	5	6	3
15	C9	1	1	7	1	1	1	2	7	2
15	C10	6	6	2	6	6	6	4	7	2
15	C11	5	5	6	5	5	4	6	6	4
15	C12	3	5	5	3	4	4	2	7	5
15	C13	6	5	4	5	5	5	6	7	3
15	C14	4	5	5	5	5	4	5	5	2
15	C15	3	3	6	3	2	2	2	7	5
16	C1	4	3	4	4	4	4	3	5	5
16	C2	6	6	2	7	7	7	7	2	2
16	C3	6	6	3	6	6	7	6	3	2
16	C4	5	6	2	6	6	6	6	2	2
16	C5	5	6	3	6	6	7	7	2	3
16	C6	4	4	5	4	4	4	3	6	4
16	C7	3	2	6	2	2	2	2	6	6
16	C8	3	3	6	2	3	2	2	6	7
16	C9	3	3	5	2	2	2	1	3	2
16	C10	4	4	3	4	4	4	4	5	5
16	C11	6	7	2	7	7	7	7	2	2
16	C12	4	5	5	5	5	4	5	5	4
16	C13	6	6	2	6	6	7	7	2	2
16	C14	6	6	3	6	6	6	6	3	2
16	C15	6	6	2	6	6	6	6	2	2

Table G.8: Raw demographics study data for subjects 15 and 16

Subject	Configuration	Question								
		1	2	3	4	5	6	7	8	9
17	C1	4	4	3	3	3	3	4	5	2
17	C2	3	6	4	6	4	4	6	5	4
17	C3	2	5	4	5	3	4	5	5	3
17	C4	1	5	6	5	3	2	5	3	1
17	C5	6	5	3	6	6	6	6	4	2
17	C6	4	3	5	4	3	3	4	5	2
17	C7	3	4	5	4	3	3	4	5	2
17	C8	5	4	5	4	4	4	5	5	2
17	C9	4	3	4	2	3	3	2	5	2
17	C10	6	6	3	6	5	6	6	5	2
17	C11	5	4	3	3	4	4	5	4	4
17	C12	2	2	5	3	2	2	2	5	4
17	C13	6	7	3	6	6	6	5	4	3
17	C14	6	6	2	6	6	6	6	4	2
17	C15	5	3	4	3	3	3	2	4	4
18	C1	4	7	6	6	5	4	7	4	1
18	C2	6	6	1	6	6	6	7	2	2
18	C3	3	4	2	5	4	3	5	4	3
18	C4	4	6	6	6	5	4	6	4	1
18	C5	5	5	3	5	4	6	6	4	5
18	C6	3	4	4	3	3	4	4	6	3
18	C7	4	4	6	4	3	2	4	6	1
18	C8	6	6	2	7	6	6	6	3	3
18	C9	2	1	5	2	2	1	5	7	2
18	C10	4	5	3	5	5	6	6	4	6
18	C11	3	4	6	4	4	3	5	4	1
18	C12	3	3	6	3	3	3	2	5	2
18	C13	5	6	2	6	5	6	6	2	4
18	C14	5	6	4	6	6	6	6	3	3
18	C15	4	5	5	5	4	3	5	5	2

Table G.9: Raw demographics study data for subjects 17 and 18

Subject	Configuration	Question								
		1	2	3	4	5	6	7	8	9
19	C1	2	2	6	2	2	2	2	7	2
19	C2	2	3	5	2	2	3	2	7	2
19	C3	2	2	7	2	2	2	1	7	1
19	C4	2	3	6	3	3	3	2	7	2
19	C5	3	2	6	1	2	2	1	7	1
19	C6	3	3	7	1	3	2	1	7	1
19	C7	2	2	7	2	2	2	2	7	2
19	C8	2	1	7	1	2	1	1	7	2
19	C9	2	1	7	1	2	2	1	7	2
19	C10	2	1	7	2	2	2	1	7	2
19	C11	2	2	6	2	2	2	2	7	2
19	C12	2	3	6	3	2	2	2	7	2
19	C13	2	1	7	2	1	2	1	7	2
19	C14	1	1	7	1	3	2	1	7	1
19	C15	2	2	7	2	1	2	2	7	2
20	C1	2	5	2	5	3	4	5	3	2
20	C2	3	5	3	5	3	3	5	4	4
20	C3	2	3	3	4	3	2	3	3	4
20	C4	2	5	2	5	4	2	3	3	2
20	C5	2	4	3	5	4	4	4	4	4
20	C6	2	2	4	2	2	2	2	7	4
20	C7	1	1	7	1	1	1	1	7	2
20	C8	4	4	3	4	3	3	3	4	3
20	C9	2	2	6	1	1	2	2	6	3
20	C10	3	4	3	3	3	3	4	4	4
20	C11	3	5	4	5	3	3	4	5	4
20	C12	2	4	2	4	2	2	4	4	2
20	C13	3	5	3	5	5	3	5	4	4
20	C14	3	5	3	5	4	4	4	4	2
20	C15	3	5	4	5	3	3	5	4	4

Table G.10: Raw demographics study data for subjects 19 and 20

Subject	Configuration	Question								
		1	2	3	4	5	6	7	8	9
21	C1	4	3	5	4	4	3	3	3	4
21	C2	5	5	3	5	5	5	5	3	3
21	C3	3	2	5	3	3	2	2	5	5
21	C4	6	5	3	6	5	5	5	3	2
21	C5	3	4	3	4	4	3	3	4	4
21	C6	6	6	2	5	5	5	5	2	2
21	C7	5	4	4	5	5	5	4	3	3
21	C8	4	4	3	4	4	4	5	4	3
21	C9	3	4	3	3	2	3	3	5	5
21	C10	5	5	3	5	4	5	4	3	4
21	C11	5	5	3	5	5	5	5	2	3
21	C12	5	5	2	5	5	5	5	3	3
21	C13	5	5	3	5	5	5	4	3	3
21	C14	5	6	2	6	5	5	5	2	2
21	C15	5	6	2	6	5	6	5	3	2
22	C1	6	6	2	6	6	6	5	5	5
22	C2	5	6	3	6	6	5	5	4	4
22	C3	5	5	6	6	5	4	5	6	6
22	C4	5	6	2	6	6	6	5	5	5
22	C5	2	2	6	2	2	2	1	7	2
22	C6	5	3	6	4	4	3	3	6	6
22	C7	4	4	5	5	3	3	4	6	6
22	C8	5	4	3	4	5	4	4	6	4
22	C9	6	6	5	5	5	4	6	6	6
22	C10	5	5	3	5	5	5	5	5	4
22	C11	5	6	2	5	5	5	5	5	5
22	C12	6	5	5	6	4	5	5	6	6
22	C13	5	6	2	6	5	5	6	3	3
22	C14	6	6	3	6	6	5	5	6	6
22	C15	6	6	2	6	6	6	6	2	2

Table G.11: Raw demographics study data for subjects 21 and 22

Subject	Configuration	Question								
		1	2	3	4	5	6	7	8	9
23	C1	4	2	4	2	2	2	4	6	6
23	C2	4	6	6	5	4	4	7	6	2
23	C3	6	7	2	7	7	7	7	2	1
23	C4	5	5	3	5	5	6	6	6	2
23	C5	6	7	3	6	6	6	6	2	1
23	C6	6	6	3	6	6	6	6	6	2
23	C7	3	5	6	5	5	4	5	6	3
23	C8	5	3	2	2	4	6	6	6	3
23	C9	3	2	3	2	3	2	3	6	1
23	C10	5	5	1	6	6	5	7	6	5
23	C11	4	6	6	5	5	4	5	5	5
23	C12	5	6	4	6	5	5	6	3	2
23	C13	4	5	2	5	4	5	7	5	6
23	C14	7	7	2	6	7	7	7	4	1
23	C15	4	4	7	5	4	5	6	7	5
24	C1	5	6	5	5	6	5	6	6	3
24	C2	5	6	6	6	5	4	6	5	6
24	C3	6	6	4	6	6	6	7	5	4
24	C4	3	2	5	3	3	2	2	5	3
24	C5	5	5	4	4	4	4	5	5	6
24	C6	6	6	4	6	6	7	6	6	4
24	C7	6	6	5	6	5	5	5	6	5
24	C8	4	3	5	4	4	5	5	6	6
24	C9	6	6	5	4	5	5	5	6	5
24	C10	3	2	6	3	2	3	2	6	2
24	C11	6	6	6	5	5	4	5	6	6
24	C12	7	6	4	6	6	6	6	4	5
24	C13	5	5	5	4	5	4	5	5	5
24	C14	5	6	7	5	5	6	6	6	6
24	C15	6	7	5	6	6	6	7	5	5

Table G.12: Raw demographics study data for subjects 23 and 24

Subject	Configuration	Question								
		1	2	3	4	5	6	7	8	9
25	C1	6	6	4	6	6	6	4	5	3
25	C2	6	5	4	6	5	5	5	4	3
25	C3	6	5	4	6	6	6	5	3	3
25	C4	6	6	4	6	6	6	5	5	4
25	C5	6	6	3	6	6	6	5	3	3
25	C6	6	5	5	6	6	6	5	6	4
25	C7	5	4	5	5	4	4	4	6	4
25	C8	6	6	4	6	6	6	5	7	3
25	C9	6	5	6	6	6	6	4	6	4
25	C10	6	6	4	6	6	5	4	7	3
25	C11	6	6	6	6	6	6	5	4	3
25	C12	6	6	4	6	6	6	4	5	3
25	C13	5	4	3	5	4	3	3	4	4
25	C14	6	6	4	6	6	6	6	5	3
25	C15	6	6	3	6	6	6	6	5	3
26	C1	4	7	2	6	5	5	6	6	6
26	C2	4	4	3	5	5	5	7	6	4
26	C3	4	5	6	6	4	4	5	7	5
26	C4	4	6	2	5	5	5	6	4	6
26	C5	5	7	6	6	5	5	6	6	4
26	C6	4	5	7	2	3	4	6	7	6
26	C7	3	1	7	2	4	3	2	7	6
26	C8	3	1	7	1	1	3	4	7	7
26	C9	1	1	7	1	1	1	1	7	6
26	C10	2	3	7	1	3	3	5	7	6
26	C11	4	5	3	4	5	5	5	7	6
26	C12	3	7	1	6	5	4	5	3	6
26	C13	3	5	7	5	5	5	5	7	5
26	C14	3	6	6	7	4	4	6	6	5
26	C15	4	3	6	3	5	6	6	7	6

Table G.13: Raw demographics study data for subjects 25 and 26

Subject	Configuration	Question								
		1	2	3	4	5	6	7	8	9
27	C1	5	5	4	6	5	5	5	6	5
27	C2	5	6	2	6	6	6	6	4	2
27	C3	3	3	5	3	3	4	2	7	5
27	C4	5	6	3	6	6	5	6	4	2
27	C5	6	6	3	6	6	5	6	4	2
27	C6	5	5	4	5	6	5	5	6	4
27	C7	5	3	3	4	4	4	4	7	3
27	C8	6	6	3	6	6	6	6	4	3
27	C9	6	6	3	6	6	6	6	6	2
27	C10	4	3	4	4	3	4	3	7	4
27	C11	2	2	6	1	1	2	2	6	2
27	C12	4	5	3	6	6	5	5	6	4
27	C13	5	5	3	5	5	4	5	5	3
27	C14	3	4	4	4	3	4	3	6	5
27	C15	4	3	5	2	2	2	4	6	4
28	C1	3	4	3	3	2	3	2	3	3
28	C2	7	6	1	6	5	5	5	4	1
28	C3	2	2	3	2	3	3	2	2	3
28	C4	3	4	2	3	3	2	2	2	4
28	C5	5	5	1	6	6	5	5	2	3
28	C6	3	2	2	2	2	1	3	3	2
28	C7	2	2	4	3	3	3	2	3	2
28	C8	5	5	2	6	6	6	5	4	2
28	C9	5	4	3	5	5	4	4	3	3
28	C10	6	5	6	5	5	5	5	4	2
28	C11	3	3	4	5	3	5	3	6	1
28	C12	2	3	4	2	3	2	3	5	2
28	C13	7	6	1	6	6	6	7	3	1
28	C14	4	3	3	3	5	5	4	3	3
28	C15	7	6	1	7	7	7	7	2	2

Table G.14: Raw demographics study data for subjects 27 and 28

Subject	Configuration	Question								
		1	2	3	4	5	6	7	8	9
29	C1	4	3	4	4	4	5	5	4	3
29	C2	5	5	3	5	5	5	5	2	3
29	C3	4	5	2	5	5	5	5	3	3
29	C4	3	4	5	5	4	4	3	5	3
29	C5	5	5	3	5	5	5	5	2	2
29	C6	3	5	5	5	5	5	5	3	3
29	C7	3	4	5	3	3	3	3	5	3
29	C8	5	5	4	5	5	5	5	5	2
29	C9	2	3	5	3	3	3	3	5	3
29	C10	4	3	5	3	3	2	3	5	6
29	C11	4	4	5	3	3	3	3	6	3
29	C12	6	6	2	6	6	6	6	2	2
29	C13	6	6	2	6	6	6	6	2	2
29	C14	5	5	3	5	5	5	5	3	3
29	C15	6	6	3	6	6	6	6	4	5
30	C1	3	2	6	3	5	3	2	6	2
30	C2	5	5	3	5	5	5	5	3	3
30	C3	5	6	4	5	5	5	5	3	5
30	C4	3	3	5	3	3	3	3	5	3
30	C5	3	3	4	3	3	3	3	5	3
30	C6	1	1	7	1	1	1	1	7	7
30	C7	5	5	4	5	4	4	4	2	2
30	C8	5	4	5	4	3	3	3	5	4
30	C9	5	2	5	2	2	2	2	5	5
30	C10	5	5	4	5	4	4	4	4	3
30	C11	6	6	2	6	6	6	6	2	2
30	C12	5	4	4	5	5	4	4	5	5
30	C13	6	6	2	6	6	6	6	3	3
30	C14	6	6	2	6	6	6	6	2	4
30	C15	6	6	2	6	6	6	6	2	2

Table G.15: Raw demographics study data for subjects 29 and 30

Subject	Configuration	Question								
		1	2	3	4	5	6	7	8	9
31	C1	4	5	2	7	6	6	7	2	3
31	C2	6	7	3	7	7	7	7	1	1
31	C3	6	6	2	6	6	6	6	2	2
31	C4	7	7	1	7	7	7	7	1	1
31	C5	7	7	1	7	7	7	6	2	2
31	C6	5	5	3	5	5	4	5	6	4
31	C7	5	2	3	7	6	3	2	6	3
31	C8	6	4	5	5	6	5	5	6	4
31	C9	4	4	3	5	5	3	4	6	4
31	C10	6	5	4	6	6	4	4	4	3
31	C11	7	7	1	7	7	7	7	1	1
31	C12	6	5	5	6	6	5	6	3	4
31	C13	7	7	2	7	7	7	7	1	1
31	C14	6	6	1	7	7	6	7	2	3
31	C15	7	7	1	6	7	7	7	1	1
32	C1	4	6	3	6	6	6	5	5	7
32	C2	2	3	5	3	3	4	4	5	7
32	C3	1	1	3	2	1	2	4	7	7
32	C4	3	5	3	5	5	5	4	7	7
32	C5	1	4	4	3	2	3	7	7	7
32	C6	1	3	4	3	2	3	3	7	7
32	C7	3	4	4	5	5	5	4	7	7
32	C8	3	6	4	4	5	3	5	5	6
32	C9	1	4	4	1	1	1	3	7	7
32	C10	3	4	3	4	4	4	5	7	7
32	C11	2	5	3	5	5	5	4	7	7
32	C12	2	1	4	1	1	1	2	7	7
32	C13	2	5	3	5	5	5	4	7	7
32	C14	3	5	4	3	4	4	6	7	7
32	C15	2	5	2	5	5	5	4	5	7

Table G.16: Raw demographics study data for subjects 31 and 32

Subject	Configuration	Question								
		1	2	3	4	5	6	7	8	9
33	C1	3	4	5	4	3	3	5	6	3
33	C2	3	2	5	4	4	4	5	6	4
33	C3	4	4	6	2	2	2	2	7	1
33	C4	3	3	5	3	3	2	4	4	4
33	C5	4	4	7	2	2	2	2	7	4
33	C6	1	1	7	1	1	1	1	7	5
33	C7	5	3	6	5	3	3	5	7	3
33	C8	3	1	7	2	2	1	2	7	4
33	C9	4	2	5	2	1	1	3	7	6
33	C10	2	3	4	4	3	2	2	5	4
33	C11	4	4	5	3	2	3	4	7	3
33	C12	4	3	6	3	3	3	4	5	4
33	C13	4	5	7	4	3	3	6	7	3
33	C14	4	5	3	4	3	3	3	7	5
33	C15	3	3	4	6	4	4	5	6	4
34	C1	3	3	4	4	3	3	5	5	5
34	C2	4	6	2	6	6	5	7	3	2
34	C3	3	6	4	5	4	5	6	5	3
34	C4	3	3	5	2	2	2	4	6	3
34	C5	4	5	3	5	3	6	6	5	4
34	C6	1	2	5	1	1	2	4	6	4
34	C7	4	7	1	6	6	6	6	2	3
34	C8	4	6	2	6	5	3	6	7	5
34	C9	3	3	5	3	2	3	4	6	5
34	C10	2	2	4	3	2	3	1	7	6
34	C11	4	5	5	3	3	3	5	5	4
34	C12	4	5	2	6	4	3	5	5	4
34	C13	4	6	3	4	4	3	6	6	2
34	C14	1	1	4	1	1	1	3	6	4
34	C15	5	6	1	6	6	5	6	4	2

Table G.17: Raw demographics study data for subjects 33 and 34

Subject	Configuration	Question								
		1	2	3	4	5	6	7	8	9
35	C1	5	5	3	5	5	6	6	3	3
35	C2	5	5	4	5	5	5	5	5	4
35	C3	4	3	3	3	3	4	4	5	4
35	C4	5	5	2	6	6	5	6	4	3
35	C5	5	5	3	5	5	5	5	4	3
35	C6	4	3	4	3	3	3	4	5	5
35	C7	2	1	2	2	2	2	1	5	5
35	C8	4	3	5	3	4	4	4	5	4
35	C9	1	1	6	2	2	2	2	5	6
35	C10	4	4	4	3	3	4	4	5	5
35	C11	4	3	4	3	3	3	3	5	5
35	C12	4	4	4	4	4	5	4	3	4
35	C13	5	5	3	5	5	5	5	5	4
35	C14	5	5	4	5	5	5	5	4	3
35	C15	5	4	4	4	4	5	4	5	4
36	C1	2	3	1	4	4	3	4	3	1
36	C2	2	2	2	3	3	3	3	3	2
36	C3	3	2	5	1	1	2	3	7	5
36	C4	2	3	1	3	4	2	3	3	2
36	C5	3	2	5	2	1	2	2	5	5
36	C6	2	2	3	2	3	2	3	3	4
36	C7	2	1	1	1	2	2	1	6	2
36	C8	1	1	2	1	1	2	3	5	7
36	C9	2	2	1	2	2	2	3	6	7
36	C10	2	2	2	2	2	2	3	3	2
36	C11	2	2	3	1	2	3	2	1	1
36	C12	3	6	1	6	5	5	6	5	1
36	C13	2	3	3	2	3	2	3	3	1
36	C14	2	4	2	5	5	3	4	3	1
36	C15	2	3	1	3	4	3	3	2	2

Table G.18: Raw demographics study data for subjects 35 and 36

Subject	Configuration	Question								
		1	2	3	4	5	6	7	8	9
37	C1	4	4	2	5	4	4	5	5	2
37	C2	4	4	2	5	5	5	5	4	3
37	C3	3	4	2	4	5	5	5	5	2
37	C4	3	3	2	3	5	5	5	5	3
37	C5	4	2	3	2	2	2	5	6	3
37	C6	4	5	2	5	5	5	5	5	2
37	C7	4	4	2	3	3	4	5	5	2
37	C8	4	4	3	2	2	5	5	6	3
37	C9	4	3	3	4	4	4	5	5	4
37	C10	4	2	2	2	2	3	4	6	4
37	C11	4	3	2	3	2	3	5	5	2
37	C12	4	5	3	5	5	5	5	5	2
37	C13	4	2	2	2	2	4	5	6	3
37	C14	4	5	2	5	4	4	5	6	4
37	C15	3	2	3	3	4	3	4	5	3
38	C1	5	6	2	6	6	6	6	6	4
38	C2	5	5	5	4	5	3	4	4	4
38	C3	6	6	3	6	6	6	6	3	6
38	C4	6	6	2	6	6	6	6	3	3
38	C5	6	6	3	6	6	6	5	2	6
38	C6	5	5	5	2	5	5	4	6	6
38	C7	6	6	6	2	6	5	5	5	5
38	C8	2	2	6	2	2	2	2	6	5
38	C9	6	6	4	6	5	4	4	6	4
38	C10	5	2	4	4	5	4	4	6	3
38	C11	5	3	4	3	4	4	3	6	4
38	C12	6	6	2	7	6	6	6	2	4
38	C13	6	6	2	6	6	6	6	5	3
38	C14	7	7	2	7	7	7	7	3	3
38	C15	6	6	2	6	6	6	6	3	6

Table G.19: Raw demographics study data for subjects 37 and 38

Subject	Configuration	Question								
		1	2	3	4	5	6	7	8	9
39	C1	5	3	3	4	4	5	5	6	4
39	C2	4	3	4	3	3	4	5	4	5
39	C3	3	3	5	3	3	3	3	5	5
39	C4	3	4	3	5	4	4	5	5	3
39	C5	5	4	4	4	5	5	5	6	4
39	C6	4	3	5	3	4	3	4	6	4
39	C7	3	2	5	2	2	3	3	5	3
39	C8	4	3	5	3	5	3	4	6	5
39	C9	3	3	5	3	3	3	4	6	3
39	C10	3	1	4	1	3	2	3	6	6
39	C11	3	3	4	4	3	3	4	5	3
39	C12	5	4	3	5	5	4	5	6	4
39	C13	4	3	5	2	3	2	4	5	5
39	C14	4	4	4	3	3	4	5	5	4
39	C15	4	4	5	4	4	3	4	5	4
40	C1	6	6	2	6	6	5	6	1	1
40	C2	4	5	2	5	4	5	6	3	2
40	C3	6	6	3	6	7	4	5	4	2
40	C4	6	6	3	5	5	6	6	3	3
40	C5	6	5	1	6	6	7	7	2	2
40	C6	4	3	4	3	3	3	4	4	6
40	C7	4	4	2	5	3	5	5	3	2
40	C8	5	6	2	3	5	4	5	3	2
40	C9	5	5	3	6	5	4	5	3	4
40	C10	4	5	3	5	5	4	5	3	2
40	C11	4	5	3	4	4	3	4	4	4
40	C12	6	6	2	6	5	6	7	2	2
40	C13	2	1	6	1	2	1	2	6	6
40	C14	3	2	3	2	3	2	2	5	6
40	C15	3	3	5	3	2	2	3	5	6

Table G.20: Raw demographics study data for subjects 39 and 40

Subject	Configuration	Question								
		1	2	3	4	5	6	7	8	9
41	C1	3	5	2	5	5	5	5	5	3
41	C2	4	6	2	6	3	5	5	4	3
41	C3	4	6	2	6	6	6	6	2	4
41	C4	3	4	4	3	3	4	4	4	4
41	C5	4	6	2	6	6	6	6	2	2
41	C6	2	4	6	3	4	4	3	6	3
41	C7	2	3	6	2	3	3	2	6	5
41	C8	4	2	5	2	2	3	3	6	5
41	C9	2	2	6	2	2	2	2	6	2
41	C10	4	2	6	2	2	2	2	5	4
41	C11	3	3	5	3	3	3	3	6	4
41	C12	4	6	3	6	5	5	5	4	3
41	C13	4	5	4	6	6	5	5	5	2
41	C14	4	4	4	5	5	5	4	4	3
41	C15	3	4	5	4	3	3	3	6	4
42	C1	4	5	3	5	5	5	5	3	3
42	C2	4	5	3	6	6	5	5	2	3
42	C3	4	5	3	6	5	5	6	3	4
42	C4	3	4	3	4	4	4	4	4	5
42	C5	4	4	3	4	4	4	5	3	4
42	C6	3	3	5	3	3	3	3	5	5
42	C7	2	1	6	1	1	1	1	6	6
42	C8	5	1	5	2	2	1	2	6	5
42	C9	3	2	5	2	3	3	4	5	5
42	C10	4	5	4	5	5	5	5	4	4
42	C11	3	3	4	3	4	3	3	5	5
42	C12	4	5	4	5	5	4	5	3	4
42	C13	4	4	3	5	5	4	4	3	4
42	C14	4	3	5	4	4	4	4	4	4
42	C15	3	3	4	3	3	3	3	6	5

Table G.21: Raw demographics study data for subjects 41 and 42

Subject	Configuration	Question								
		1	2	3	4	5	6	7	8	9
43	C1	6	7	2	7	7	7	7	3	3
43	C2	6	7	3	7	7	7	7	1	3
43	C3	6	7	2	7	7	7	7	2	2
43	C4	5	6	3	6	7	5	6	5	3
43	C5	6	7	1	7	7	7	7	1	2
43	C6	4	5	6	4	4	3	4	5	5
43	C7	4	1	7	1	1	1	1	7	4
43	C8	5	5	4	5	5	4	7	5	4
43	C9	3	3	5	3	3	3	4	4	4
43	C10	5	4	4	4	4	4	5	5	4
43	C11	4	3	6	3	2	3	4	7	4
43	C12	5	6	3	5	5	5	6	4	4
43	C13	6	7	5	7	7	7	7	5	2
43	C14	4	5	5	5	5	5	6	4	4
43	C15	6	7	2	7	7	7	7	4	4

Table G.22: Raw demographics study data for subject 43

Appendix H

Simulator Operation

The Clemson University steering simulator was developed in modules. As such, the operation of the simulator was not a simple turn-key operation. The follow are sets of direction with accompanying photos for starting, changing, resetting, and shutting down the simulator.

Hardware Startup

1. Turn on power strips/3 phase

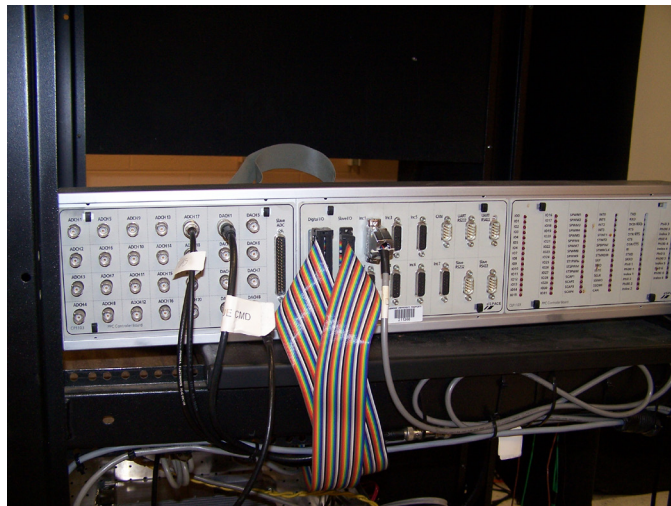


2. Power on both computers (password: tronics)

3. Power on Projectors



4. Power on dSPACE board



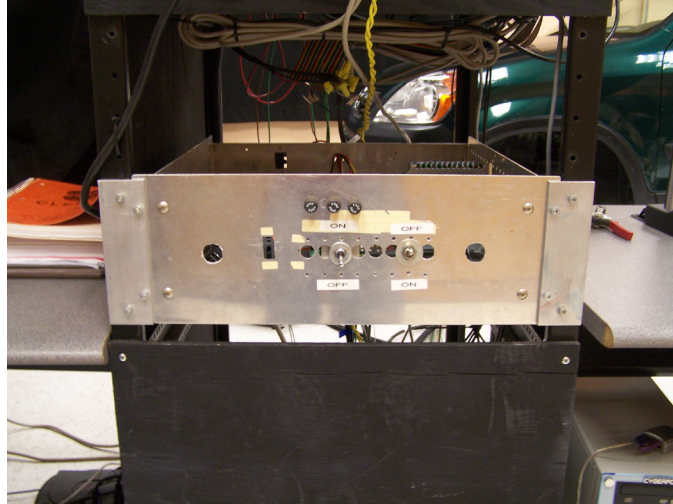
5. Power on audio amplifier



6. Power on dashboard amplifier



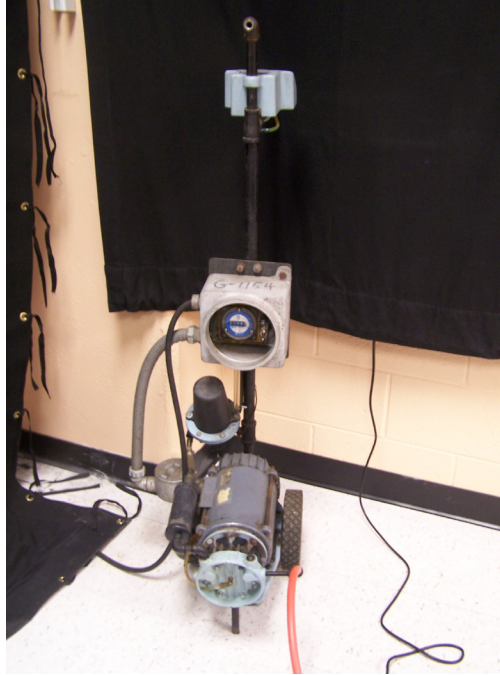
7. Power on motor controller (left first)



8. Power on motion control box (leave E-stop engaged)



9. Power on Vacuum Pump



10. Ensure Steering Wheel is centered

Software Startup from Scratch

1. Start CarSim 7
2. Select scenario from menu: Datasets > Honda Simulator
3. Start dSPACE ControlDesk
4. In ControlDesk: Platform > Initialization > Refresh Platform Connection (Ctrl-Shift-R)
5. In CarSim: More > Download Program to Target
6. In CarSim: More > Download Parsfiles to Target
7. On Image Generation (IG) computer: Run “3 screen” from desktop
8. In CarSim: Start Live Video
9. On IG: Click mouse on bottom right corner of right monitor
10. In CarSim: Load/Run
11. Disengage Motion E-stop
12. Adjust steering variables in ControlDesk as desired
13. Use Red Stop Button in ControlDesk to stop simulation

Start after Stop

1. Ensure ControlDesk is in “Animation Mode”
2. In CarSim: Run

Scene Change

1. Stop current run with Red Stop Button in ControlDesk
2. Change ControlDesk to Edit Mode
3. In ControlDesk: Platform > Initialization > Refresh Platform Connection (Ctrl-Shift-R)
4. Close all 3 Animation windows
5. In CarSim: Select new scenario from menu: Datasets > Honda Simulator
6. In CarSim: More > Download Program to Target
7. In CarSim: More > Download Parsfiles to Target
8. On Image Generation (IG) computer: Run “3 screen” from desktop
9. In CarSim: Start Live Video
10. On IG: Click mouse on bottom right corner of right monitor
11. In CarSim: Load/Run

Software Reset

1. Stop current run with Red Stop Button in ControlDesk
2. Change ControlDesk to Edit Mode
3. In ControlDesk: Platform > Initialization > Refresh Platform Connection (Ctrl-Shift-R)
4. In CarSim: Load/Run

Full Shutdown

1. Stop current run with Red Stop Button in ControlDesk
2. Engage Motion E-Stop
3. Close Animation Windows
4. Change ControlDesk to Edit Mode
5. In ControlDesk: Platform > Initialization > Refresh Platform Connection (Ctrl-Shift-R)
6. Close ControlDesk
7. Close CarSim
8. Power Off vacuum pump
9. Power Off motion control box
10. Power Off motor controller (right first)
11. Power Off dashboard amplifier
12. Power Off audio amplifier
13. Power Off projectors
14. Power Off dSPACE box
15. Shutdown computers

Appendix I

Active Steering Controller Simulink Block Diagram

The modeling, estimation, and control during the run-off-road vehicle event were performed within Matlab/Simulink. The Simulink block diagram has been shown.

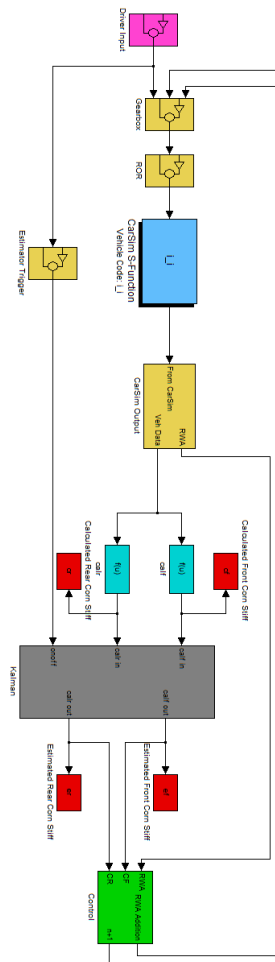


Figure H.1: Simulink block diagram for active steering controller with subsystems for modeling the driver, steering gearbox, road event, CarSim vehicle dynamics, cornering stiffness estimator, and steering controller

Appendix J

Normalized Objective Metrics

The data channels collected during the demographics study were converted into individual objective metrics and normalized according to equations (5.4) and (5.5). A separate metric was created for each combination of driver (39), steering configuration (5), and data channel (13) for a total of 2,535 metrics.

Subject	Config	Data Channel												
		1	2	3	4	5	6	7	8	9	10	11	12	13
1	1	1.11	0.73	0.75	0.71	0.74	0.93	1.01	0.92	1.03	0.84	0.83	1.03	1.00
1	2	0.78	1.04	1.05	1.08	1.06	1.05	1.05	1.07	1.06	1.03	1.05	1.18	1.03
1	3	1.15	0.56	0.73	0.55	0.72	0.90	0.88	0.91	0.78	0.64	0.65	0.76	0.97
1	4	0.87	0.84	0.83	0.88	0.85	0.96	1.18	0.90	1.32	0.93	0.99	1.05	0.94
1	5	1.08	1.84	1.64	1.78	1.63	1.16	0.87	1.21	0.82	1.56	1.49	0.98	1.06
2	1	0.84	0.55	0.56	0.46	0.58	0.94	1.26	0.68	2.16	1.20	1.15	0.84	0.75
2	2	1.25	2.00	1.88	2.27	1.94	1.08	1.19	1.34	0.91	0.97	1.07	1.05	1.07
2	3	0.88	0.86	0.93	0.83	0.89	1.01	0.61	1.13	0.00	0.85	0.84	1.29	1.20
2	4	1.15	0.73	0.72	0.59	0.71	1.04	1.27	0.81	1.91	1.20	1.14	0.80	0.83
2	5	0.88	0.85	0.90	0.85	0.87	0.93	0.67	1.04	0.01	0.79	0.80	1.02	1.15
3	1	1.68	0.08	0.15	0.09	0.14	0.55	0.61	0.35	0.45	0.43	0.42	0.61	0.63
3	2	0.58	2.32	2.00	2.25	1.99	1.36	1.31	1.54	0.01	1.78	1.77	1.43	1.23
3	3	0.78	0.65	0.83	0.70	0.83	0.99	1.19	1.02	4.45	0.76	0.79	1.05	1.07
3	4	1.07	0.79	0.91	0.81	0.92	1.10	1.00	1.07	0.03	0.95	0.95	0.95	1.01
3	5	0.89	1.16	1.11	1.15	1.13	1.00	0.89	1.03	0.05	1.07	1.07	0.96	1.06
4	1	1.32	1.12	1.11	1.11	1.12	1.14	0.94	1.06	1.51	1.20	1.20	1.00	0.95
4	2	1.14	0.86	0.92	0.85	0.92	0.97	0.99	0.99	1.02	0.93	0.91	1.03	1.02
4	3	0.72	0.89	0.99	0.89	0.97	1.02	1.20	1.08	0.07	0.94	0.94	0.99	1.10
4	4	0.60	0.78	0.87	0.81	0.87	0.90	1.14	0.96	1.22	0.82	0.83	1.14	1.07
4	5	1.22	1.35	1.10	1.33	1.12	0.96	0.74	0.91	1.19	1.11	1.13	0.85	0.86

Table J.1: Normalized objective metric data, $J_{norm_{ick}}$, for the $c = 13$ data channels, H_c , and subjects $i = 1-4$

Subject	Config	Data Channel												
		1	2	3	4	5	6	7	8	9	10	11	12	13
5	1	0.39	0.50	0.70	0.48	0.61	0.96	0.92	0.75	0.62	0.83	0.82	1.00	0.79
5	2	0.77	0.65	0.70	0.73	0.62	0.87	0.55	0.84	0.30	0.75	0.81	0.75	0.90
5	3	1.01	0.96	1.24	0.94	1.12	1.12	0.92	1.12	0.72	0.96	0.94	1.09	1.10
5	4	1.01	0.50	0.65	0.55	0.58	0.86	0.56	0.89	0.26	0.63	0.68	0.73	1.02
5	5	1.83	2.39	1.70	2.30	2.06	1.18	2.05	1.39	3.10	1.82	1.75	1.44	1.19
6	1	1.41	0.51	0.65	0.43	0.63	0.88	1.53	0.83	1.81	0.78	0.72	0.93	1.02
6	2	0.83	0.55	0.70	0.52	0.70	0.94	1.23	0.85	1.43	0.83	0.83	0.94	0.92
6	3	1.45	0.26	0.36	0.29	0.35	0.81	0.33	0.58	0.12	0.78	0.76	0.52	0.69
6	4	0.80	3.00	2.38	3.09	2.41	1.35	0.43	1.73	0.00	1.72	1.79	1.29	1.29
6	5	0.51	0.69	0.91	0.67	0.91	1.01	1.48	1.01	1.64	0.90	0.90	1.33	1.08
7	1	0.90	1.03	1.05	1.15	1.04	0.96	0.66	1.14	0.04	0.78	0.82	0.89	1.17
7	2	1.24	1.47	1.48	1.56	1.54	1.05	0.99	1.19	1.09	0.93	0.96	1.27	1.15
7	3	0.88	0.43	0.44	0.39	0.46	0.85	1.76	0.56	2.91	1.25	1.21	0.99	0.58
7	4	1.24	1.00	1.00	0.87	0.94	0.96	0.95	0.99	0.46	0.88	0.86	1.15	1.16
7	5	0.74	1.07	1.03	1.02	1.02	1.18	0.64	1.13	0.50	1.16	1.15	0.70	0.94
8	1	0.58	0.13	0.32	0.16	0.32	0.55	0.52	0.48	0.05	0.31	0.34	0.56	0.85
8	2	0.80	1.00	1.31	1.03	1.28	1.16	1.06	1.34	1.00	0.92	0.95	1.32	1.18
8	3	2.63	2.13	1.24	2.01	1.23	1.38	1.52	1.31	0.18	2.04	1.94	1.20	1.04
8	4	0.26	0.41	0.71	0.47	0.73	0.80	0.72	0.70	2.14	0.57	0.61	0.67	0.85
8	5	0.72	1.33	1.42	1.33	1.44	1.12	1.17	1.18	1.63	1.15	1.15	1.25	1.08
9	1	1.01	2.57	2.09	2.54	2.10	1.23	0.69	1.64	0.20	1.25	1.27	1.41	1.29
9	2	0.37	0.49	0.59	0.49	0.60	0.91	0.61	0.73	0.32	0.94	0.96	0.55	0.81
9	3	0.67	1.12	1.22	1.15	1.22	1.11	0.64	1.20	0.22	1.02	1.03	1.09	1.12
9	4	0.61	0.34	0.45	0.34	0.43	0.77	0.53	0.63	0.39	0.74	0.74	0.90	0.92
9	5	2.34	0.49	0.65	0.48	0.65	0.98	2.53	0.80	3.87	1.05	1.00	1.05	0.86
10	1	0.85	1.15	1.19	1.15	1.18	1.14	1.01	1.23	0.20	1.07	1.08	1.10	1.12
10	2	0.63	1.72	1.51	1.71	1.56	1.24	0.96	1.17	0.83	1.41	1.42	1.10	0.93
10	3	1.25	0.42	0.48	0.41	0.47	0.75	1.03	0.64	0.59	0.76	0.74	0.68	0.83
10	4	1.48	1.20	1.24	1.20	1.23	1.07	1.04	1.17	3.08	1.01	1.02	1.22	1.12
10	5	0.80	0.51	0.58	0.52	0.56	0.80	0.97	0.78	0.30	0.74	0.73	0.90	0.99

Table J.2: Normalized objective metric data, $J_{norm_{ick}}$, for the $c = 13$ data channels, H_c , and subjects $i = 6-10$

Subject	Config	Data Channel												
		1	2	3	4	5	6	7	8	9	10	11	12	13
11	1	0.86	0.85	0.68	0.86	0.70	1.01	1.00	0.88	0.96	1.17	1.19	0.86	0.94
11	2	1.11	0.17	0.38	0.20	0.40	0.79	0.67	0.71	0.31	0.38	0.40	0.86	0.85
11	3	1.10	0.64	1.36	0.55	1.27	0.85	1.67	0.72	1.63	0.68	0.66	1.01	0.91
11	4	0.89	2.72	1.60	2.75	1.62	1.35	1.08	1.57	1.77	2.19	2.16	1.47	1.23
11	5	1.04	0.63	0.99	0.65	1.01	1.00	0.58	1.12	0.33	0.58	0.59	0.81	1.08
12	1	0.54	0.88	0.94	0.92	1.00	0.96	0.56	1.12	0.01	0.81	0.85	1.05	1.13
12	2	1.48	3.10	2.67	3.05	2.58	1.66	2.80	1.67	4.99	2.36	2.32	1.54	1.15
12	3	1.10	0.20	0.30	0.21	0.31	0.70	0.57	0.63	0.00	0.51	0.52	0.70	0.89
12	4	0.88	0.38	0.53	0.36	0.53	0.82	0.59	0.79	0.00	0.61	0.59	0.91	0.90
12	5	1.00	0.44	0.56	0.46	0.59	0.87	0.48	0.80	0.00	0.71	0.72	0.80	0.92
13	1	0.46	1.00	1.01	1.02	1.03	0.99	1.16	1.00	1.04	0.98	1.00	1.01	1.02
13	2	1.67	0.93	0.95	0.87	0.93	1.05	1.02	1.01	3.62	1.04	1.01	1.20	1.01
13	3	1.05	0.64	0.66	0.62	0.65	0.87	0.96	0.76	0.32	0.92	0.91	0.68	0.88
13	4	1.18	1.06	1.09	1.06	1.09	1.04	0.96	1.07	0.03	1.01	1.01	1.04	1.01
13	5	0.63	1.36	1.29	1.43	1.30	1.06	0.89	1.15	0.00	1.05	1.07	1.08	1.07
14	1	1.00	1.46	1.44	1.46	1.44	1.19	1.08	1.32	0.01	1.14	1.15	1.15	1.14
14	2	0.73	1.43	1.39	1.42	1.41	1.17	1.49	1.24	4.75	1.16	1.17	1.33	1.05
14	3	1.33	0.45	0.49	0.46	0.48	0.78	0.74	0.62	0.02	0.85	0.84	0.65	0.79
14	4	0.89	0.76	0.78	0.74	0.76	0.96	0.81	0.91	0.22	0.96	0.94	0.98	1.00
14	5	1.05	0.90	0.90	0.93	0.90	0.90	0.87	0.91	0.00	0.89	0.91	0.90	1.02
15	1	0.93	1.50	1.45	1.52	1.48	1.19	1.00	1.26	3.20	1.25	1.26	1.00	1.02
15	2	0.95	0.30	0.44	0.33	0.43	0.84	0.88	0.74	0.32	0.71	0.72	0.96	0.94
15	3	1.30	2.14	1.72	2.06	1.73	1.09	1.24	1.26	0.02	1.36	1.34	1.14	1.10
15	4	0.99	0.26	0.38	0.28	0.36	0.84	0.60	0.64	1.15	0.81	0.79	0.63	0.79
15	5	0.84	0.79	1.01	0.81	1.00	1.04	1.28	1.11	0.31	0.87	0.88	1.27	1.16
16	1	0.88	0.41	0.43	0.42	0.44	0.81	0.90	0.66	1.69	0.74	0.74	0.66	0.79
16	2	0.97	2.14	1.74	2.12	1.76	1.17	0.99	1.33	0.01	1.65	1.64	1.26	1.21
16	3	0.74	0.94	1.22	0.94	1.18	1.15	1.90	1.27	3.26	0.92	0.92	1.42	1.18
16	4	1.24	0.23	0.31	0.24	0.30	0.82	0.40	0.58	0.02	0.68	0.67	0.52	0.75
16	5	1.17	1.28	1.31	1.29	1.31	1.05	0.81	1.17	0.02	1.01	1.03	1.14	1.07

Table J.3: Normalized objective metric data, $J_{norm_{ick}}$, for the $c = 13$ data channels, H_c , and subjects $i = 11-16$

Subject	Config	Data Channel												
		1	2	3	4	5	6	7	8	9	10	11	12	13
17	1	0.73	0.48	0.56	0.48	0.54	0.95	0.80	0.97	0.64	0.75	0.76	0.90	1.01
17	2	1.04	0.67	0.82	0.69	0.80	1.01	1.43	1.07	1.13	0.83	0.87	1.28	1.15
17	3	0.62	0.25	0.31	0.27	0.31	0.75	0.43	0.65	0.30	0.61	0.63	0.75	0.86
17	4	1.92	2.87	2.53	2.73	2.56	1.29	1.95	1.23	2.92	1.98	1.85	1.21	0.98
17	5	0.69	0.73	0.77	0.83	0.79	0.99	0.39	1.08	0.00	0.83	0.89	0.85	1.00
18	1	1.14	2.48	1.92	2.39	1.97	1.27	3.35	1.35	4.86	1.70	1.69	1.56	1.03
18	2	1.05	0.45	0.59	0.49	0.57	0.89	0.38	0.81	0.05	0.79	0.79	0.79	0.96
18	3	0.99	1.06	1.19	1.09	1.20	1.07	0.50	1.08	0.09	1.00	1.01	0.88	0.97
18	4	0.83	0.33	0.46	0.36	0.45	0.80	0.37	0.70	0.01	0.71	0.71	0.73	0.93
18	5	1.00	0.68	0.84	0.68	0.81	0.98	0.41	1.06	0.00	0.81	0.79	1.04	1.11
19	1	1.19	1.24	1.22	1.26	1.21	1.15	0.77	1.20	0.06	1.11	1.11	1.03	1.09
19	2	0.83	1.14	1.16	1.17	1.18	1.08	1.21	1.14	0.75	1.00	1.01	1.19	1.06
19	3	1.30	0.58	0.60	0.56	0.60	0.83	0.74	0.64	0.47	0.99	0.99	0.62	0.78
19	4	0.86	1.37	1.35	1.36	1.32	1.10	1.48	1.30	1.86	0.96	0.97	1.46	1.21
19	5	0.82	0.67	0.67	0.65	0.69	0.83	0.80	0.72	1.87	0.93	0.93	0.70	0.86
20	1	0.69	0.47	0.55	0.51	0.55	0.75	0.55	0.71	0.00	0.64	0.66	0.67	0.97
20	2	1.25	1.91	1.52	1.88	1.52	1.24	0.60	1.40	0.00	1.44	1.46	1.32	1.21
20	3	0.89	0.29	0.33	0.27	0.35	0.88	1.62	0.59	2.21	0.88	0.82	0.73	0.71
20	4	1.60	1.39	1.51	1.42	1.43	1.21	0.71	1.50	0.06	1.12	1.14	1.26	1.31
20	5	0.57	0.93	1.09	0.93	1.15	0.92	1.51	0.80	2.72	0.92	0.92	1.02	0.80
21	1	1.29	1.47	1.62	1.52	1.60	1.19	0.70	1.50	0.00	0.96	0.99	1.30	1.30
21	2	1.00	0.19	0.29	0.20	0.27	0.71	0.32	0.52	0.02	0.62	0.61	0.67	0.81
21	3	1.01	0.23	0.29	0.17	0.29	0.75	2.81	0.51	4.98	1.12	1.06	0.82	0.73
21	4	0.93	0.50	0.65	0.57	0.65	0.96	0.38	0.88	0.00	0.77	0.81	0.90	1.02
21	5	0.78	2.61	2.16	2.55	2.19	1.38	0.79	1.58	0.01	1.52	1.53	1.31	1.14
22	1	0.16	0.03	0.01	0.03	0.01	0.63	0.56	0.93	0.61	0.22	0.24	0.97	1.10
22	2	0.22	0.04	0.01	0.04	0.01	0.67	0.50	0.94	0.38	0.34	0.35	1.00	1.02
22	3	0.44	0.00	0.00	0.00	0.00	0.24	0.88	0.14	1.73	0.15	0.14	0.34	0.33
22	4	2.88	1.48	1.11	1.24	1.02	1.45	1.67	2.06	0.71	0.98	0.95	2.08	2.03
22	5	1.30	3.45	3.87	3.69	3.96	2.01	1.39	0.93	1.56	3.32	3.32	0.61	0.52

Table J.4: Normalized objective metric data, $J_{norm_{ck}}$, for the $c = 13$ data channels, H_c , and subjects $i = 17-22$

Subject	Config	Data Channel												
		1	2	3	4	5	6	7	8	9	10	11	12	13
23	1	0.70	0.31	0.41	0.32	0.39	0.77	0.44	0.62	0.64	0.75	0.74	0.82	0.90
23	2	0.35	0.75	0.91	0.80	0.92	1.11	0.63	1.06	0.49	1.00	1.04	1.03	1.03
23	3	0.58	3.05	2.61	2.98	2.50	1.39	0.62	1.83	0.60	1.41	1.43	1.55	1.37
23	4	0.53	0.37	0.50	0.42	0.48	0.85	0.49	0.71	0.58	0.78	0.80	0.87	0.91
23	5	2.84	0.52	0.57	0.48	0.71	0.88	2.83	0.78	2.68	1.06	1.00	0.72	0.80
24	1	0.51	0.18	0.41	0.21	0.40	0.63	0.46	0.61	3.12	0.25	0.28	0.82	0.90
24	2	0.92	2.84	2.01	2.72	2.02	1.34	1.40	1.13	0.01	2.58	2.48	1.07	1.01
24	3	0.81	0.26	0.63	0.29	0.63	0.84	0.52	0.84	0.20	0.33	0.36	0.84	1.02
24	4	2.08	1.23	1.07	1.26	1.07	1.25	1.78	1.50	0.20	1.29	1.30	1.27	1.04
24	5	0.67	0.50	0.88	0.52	0.89	0.94	0.84	0.93	1.47	0.56	0.58	1.00	1.01
25	1	1.16	0.68	0.70	0.68	0.70	0.90	0.91	0.79	0.00	0.90	0.88	0.83	0.88
25	2	0.60	1.56	1.41	1.53	1.44	1.13	1.66	1.20	3.90	1.28	1.29	1.17	1.09
25	3	0.94	0.42	0.54	0.46	0.54	0.89	0.60	0.77	0.13	0.75	0.76	0.74	0.87
25	4	1.50	0.32	0.45	0.34	0.44	0.91	0.61	0.75	0.83	0.73	0.73	0.71	0.86
25	5	0.80	2.02	1.91	1.98	1.89	1.18	1.21	1.49	0.15	1.35	1.35	1.54	1.30
26	1	0.58	0.04	0.08	0.03	0.08	0.46	0.79	0.20	0.78	0.52	0.49	0.37	0.45
26	2	0.76	0.62	0.80	0.65	0.82	0.91	0.92	0.92	0.72	0.72	0.74	1.16	1.02
26	3	0.67	0.32	0.56	0.34	0.55	0.89	0.37	0.91	0.06	0.55	0.56	0.70	1.06
26	4	1.52	2.61	1.85	2.63	1.91	1.52	1.10	1.52	0.61	2.16	2.17	1.32	1.12
26	5	1.48	1.42	1.72	1.35	1.64	1.23	1.82	1.45	2.83	1.04	1.04	1.46	1.35
27	1	1.31	0.30	0.38	0.32	0.38	0.82	0.65	0.64	0.03	0.75	0.73	0.62	0.81
27	2	0.71	0.80	0.90	0.88	0.92	0.92	0.74	1.03	0.04	0.79	0.83	1.08	1.12
27	3	0.86	1.01	1.09	0.95	1.06	1.09	1.12	1.15	0.14	1.03	1.00	1.22	1.07
27	4	1.41	0.43	0.50	0.47	0.52	0.93	0.68	0.70	0.25	0.92	0.93	0.48	0.73
27	5	0.72	2.46	2.14	2.38	2.12	1.24	1.81	1.49	4.55	1.51	1.51	1.60	1.27
28	1	0.99	2.14	3.11	1.84	2.90	1.40	2.31	1.24	4.22	1.60	1.58	1.29	1.04
28	2	1.12	1.52	0.92	1.89	1.07	1.12	0.72	1.45	0.00	0.98	1.06	1.31	1.29
28	3	1.35	0.18	0.15	0.20	0.16	0.65	0.26	0.45	0.00	0.74	0.74	0.47	0.66
28	4	0.58	0.80	0.53	0.65	0.55	0.98	1.10	1.03	0.77	0.93	0.86	1.09	1.04
28	5	0.96	0.36	0.29	0.41	0.32	0.86	0.60	0.83	0.00	0.75	0.76	0.85	0.98

Table J.5: Normalized objective metric data, $J_{norm_{ck}}$, for the $c = 13$ data channels, H_c , and subjects $i = 23-28$

Subject	Config	Data Channel												
		1	2	3	4	5	6	7	8	9	10	11	12	13
29	1	0.84	1.41	0.92	1.65	1.04	1.26	0.50	1.54	0.01	0.95	1.01	1.19	1.21
29	2	0.94	0.59	0.40	0.64	0.43	0.94	0.54	1.02	0.05	0.71	0.72	1.03	1.10
29	3	1.21	0.36	0.26	0.42	0.29	0.87	0.42	0.80	0.09	0.69	0.71	0.89	0.96
29	4	0.83	2.03	2.99	1.65	2.78	1.03	2.99	0.67	4.61	1.95	1.87	1.13	0.73
29	5	1.18	0.61	0.42	0.64	0.46	0.90	0.55	0.97	0.25	0.70	0.70	0.77	1.00
30	1	1.15	2.02	1.56	1.91	1.56	1.26	0.90	1.37	0.00	1.44	1.42	1.11	1.11
30	2	0.96	1.03	1.15	1.13	1.17	1.04	0.73	1.09	0.02	0.97	1.03	1.06	1.05
30	3	1.10	0.19	0.28	0.16	0.25	0.65	1.45	0.45	3.85	0.69	0.65	0.69	0.76
30	4	0.81	1.29	1.38	1.31	1.40	1.12	1.04	1.21	1.13	1.09	1.11	1.14	1.10
30	5	0.99	0.47	0.63	0.48	0.62	0.93	0.88	0.87	0.00	0.80	0.80	1.00	0.98
31	1	1.01	0.04	0.09	0.03	0.09	0.51	1.97	0.20	4.88	0.71	0.65	0.43	0.48
31	2	1.33	2.84	1.59	2.73	1.62	1.11	1.13	1.27	0.07	1.81	1.78	1.42	1.17
31	3	0.72	0.25	0.52	0.29	0.51	1.00	0.55	0.82	0.03	0.71	0.73	0.70	0.91
31	4	0.51	1.09	1.66	1.15	1.65	1.17	0.74	1.46	0.00	0.84	0.88	1.39	1.38
31	5	1.44	0.77	1.14	0.80	1.13	1.22	0.61	1.25	0.02	0.94	0.95	1.07	1.05
32	1	0.66	0.62	0.94	0.69	0.92	0.96	0.76	1.09	3.74	0.67	0.73	1.00	1.13
32	2	0.88	1.22	0.73	1.18	0.78	0.94	1.11	0.78	0.53	1.27	1.25	0.81	0.92
32	3	1.54	1.30	1.48	1.39	1.46	1.33	1.30	1.43	0.00	1.29	1.28	1.09	1.09
32	4	1.44	0.27	0.59	0.26	0.57	0.72	0.83	0.64	0.73	0.50	0.48	0.82	0.88
32	5	0.47	1.59	1.27	1.49	1.27	1.05	1.00	1.06	0.00	1.27	1.25	1.27	0.98
33	1	1.05	0.27	0.32	0.25	0.32	0.71	0.85	0.52	4.23	0.78	0.75	0.69	0.81
33	2	1.14	2.25	2.07	2.27	2.12	1.31	1.31	1.57	0.00	1.28	1.32	1.31	1.21
33	3	1.28	0.31	0.36	0.25	0.35	0.78	0.93	0.53	0.63	0.94	0.88	0.72	0.80
33	4	0.88	1.16	1.17	1.10	1.14	1.12	1.01	1.22	0.02	1.02	1.03	1.17	1.10
33	5	0.65	1.01	1.07	1.12	1.07	1.08	0.89	1.16	0.12	0.97	1.03	1.12	1.08
34	1	1.08	2.12	1.47	2.03	1.47	1.23	0.54	1.26	0.00	1.70	1.64	0.98	1.08
34	2	0.97	0.75	0.95	0.77	0.93	0.98	0.74	0.97	0.00	0.84	0.85	0.88	0.97
34	3	0.97	0.16	0.22	0.19	0.23	0.63	1.94	0.45	2.90	0.60	0.62	0.83	0.73
34	4	0.94	0.65	0.80	0.68	0.80	0.94	0.60	0.97	0.01	0.77	0.77	0.90	1.06
34	5	1.04	1.32	1.56	1.33	1.57	1.22	1.18	1.35	2.08	1.10	1.11	1.41	1.17

Table J.6: Normalized objective metric data, $J_{norm_{ck}}$, for the $c = 13$ data channels, H_c , and subjects $i = 29-34$

Subject	Config	Data Channel												
		1	2	3	4	5	6	7	8	9	10	11	12	13
35	1	0.40	1.01	1.18	1.05	1.18	1.09	0.95	1.25	0.22	0.91	0.94	1.23	1.24
35	2	0.64	1.36	1.03	1.35	1.06	1.09	0.80	1.04	1.48	1.33	1.33	1.13	1.00
35	3	0.91	1.56	1.29	1.52	1.33	1.10	1.40	1.13	3.30	1.32	1.29	1.02	1.02
35	4	2.06	0.92	1.24	0.93	1.19	1.09	1.07	1.10	0.00	0.96	0.95	0.98	0.98
35	5	1.00	0.14	0.26	0.16	0.25	0.64	0.77	0.48	0.00	0.48	0.49	0.64	0.77
36	1	0.75	0.85	1.00	0.93	1.01	1.08	1.41	1.17	2.06	0.94	0.98	1.18	1.15
36	2	0.80	0.40	0.52	0.40	0.52	0.91	1.40	0.83	2.00	0.76	0.75	0.90	0.90
36	3	0.97	0.67	0.84	0.72	0.86	0.93	0.76	0.95	0.49	0.81	0.83	0.93	1.00
36	4	1.27	0.30	0.43	0.34	0.43	0.88	0.67	0.76	0.45	0.69	0.71	0.79	0.85
36	5	1.20	2.78	2.21	2.62	2.18	1.19	0.76	1.29	0.00	1.81	1.74	1.21	1.11
37	1	0.54	0.58	0.85	0.63	0.86	0.93	0.79	0.93	0.33	0.68	0.71	1.00	1.01
37	2	1.36	1.38	0.80	1.32	0.80	1.05	0.77	0.98	1.67	1.47	1.42	1.00	0.93
37	3	0.97	0.55	0.82	0.59	0.83	0.99	0.92	0.94	0.71	0.73	0.76	0.92	0.99
37	4	1.37	1.33	1.42	1.31	1.39	0.98	1.45	1.12	2.27	1.03	1.02	1.07	1.09
37	5	0.76	1.16	1.11	1.15	1.12	1.05	1.06	1.04	0.01	1.10	1.10	1.02	0.98
38	1	1.18	2.22	1.43	2.08	1.38	1.15	0.76	1.28	0.00	1.61	1.59	1.02	1.11
38	2	1.61	1.30	1.58	1.37	1.65	1.25	2.65	1.33	4.96	1.27	1.22	1.71	1.08
38	3	0.77	0.50	0.73	0.55	0.73	0.84	0.47	0.83	0.03	0.65	0.70	0.72	0.93
38	4	0.70	0.53	0.66	0.54	0.65	0.94	0.48	0.83	0.00	0.79	0.81	0.85	0.96
38	5	0.73	0.45	0.60	0.45	0.60	0.82	0.64	0.73	0.00	0.67	0.69	0.71	0.92
39	1	0.85	0.24	0.55	0.28	0.51	0.81	0.71	0.78	0.00	0.61	0.62	0.79	0.96
39	2	1.64	3.82	2.37	3.59	2.47	1.66	1.88	1.65	4.85	2.54	2.43	1.58	1.07
39	3	0.75	0.28	0.63	0.34	0.60	0.80	0.84	0.83	0.04	0.57	0.60	0.86	1.03
39	4	0.87	0.29	0.65	0.35	0.61	0.89	0.66	0.82	0.08	0.70	0.73	0.81	0.87
39	5	0.89	0.37	0.80	0.45	0.80	0.83	0.91	0.93	0.03	0.59	0.62	0.95	1.07

Table J.7: Normalized objective metric data, $J_{norm_{ick}}$, for the $c = 13$ data channels, H_c , and subjects $i = 35-39$

REFERENCES

- Ancha, S., Baviskar, A., Wagner, J., and Dawson, D., "Ground Vehicle Steering Systems – Modeling, Control and Analysis of Hydraulic, Electric, and Steer-by-Wire Configurations", *International Journal of Vehicle Design*, vol. 44, nos. 1/2, pp. 188-208, 2007.
- Andonian, B., Rauch, W., and Bhise, V., "Driver Steering Performance Using Joystick vs. Steering Wheel Controls", SAE Paper, 2003-0100118, 2003.
- Black, J., Wagner, J., Alexander, K., and Pidgeon, P., "Vehicle Road Runoff - Active Steering Control for Shoulder Induced Accidents", Proceedings of the American Control Conference, pp. 3237-3244, Seattle, 2008.
- Brown, R. G., and Hwang, P. Y. C., *Introduction to Random Signals and Applied Kalman Filtering*, Third Edition, John Wiley & Sons, Inc.: New York, 1997.
- Campbell, B. N., Smith, J. D., and Najm, W. G., "Examination of Crash Contributing Factors Using National Crash Databases", Volpe National Transportation Systems Center, US National Highway Traffic Safety Administration, DOT HS 809 664, 2003.
- Català, A., Hoppenot, S., Puig, J., and Waare, R., "Laboratory and Road Methods for the Evaluation of the Performance of Steering Systems", FISITA 2004 World Automotive, Barcelona, Spain, F2004U118, 2004.
- Deram, P., "Vehicle Based Detection of Inattentive Driving for Integration in an Adaptive Lane Departure Warning System - Distraction Detection", Master's Thesis, Royal Institute of Technology, Sweden, 2004.
- Gillespie, T. D., *Fundamentals of Vehicle Dynamics*, Society of Automotive Engineers: Warrendale, PA, 1992.

- Green, M., "Methodological Analysis of Driver Perception-Brake Times", *Transportation Human Factors*, vol. 2, no. 3, pp. 195-216, 2000.
- Hadden, J. A., Everson, J. H., Pape, D. B., Narendran, V. K., and Pomerleau, D., "Modeling and Analysis of Driver/Vehicle Dynamics with Run-Off-Road Crash Avoidance Systems", 30th International Symposium on Automotive Technology and Automation, pp. 343-350, Florence, Italy, June 1997.
- Heathershaw, A., "Optimizing Variable Ratio Steering for Improved On-Center Sensitivity and Cornering Control", SAE Paper, 2000-01-0821, 2000.
- Heydinger, G.J., Salaani, M.K., Garott, W.R., and Grygier, P.A., "Vehicle dynamics modeling for the National Advanced Driving Simulator", *Proceedings of the Institution of Mechanical Engineers, Part D. Journal of Automobile Engineering*, vol. 216, no. 4, pp. 307-318, 2002.
- Hickey, J., "Shoulder Rumble Strip Effectiveness: Drift-Off-Road Accident Reductions on the Pennsylvania Turnpike", *Transportation Research Record: Journal of the Transportation Research Board*, vol. 1573, no. 17, pp.105-109, 1997.
- Iyasere, E., Black, J., Kinstle, M., Post, B., Wagner, J., and Dawson, D., "A Real Time Re-configurable Steering Simulator for System Design Studies", 2007 American Control Conference, 2289-2295, New York, 2007.
- Jaksch, F., "Driver-Vehicle Interaction with Respect to Steering Controllability", SAE Paper, 790740, 1979.
- Janssen, W., De Ridder, S., Brouwer, R. F. T., Thomson, R., Fagerlind, H., Lanner, G., Dupre, G., Bisson, O., Garcia, J. M., Figaredo, A., Papi, J., Martinez, A. V., Amengual, A., Valtonen, J., Kelkka, M., Goose, U., Klootwijk, C. W., Hooi, H., Hoschopf, H., Naing, C. L., Hill, J., and Wink, W., "Road Side Infrastructure for Safer European Roads: D02-Summary of Driver Behaviour and Driver Interactions with Roadside Infrastructure", Project RISER, European Community under the Competitive and Sustainable Growth Program, 2006.

Kalman, R. E., "A New Approach to Linear Filtering and Prediction Problems", *Journal of Basic Engineering*, pp. 35-45, March 1960.

LeBlanc, D., Sayer, J., Winkler, C., Ervin, R., Bogard, S., Devonshire, J. Mefford, M., Hagan, M., Bareket, Z., Goodsell, R., and Gordon, T., "Road Departure Crash Warning System Field Operational Test: Methodology and Results", University of Michigan Transportation Research Institute, Technical Report, Ann Arbor, MI, 2006.

Mandhata, U., Parker, R., Wagner, J., Dawson, D., and Post, B., "Investigation of Operator Feedback in Human-Machine Haptic Interface Steer-By-Wire Transportation Systems", Proceedings of the ASME/IMECE Dynamic Systems and Control Division, Anaheim, CA, 2004.

Pape, D. B., Hadden, J. A., McMillan, N. J., Narendran, V. K., Everson, J. H., and Pomerleau, D. A., "Performance Considerations for Run-Off-Road Countermeasure Systems for Cars and Trucks", SAE paper 1999-01-0820, 1999.

Pohl, J., Birk, W., and Westervall, L., "A Driver-Distraction-Based Lane-Keeping Assistance System", *Proceedings of the Institution of Mechanical Engineers, Part I: Journal of Systems and Control Engineering*, vol. 221, no. 4, pp. 541-552, 2007.

Räsänen, M., "Effects of a Rumble Strip Barrier Line on Lane Keeping in a Curve", *Accident Analysis and Prevention*, vol. 37, no. 3, pp. 575-581, 2005.

Sayer, J. R., LeBlanc, D. J., Mefford, M. L., and Devonshire, J., "Field Test Results of a Road Departure Crash Warning System: Driver Acceptance, Perceived Utility and Willingness to Purchase", proceedings of the Fourth International Driving Symposium on Human Factors in Driver Assessment, Training and Vehicle Design, Stevenson, WA, 2007.

Setlur, P., Wagner, J., and Dawson, D., "A Hardware-in-the-Loop and Virtual Reality Test Environment for Hybrid Vehicle Steer-by-Wire System Evaluation", proceedings of the American Control Conference, vol. 3, pp. 2584-2589, Denver, CO, June 2003.

- Sierra, C., Tseng, E., Jain, A., and Peng, H., "Cornering Stiffness Estimation Based on Vehicle Lateral Dynamics", *Vehicle System Dynamics*, vol. 44, suppl., pp. 24-38, 2006.
- Sugita, S., Tomizuka, M., and El-Shaer, A., "Human-Machine Interaction in Vehicle Steering", SAE Paper, 2009-01-0359, 2009.
- Xia, X., "A Nonlinear Analysis of Closed Loop Driver/Vehicle Performance with Four Wheel Steering Control," Ph.D. Dissertation, Department of Mechanical Engineering, Clemson University, Clemson, SC, 1990.
- Yamaguchi, Y., and Murakami, T., "Adaptive Control for Virtual Steering Characteristics on Electric Vehicle Using Steer-by-Wire System", *IEEE Transactions on Industrial Electronics*, vol. 56, no. 5, pp 1585-1594, 2009.
- Yi, K., and Chung, J., "Nonlinear Brake Control for Vehicle CW/CA Systems", *IEEE/ASME Transactions on Mechatronics*, vol. 6, no. 1, pp 17-25, 2001.
- Yih, P., and Gerdes, J. C., "Modification of Vehicle Handling Characteristics via Steer-By-Wire", *IEEE Transactions on Control Systems Technology*, vol. 13, pp. 965-976, 2005.
- Zegeer, C. V., Reinfurt, D. W., Hummer, J., and Herf, L., "Safety Effects of Cross-Section Design for Two-Lane Roads", *Transportation Research Record 1195*, Transportation Research Board, National Research Council, Washington, D.C., pp. 30-32, 1988.
- Zhang, N., and Wang, M., "Dynamic Modeling of Hydraulic Power Steering System with Variable Ratio Rack and Pinion Gear", *Japanese Society of Mechanical Engineers International Journal, Series C: Mechanical Systems, Machine Elements and Manufacturing*, vol. 48, no. 2 SPEC, pp. 251-260, 2005.